Reply to the comments of Referee #1 on the paper

In situ observations of CH_2Cl_2 and $CHCl_3$ show efficient transport pathways for very short-lived species into the lower stratosphere via the Asian and North American summer monsoons

by V. Lauther et al.

We thank Referee #1 for the thorough reading of and the very helpful remarks on our manuscript. The comments have been considered carefully while revising the draft and resulting modifications are addressed point-py-point in the following (Referee's comments are cited in bold face):

Specific comments:

1. This distinction between tropospheric and stratospheric air is clear in the figures but does get lost in some of the text. For stratospherically relevant numbers reported, these should be calculated with only observations collected above the thermal tropopause. If that is already being done, it is not clearly communicated in the main text. For example, on line 19 in the abstract and in the main text it is not clear if the reported "1-5 weeks into the Ex-LS" was calculated only with observations collected above the thermal tropopause.

This is a very good remark! We agree and have now specified the given transport times at the respective locations in the paper. In addition, we have added an overview table with median transport times derived from back-trajectories of different lengths (from the model boundary layer and from the location of maximum convection) for all observations in the UTLS and either only for those in the UT or only for those in the LS. The used data set in the new table (Table 2) is also filtered to include only measurements of CH_2Cl_2-poor air linked to the NAM as well as measurements of CH_2Cl_2-rich air linked to the ASM. We consistently use median transport times now and provide ranges of transport times derived from the 25. and 75. percentile of the respective data set. For details, we refer to the track change version of the manuscript.

In addition, we noticed that the separation between measurements in the UT and the LS shown in the figures was based on ECMWF's ERA5 reanalysis data (Hersbach et al., 2020). There are but a few differences regarding the discrimination between UT and LS of individual data points when using ERA5 instead of ERA-Interim data. However, to be consistent, we changed the displayed separation between UT and LS in all relevant figures (3, 12 (now 13), 13 (now 14), B1 (now C1); no changes were necessary in Fig. 9 (now 10)) to the calculations based on ERA-Interim.

2. It is misleading to place N2O and month on the same axis in Figure 4. Measurements of CH2Cl2 at N2O mixing ratios of 325 ppb should not necessarily be compared to surface observations in June; some of the low mixing ratios of CH2Cl2 shown here are likely due to photochemical processing in the stratosphere, not seasonal surface trends.

This is true and we thought about that while carefully choosing the wording of this section (i.e. "Although this simplified view ignores the impact of mixing processes and chemical reduction of CH_2Cl_2 it qualitatively explains the lower branch of the correlation curve for air parcels younger than a few months."). However, we think Figure 4 is an interesting qualitative comparison between two different data sets providing the reader a good first impression of a plausible explanation for one part of the rather complex CH_2Cl_2-N_2O relationship. Nevertheless, we agree that Figure 4 should be interpreted with care and not be used out of context. In the caption of Figure 4 we thus refer to the similarities between the CH_2Cl_2-N_2O relationship and the ground-based CH_2Cl_2 observations from the AGAGE network focusing only on the lower branch of the correlation — implying a comparison of the correlation with AGAGE data from about July to September. This range for a plausible comparison is also stated in the main text ("The observed decrease of low CH_2Cl_2 mixing ratios for increasing N_2O mixing ratios (from older to younger air) agrees well with the decreasing tropical monthly averaged CH_2Cl_2 mixing ratios from about July to September

2017, as observed by AGAGE."). However, we agree that the figure might be misleading to some readers and therefore we have now included vertical lines highlighting the comparison between July and September to clarify the plausible range of the comparison. In addition, we have specified the respective text in the Figure 4 caption as follows:

"The gradient of the CH_2Cl_2-N_2O relationship's lower branch (low CH_2Cl_2 mixing ratios between vertical lines) qualitatively fits the temporal variation of the ground-based CH_2Cl_2 measurements."

It should also be noted that biases between NOAA and Advanced Global Atmospheric Gas Experiment (AGAGE) records of CH2Cl2, particularly in the northern tropic station shown in Figure 4, have been identified, suggesting either calibration errors or longitudinal gradients in mixing ratios of CH2Cl2 (Engel et al., 2018).

Additionally, the CH2Cl2-poor air is connected to the OH-driven seasonality based on ground-based observations at one AGAGE station without discussing other explanations. However, since CH2Cl2 is not well mixed in the troposphere, a contributing factor could be the uplift of air with less anthropogenic influence than measured at the ground-based station. This option is alluded to on line 402, but it is not clearly introduced as a separate mechanism for low CH2Cl2 mixing ratios

These are good points and we have included them in the text of Section 3.1 as follows:

"It is thus very likely that the lower branch of the CH_2Cl_2-N_2O ~~correlation~~relationship is caused by the tropical Atlantic CH_2Cl_2 surface seasonality. However, the low CH_2Cl_2 mixing ratios observed during WISE could also be impacted by air uplifted from regions less influenced by CH_2Cl_2 sources than the observations from the AGAGE network at Barbados. Ground-based observations of CH_2Cl_2 surface mixing ratios from the AGAGE and the NOAA network show strong regional differences particularly in the NH tropics. However, it is unclear if these differences are caused by calibration biases or are of a natural origin (Engel et al., 2018)."

3. Variations of "first study" statements appear throughout the paper. I would caution against that phrasing since it seems unnecessary for the importance of the paper and can be untrue if one of the qualifications in these statements are removed. From a literature search, at least Adcock et al. (2021) provides back-trajectory analysis and identifies source regions of measurements of CH2Cl2 in the UTLS. Additionally, Rotermund et al. (2021), which is properly referenced in the discussion section, should also be acknowledged in the introduction as a study that employed similar methods to investigate source regions of brominated VSLS during the WISE campaign.

We agree and have removed the respective statements of "first study" from the paper. Also Adcock et al. (2021) is discussed in the paper. For details, we refer to the track change version of the manuscript.

Rotermund et al. (2021) is now acknowledged in the introduction of the paper in the following way:

A study by Rotermund et al. (2021) employed similar methods to identify source regions and the impact on the Ex-LS of Br-VSLS using measurements from the same aircraft campaign as the measurements used in the present paper and is compared to our results in Section 4.

4. It would be helpful to either place the results of the present study in the context of similar studies conducted with observations of other VSLS (e.g., Aschmann et al., 2009; Ashfold et al., 2012; Levine et al., 2007; Liang et al., 2014), or explain in the introduction why the results of those studies have limited applications for studying the transport of Cl-VSLS.

The results of similar transport studies focused on other VSLS (usually Br-VSLS with mainly natural, oceanic sources) cannot necessarily be used to describe the transport of Cl-VSLS (mainly anthropogenic, land-based sources) because of their different source distribution in the troposphere. Therefore it is necessary to describe transport pathways into the stratosphere for VSLS (particularly for those with strongly varying mixing ratios in the troposphere) specifically for the respective VSLS or group of VSLS with similar characteristics (e.g., photochemical lifetime and source distribution). To point this out, we have now added the following explanations to the introduction of the paper:

"Observational evidence for Cl-VSLS being transported into the stratosphere is extremely rare~~ and their main transport pathways into the stratosphere have not been described on an observational basis~~ (e.g., Schauffler et al., 1993; Woodbridge et al., 1995; Schauffler et al., 2003; Laube et al., 2008; Park et al., 2010; Adcock et al., 2021). Transport pathways into the stratosphere for VSLS have been derived from observations of bominated VSLS (Br-VSLS; e.g., Sturges et al., 2000; Ashfold et al., 2012; Wales et al., 2018; Filus et al., 2020; Keber et al., 2020; Rotermund et al., 2021) or modeled specifically for Br-VSLS (e.g., Levine et al., 2007; Aschmann et al., 2009; Ashfold et al., 2012; Liang et al., 2014) which have mainly natural emission sources (Engel et al., 2018). However, the only Br-VSLS with a photochemical lifetime comparable to those of CH_2Cl_2 and $CHCl_3$ is CH_2Br_2 (150 days; WMO, 2018) which is mostly emitted by the oceans and, consequently, is differently distributed in the troposphere than the mainly anthropogenically (land-based) emitted CH_2Cl_2 and most Cl-VSLS (e.g., Engel et al., 2018). Thus, transport studies of Br-VSLS focus on transport into the stratosphere from likely different source regions than those of Cl-VSLS and their results might not necessarily be directly applicable to the transport into the stratosphere of CH_2Cl_2 and $CHCl_3$. In addition, in order to specifically study transport into the stratosphere via the ASM it is beneficial to observe VSLS with their strongest sources being located in the core region of the ASM. This is the case for CH_2Cl_2 while most Asian Br-VSLS sources are located only in adjacent regions of the ASM."

5. "...two most efficient and fast transport pathways from (sub-)tropical source regions into the extratropical lower stratosphere (Ex-LS)..." (Line 7) This study has identified the ASMA as an efficient pathway into the extratropical stratosphere and the North American monsoon as a fast transport pathway into the Northern Hemisphere upper troposphere/lower stratosphere. However, from the observations presented in this paper, it is not clear how efficiently Cl-VSLS lofted into the upper troposphere by hurricanes are mixed into the stratosphere. This sentence could be simplified to: "...two transport pathways from (sub-)tropical source regions into the extratropical lower stratosphere and upper troposphere...". Further detail of the difference between the two pathways is provided later in the abstract.

This is true. We changed the sentence as suggested.

6. Line 132: Please state why earlier flights are not included in this study. Also, altitude and pressure ranges are not given for the measurements. Were any filtering criteria used to limit observations to the UTLS?

We have reconsidered the wording of Line 132 and added the full ranges of the used data set regarding potential temperature, altitude, and pressure. No explicit filtering of the data set was used to confine the presented observations to the UTLS region. However, due to a malfunctioning water trap of the HAGAR-V instrument, we could perform CH_2Cl_2 and $CHCl_3$ measurements only at ambient water vapor levels below about 100 ppm (measuring mainly at around 6 ppm), thus "naturally" confining the observations to the upper part of the troposphere and above. This is briefly explained in Section 2.2.1 to which we now refer in the introduction to the used data set (Sect. 2.1). We also added to Section 2.2.1 why we were able to measure only during the last ten flights of the WISE campaign. The respective parts of the manuscript are modified as follows (sections 2.1 and 2.2.1, respectively):

"In this study we present UTLS measurements ~~up to~~between a potential temperature of 315 K and 404 K (i.e., 7.4 – 14.5 km altitude; 388 – 130 hPa pressure) of the last ten WISE flights, i.e., from 28 September to 21 October 2017 (Figure 1). Due to technical issues of the instrument, CH_2Cl_2 and $CHCl_3$ measurements below the given range and during earlier flights of the WISE campaign were not performed (cf. Section 2.2.1)."

"However, during WISE the dehydration system of HAGAR-V was malfunctioning.~~ could not be used. Consequently,~~ For the last 10 WISE flights that system was bypassed and the MS module measured only at low ambient water vapor levels (mainly at $H_2O < 100$ ppm; median: 5.6 ppm), i.e., in the UTLS region~~. With this solution the MS module measured~~ thus yielding measurements during about 90% of a typical ~~WISE~~ flight's duration (i.e., about 7.6 h per flight). MS measurements of WISE flights before 28 September could not be used for analysis due to the malfunctioning sample dehydration unit."

7. Section 3.1.3 would read more clearly if the "Analysis of transport pathways" is discussed before "Case study: convective uplift by hurricane Maria". As written, what is meant by fast transport time

We agree and have rearranged the respective paragraphs and figures. Note, that this is not directly marked in the track changes version of the manuscript to keep changes within the text highlighted.

8. Line 370: Please explain why the comparison to August and September ground-based observations is justified based on the transport time since maximum $\Delta\Theta_{18h}$ and not transport time since the boundary layer? Similarly, is the uplift described on line 373 recent or fast uplift of CH2Cl2-poor air (since max $\Delta\Theta_{18h}$ or since the boundary layer, respectively)?

This is a good point and by providing the different calculated transport times (Table 2; cf. response to specific comment "1.") this should be clear now. We additionally included the information about the transport time since the boundary layer to the sentence (see quote below). For CH_2Cl_2-poor air parcels with maximum convection above Central America the difference between median transport times from the location of maximum convection and from the model boundary layer is only about one week. Thus 'recent transport' can also be considered 'fast transport'. We agree that this was not clear before we added Table 2 to the paper. In regard to specific comment "8.", the text of Sect. 3.1.3 - "Locations of maximum diabatic ascent rate and transport times" was modified as follows:

"The transport times to the UTLS since the ascent above Central America mainly range between ~~1~~2 – 5 weeks~~ and are much shorter than for those air parcels lifted up above Asia~~ (cf. Table 2). The main uplift of CH_2Cl_2-poor air above Central America thus falls in the time period of late August and throughout the entire September. ~~T~~With transport times from the BL being only about one week longer (Table 2), this result supports the comparison of CH_2Cl_2-poor air with the seasonal minimum CH_2Cl_2 mixing ratios observed by AGAGE at Barbados"

9. In the discussion section, line 504, the authors state "...clearly benefits the use of CH2Cl2 observations to derive details about the different transport mechanisms and pathways...". It is an interesting and novel way to frame the paper, and if the authors would like to highlight that aspect, it should be introduced at the end of Section 1. However, in the discussion please note that CH2Cl2 and CH2Br2 have similar atmospheric lifetimes, and regionally varying surface mixing ratios, not just the OH seasonal cycle, can influence the low CH2Cl2 observed in the UTLS. The use of the CHCl3:CH2Cl2 ratio as a diagnostic tracer could also be better highlighted.

These are good points. With our revision of the introduction regarding the specific comment number "4." we also highlighted the beneficial use of a VSL tracer like CH_2Cl_2 with its main sources located in the core region of the ASM to analyze transport into the stratosphere via the ASM.

We also changed the wording regarding the advantage of CH_2Cl_2 over the Br-VSLS analyzed by Rotermund et al. (2021) due to its very strong Asian emission sources and very low mixing ratios in other regions of strong convection. Thereby we highlight the more general fact that we could derive the two transport pathways so clearly due to the strong contrast of tropospheric CH_2Cl_2 mixing ratios in the regions of significant convection. The possible reasons for the low CH_2Cl_2 mixing ratios are already discussed in Section 3.1 (see our response to the specific comment nr. "2."). However, we wanted to keep the phrasing "[...] a longer lifetime [...]" when comparing CH_2Cl_2 to the Br-VSLS analyzed by Rotermund et al. (2021) without specifically commenting on the comparable atmospheric lifetime of CH_2Br_2 (this is already mentioned in the introduction, cf. answer to specific comment nr. "4.") because of two reasons: (1) our statement is correct (CH_2Cl_2 and CH_2Br_2 have similar atmospheric lifetimes, but on average that of CH_2Cl_2 is up to one month longer; WMO, 2018); (2) we write that not a single but the combination of attributes (lifetime and source distribution) is the reason why CH_2Cl_2 is the preferred tracer for the analysis of details on the transport pathways into the Ex-UTLS in NH late summer. The respective part of the discussion is now modified as follows:

"Nevertheless, compared to the very short-lived bromine species analyzed by Rotermund et al. (2021), the combination of a longer lifetime, highly significant Asian emission sources~~, and a strong seasonal cycle~~ and very low mixing ratios in other regions of strong convection clearly benefits the use of CH_2Cl_2 observations to derive details about the different transport mechanisms and pathways from the source region into the NH summertime UTLS. In addition, using the $CHCl_3$:CH_2Cl_2 ratio to support the analysis of air mass origin is a unique and helpful tool in the analysis of transport pathways."

10. The discussion of the flight on 1 October (lines 542 – 556) could be moved to the hurricane case study section. Having this text at the end of Section 4 somewhat distracts from the big picture highlights given. Please note on line 553 and in similar text that while NAMA was observed to be a fast transport pathway to the UTLS, a low fraction of stratospheric air originates from central and western ITCZ (Figure 6).

We agree and moved this paragraph and Figure 14 (now Fig. 11) to the hurricane case study section which itself has also been moved further below in the text (cf. specific comment number "7."). Note, that the moving of figures and paragraphs is not directly marked in the track changes version of the manuscript to keep changes within the text highlighted.

When discussing the transport pathway into the Ex-LS via the NAMA we now added the information about the relatively low fractions of central and western ITCZ air mass origin in stratospheric air as well as the note that we actually observed only 25 % of the air parcels transported by the NAMA within the Ex-LS. We modified the text at three different locations (Section 3.1.3 - Analysis of transport pathways, Section 4 - Discussion (now Section 3.1.3 - Case study: convective uplift by hurricane Maria), and Section 5 - Conclusion) as follows:

"Another aspect adding to the different transport times is the longer transport pathway from Asia because simulations indicated air masses~~ were always observed to reach~~ reached the location of measurement always from the west. Nevertheless, air parcels observed in the Ex-LS are impacted more strongly by air masses transported via the ASMA than via the NAMA (cf. figures 6 and 14)."

"We have thereby shown that tropical surface mixing ratios of VSLS from the region of Central America and the Atlantic Ocean can be efficiently transported into the Ex-LS during the late North American monsoon season. For instance, this is of particular importance for brominated short-lived substances (e.g., CH_2Br_2 and $CHBr_3$) that have a high ODP and some of their largest emission sources located in tropical oceans (e.g., Hepach et al., 2015; Rotermund et al., 2021). However, it has to be noted that only 25 % of air parcels transported by this pathway were observed in the Ex-LS and stratospheric air masses showed relatively low fractions of air originating in the region of central and western ITCZ compared to those originating in southern and eastern Asia (cf. Figure 14)."

Eventually, these air masses mixed into the LS by Rossby wave breaking and influenced the chemical composition of the NH Ex-LS $10-20$ K below the air masses dominated by transport via the ASMA. However, only 25 % of air parcels transported via this pathway were observed above the thermal TP with transport times from the BL to the location of measurement ranging from 5 to 9 weeks.

Technical comments:

- "Regionally differing … CHCl3 sources" (Lines 23 – 26): As written this sentence is confusing. Please clarify that a larger fraction of CHCl3 than CH2Cl2 is emitted by natural sources, and, consequently, a lower CHCl3:Cl2Cl2 is found in air parcels that originate from regions with significant anthropogenic influences than regions with weaker

anthropogenic emissions.

We changed the wording of the mentioned sentence in the abstract as follows:

"~~Regionally differing $CHCl_3$:CH_2Cl_2 emission ratios derived from our UTLS measurements suggest a clear similarity between $CHCl_3$ and CH_2Cl_2 when emitted by anthropogenic sources and differences between the two species mainly caused by additional, likely biogenic, $CHCl_3$ sources.~~ CH_2Cl_2 and $CHCl_3$ have similar atmospheric sinks and lifetimes but the fraction of biogenic emissions is clearly higher for $CHCl_3$ than for the mainly anthropogenically emitted CH_2Cl_2, consequently lower $CHCl_3$:CH_2Cl_2 ratios are expected in air parcels showing a higher impact of anthropogenic emissions. The observed $CHCl_3$:CH_2Cl_2 ratio suggests clearly stronger anthropogenic emissions in the region of southern and eastern Asia compared to those in the region of Central America and the tropical Atlantic."

- "Due to the sparseness of Cl-VSLS measurements in the stratosphere" (Line 36): This statement is true, but please reference some past studies that measured Cl-VSLS in the stratosphere, such as (Laube et al., 2008; Schauffler et al., 1993, 2003) in addition to some of the references already present in the paper.

References to other studies presenting Cl-VSLS measurements in the stratosphere are now given: "~~Due~~Owing to the sparseness of Cl-VSLS measurements in the stratosphere (e.g., Schauffler et al., 1993, 2003; Laube et al., 2008; Park et al., 2010; Adcock et al., 2021 the impact of changes in Cl-VSLS surface emissions on their distribution in the stratosphere has yet to be fully characterized on an observational basis."

- Paragraph beginning on Line 54: It's important for your analysis of the CHCl3:CH2Cl2 ratio that the reader understands CH2Cl2 is largely emitted by anthropogenic sources, while a larger fraction of CHCl3 is from natural sources. This should be directly stated for the reader here. Overall, the detail given for the different emissions sources for the two VSLS could be more concise and focused so that this point does not get missed.

We agree and the phrase " Nevertheless, on a global scale $CHCl_3$ has a significant fraction of biogenic emission sources in contrast to CH_2Cl_2 which is almost exclusively emitted by anthropogenic sources." was added to the mentioned paragraph to highlight this difference between the two analyzed species.

In addition and in agreement with a comment of Referee #2 we shortened the information given in the introduction to focus more on things directly relevant to the paper.

- Line 77: It may be helpful to state the atmospheric lifetimes of CH2Cl2 and CHCl3 at the beginning of this paragraph so that they are not lost in the discussion.

We agree and the mentioned paragraph is now rearranged accordingly:

"For CH_2Cl_2 Hossaini et al. (2019) suggest an average tropospheric lifetime of 168 days (about 6 months) and a stratospheric lifetime of $1-2$ years (outside the poles) was estimated by Hossaini et al. (2017). The main atmospheric sink of both CH_2Cl_2 and $CHCl_3$ is the reaction with hydroxyl radicals (OH) in the troposphere. Both species have similar reaction rates with OH implying similar photochemical lifetimes for both Cl-VSLS (Hsu and DeMore, 1994). Time series of background mixing ratios of both species are anticorrelated to the seasonal cycle of OH (Cox et al., 2003). In the NH seasonal anthropogenic use of products releasing $CHCl_3$ to the atmosphere (e.g., landfill and chlorination of water) have been observed to have a small local impact on the seasonality of $CHCl_3$ (Gentner et al., 2010). In addition, the global distribution of OH shows significant regional differences (Spivakovsky et al., 2000; Hanisco et al., 2001; Lelieveld et al., 2016). Therefore, also the photochemical lifetimes of CH_2Cl_2 and $CHCl_3$ are regionally different. ~~For CH_2Cl_2 Hossaini et al. (2019) suggest an average tropospheric lifetime of 168 days (about 6 months) and a stratospheric lifetime of $1-2$ years (outside the poles) was estimated by Hossaini et al. (2017). Both species have similar reaction rates with OH implying similar photochemical lifetimes for both~~

~~Cl-VSLS (Hsu and DeMore, 1994).~~"

- Line 104: If there are modeling studies that explored source regions of Cl-VSLS in addition to Claxton et al. (2019), they should be referenced here.

This paragraph highlights the regional dependency of the Cl-VSLS's ODP which is, to the best of our knowledge, presented only by Claxton et al. (2019).

- Lines 255 - 260: Some of the wording in this paragraph is hard to follow. A useful point that is missing here is N2O, due to its long tropospheric lifetime is well mixed in the troposphere, while CH2Cl2 is not.

We considered the comment and added the proposed additional information to the text as follows:

"With a photochemical lifetime of 123 years (Ko et al., 2013) N_2O is well mixed in the troposphere and has a much longer lifetime than CH_2Cl_2 which exhibits strongly varying mixing ratios throughout the boundary layer (e.g., Simmonds et al., 2006)."

- "measurements of AGAGE" (Line 262): Here and elsewhere in the paper, please correct to read "ground-based measurements of CH2Cl2 from the AGAGE network"

The text is now changed to the proposed phrasing at all convenient places in the manuscript. For details, we refer to the track change version of the manuscript.

- Line 299 – 304: The description of the different criteria is hard to follow. Please carefully reword. Also, readers may have to refer back to criteria (1) and (2), it could be helpful to format them as separate bullets.

We agree and reconsidered the wording and structure of the paragraph modifying it as follows:

"Further, to work out differences of air mass origin between CH_2Cl_2-rich and -poor air, ~~for each surface origin tracer the median fraction~~ the median fraction of a surface origin tracer in CH_2Cl_2-rich air parcels is compared to that in CH_2Cl_2-poor air parcels. To combine regions of air mass origin with a particularly high relative impact on either CH_2Cl_2-rich or -poor air, the ratio of these median surface origin tracer fractions in CH_2Cl_2-rich and -poor air is analyzed. Surface origin tracers with particularly high relative median fractions in either CH_2Cl_2-rich or -poor air are combined following these two criteria:

(1) considered are only surface origin tracers with median fractions $\geq 1\,\%$ in CH_2Cl_2-rich or -poor air parcels, and

(2) the ~~median~~ ratio of a median surface origin tracer fraction (CH_2Cl_2-rich/CH_2Cl_2-poor air respectively CH_2Cl_2-poor/CH_2Cl_2-rich air) must be > 1.8.

- Figure 7: Could the transport time to the boundary layer be shown in a similar figure? The lines given in Figure 10 are hard to distinguish.

Yes, we added Figure B1 to the appendix and refer to it in Section 3.1.3 as follows:

" The locations of trajectory end points at the model boundary layer color coded with transport time are given in the appendix (Figure B1)."

- Line 354: Locations of and transport times since maximum diabatic ascent rate

We have now included also transport times from the boundary layer (Table 2; see reply to specific comment number "1.") and will thus keep the title of the subsection as it is.

- Line 389: Please state how many of these air masses were collected above the thermal tropopause.

It were 5 out of 27. The sentence was modified as follows:

"This analysis directly links 27 WISE measurements (five were observed above the thermal TP) to the convection of hurricane Maria with transport times since convection ranging between one week and one month."

- "positively correlate with transport time" (Line 391): What is shown in Figure 8 is the time since max convection, not the overall transport time. Please clarify the discussion in this paragraph.

We focus on the transport since the main convection by hurricane Maria because this gives a better impression on the time scale for air parcels lofted by a major hurricane to reach the Ex-UTLS and we analyze impacts on these air parcels induced in the UTLS. However, all trajectories linked to air parcels lifted up by hurricane Maria reach the model boundary layer in September and most do so above the Atlantic Ocean, i.e., at the time of seasonal surface minimum CH_2Cl_2 mixing ratios and in a region of weak CH_2Cl_2 emission sources. We added the respective information to the text and included a note to the relationship of CH_2Cl_2 and transport time since the boundary layer as follows:

"Interestingly, CH_2Cl_2 mixing ratios of measurements linked to hurricane Maria positively correlate with transport time since maximum convection ($R_{\text{Pearson}} = 0.85$; Figure 10, top right. Note, these CH_2Cl_2 mixing ratios also correlate with transport time since the model BL but with a lower $R_{\text{Pearson}} = 0.64$ and transport times between 9 and 48 days. However, here we focus on the transport since convection by hurricane Maria to derive impacts on the air parcels induced by processes in the UTLS region). Those air samples related to short transport times contain the lowest CH_2Cl_2 mixing ratios at $N_2O > 325$ ppb measured during WISE (Figure 10, top left). According to the back-trajectories, most of the air parcels lifted up by hurricane Maria left the model boundary layer above the tropical Atlantic in September where CH_2Cl_2 sources are small (Figure 10, bottom). In addition, in that region the seasonal minimum of CH_2Cl_2 mixing ratios is in September (cf. Section 3.1)."

- Lines 411 and 434: Please clearly state that you are only performing back trajectories for observations collected above the thermal tropopause, otherwise here and elsewhere should read "into the UTLS"

We analyze the trajectories for observations in the UTLS region and corrected the wording accordingly.

- Line 447: State for the readers that a broader range of surface mixing ratios of CH2Cl2 (~10 – 70 ppt) are reported from surface stations than for CHCl3 (~5 – 15 ppt) (https://agage.mit.edu/data/agage-data).

We have considered this statement carefully and concluded that it is not necessarily helpful to the readers. The much clearer split of the CH_2Cl_2-N_2O relationship than that of the $CHCl_3$-N_2O relationship is likely not based on the different global absolute surface mixing ratio ranges of the two Cl-VSLS. For air parcels measured during WISE we identified significant regions of air mass origin only around the summertime ITCZ (cf. Figure 2). The surface mixing ratio ranges within these regions between July and September could provide a supporting argument to the discussion. However, using the monthly averaged surface mixing ratios ignores the daily variations at the given location. Including the standard deviation or any other measure of the mean surface mixing ratio scatter range within the relevant regions would actually provide a useful argument for why we can clearly resolve the two branches in the CH_2Cl_2-N_2O relationship but not so clearly in the $CHCl_3$-N_2O relationship ($CHCl_3$ has stronger relative variations of mixing ratios within the source regions than CH_2Cl_2). However, the sparseness of ground-based Cl-VSLS observations in these regions prevents us from using such an argument. In any case, we think it is not helpful if we provide the global range of monthly averaged mixing ratios of the two Cl-VSLS here.

- Line 476: Remind the reader here or earlier in the section that a larger fraction of CHCl3 emissions than CH2Cl2 are from natural sources and the two compounds have similar atmospheric lifetimes.

This is a good suggestion and it was included in the text of Section 3.2 as follows:

“The $CHCl_3$-CH_2Cl_2 correlation slope thus flattens with increasing entry of air masses originating from southern and eastern Asia.~~T~~ Knowing that both species have similar sinks and photochemical lifetimes but $CHCl_3$ has a larger fraction of emissions from biogenic sources than CH_2Cl_2, this suggests larger $CHCl_3$:CH_2Cl_2 emission ratios in the region of the central and western ITCZ region (with presumably mostly biogenic sources) than in southern and eastern Asia (where anthropogenic sources likely dominate).”

- Line 408: The ASMA pathway was also identified by Adcock et al. (2021) for CH2Cl2.

We partly agree on this point. In this paragraph we highlight the transport pathway from Asia via the ASM including eastward outflow of the ASMA into the Ex-LS derived from observations above western Europe/Atlantic. Adcock et al. (2021) present a transport pathway into the LS based on measurements within the ASMA (StratoClim 2017) and observations of westward ASMA outflow (without back-trajectory analysis) above eastern Europe and the Mediterranean (StratoClim 2016). We do not argue the point that the observations by Adcock et al. (2021) are an important contribution to observational studies regarding Cl-VSLS transport into the LS by the ASMA (and we refer to the paper elsewhere in our manuscript) but quoting their paper at line 508 would be inaccurate to the content of this paragraph.

Response to the comments of Referee #2 on the paper

In situ observations of CH_2Cl_2 and $CHCl_3$ show efficient transport pathways for very short-lived species into the lower stratosphere via the Asian and North American summer monsoons

by V. Lauther et al.

We thank Referee #2 for the thorough reading of and the very helpful remarks on our manuscript. The comments have been considered carefully while revising the draft and resulting modifications are addressed point-py-point in the following (Referee's comments are cited in bold face):

General comments:

Introduction p2-3: To me there seemed to be a lot of detail here about the overall significance of the CL-VSLS, and about sources. This is important, of course, but it does not all seem to be essential to this paper. The key points, for this paper, are the general geographical characterisation for the source regions of the different species being considered. The reader would be able to focus more effectively on the major points of this paper if some of the detail was removed.

We agree. A similar remark was made by Reviewer #1 and we reduced the information given in the introduction to focus on the most essential details about Cl-VSLS. For details, we refer to the track change version of the manuscript.

p10-11: I think that it is a bit confusing to refer to the 'lower branch of the correlation' for the CH2Cl2-N2O relationship. It looks as though there are large number of parcels for which the N2O values are around 330ppb but the CH2Cl2 values are distributed across the range 30-45ppt. I think that in some ways it weakens your case if you call something a correlation when by conventional measures the correlation is rather weak. I am not disputing the fact that there are two 'families' in the plot at high N2O values – but can you find a more neutral term to describe them?

We agree that our use of the term "correlation" is rather based on lab jargon than on mathematics. We now use the general and more precise wording of a "CH_2Cl_2-N_2O relationship" instead of "CH_2Cl_2-N_2O correlation" if "correlation" is not specifically meant. We thus refer now to the "lower branch of the CH_2Cl_2-N_2O relationship" to describe the values of particularly low CH_2Cl_2 mixing ratios at high N_2O mixing ratios (similar for the upper branch). These modifications are made throughout the manuscript and for details we refer to the track change version of it.

p12: A similar comment applies to this approach of fitting a 'mean correlation curve' and using that as a basis for separating the upper and lower branches. The quadratic fit might be intended to seem quantitative – but there is really no reason to believe that the extrapolated values have any concrete relevance to the concentrations of CH2Cl2 measured in high N2O concentration parcels – the split between the two categories is essentially being made on the basis of the appearance of the plot. It seems very reasonable to make the split – but if the authors (or the readers) felt that it was more justifiable on the basis of a quadratic fit and an extrapolation then I would say that they were confused.

It is true, the split between the two categories of data was made on the basis of the appearance of the CH_2Cl_2-N_2O relationship and we do not claim otherwise. In order to decide on the "geometry" of the split we used the 'mean correlation curve' as a best-guess proxy of the annual mean CH_2Cl_2-N_2O relationship. Other methods can be thought of to realize a similar split of the data set. We changed the extrapolation of the shown 'mean correlation curve' in Figure 5 to a dashed line to reduce a possible misunderstanding about the origin of this curve.

p21: At this stage in the paper you use the term 'convective transport' quite frequently and in association with trajectories/CLaMS. I think that you should be a bit clearer about what transport is included in trajectories/CLaMS – which I believe is simply that in the ERA-I velocity fields, i.e. there is no inclusion of convective transport by parametrisation. I suspect that ERA-I velocities tend to be rapidly upward in regions of large-scale convection – and that serves as some kind of representation of convective transport, but it is unlikely that upward velocities are quantitatively correct. Certainly this sort of interpretation has been made by many authors who have used trajectory-based approaches, including myself, and I would not quarrel with it – but I do think that it needs to be clearly stated. The uncertainty perhaps becomes a bit more serious when considering tropical cyclones. How well is vertical transport in tropical cyclones represented by something like ERA-I? One imagines that maximum vertical velocities are significantly underestimated – but it could be, for example, that vertical transport is distributed over too large a region. You may not be able to resolve this uncertainty, but I think that you should at least say that it exists.

Many thanks for this helpful comment and we confirm that in CLaMS as used here there is no inclusion of convective transport by parametrisation. We added the following text to Sect. 2.3.

" In CLaMS, the diabatic approach was applied using the diabatic heating rate as the vertical velocity with contributions from radiative heating including the effects of clouds, latent heat release, mixing, and diffusion (for details, see Ploeger et al., 2010). CLaMS employs a hybrid vertical coordinate (ζ) which, in this study, transforms from a strictly isentropic coordinate (Θ) to a pressure-based orography-following coordinate system (σ coordinates) below a threshold of approximately 300 hPa(Pommrich et al., 2014). In both three-dimensional simulations as well as in trajectory calculations, the upward transport in CLaMS is driven by ERA-Interim reanalysis data in which changes are implemented to improve deep and mid-level convection compared to previous reanalysis data (Dee et al., 2011). However small-scale rapid uplift in convective cores is not included, therefore small-scale convection is most likely underestimated in CLaMS simulations driven by ERA-Interim. Nevertheless, upward transport in larger convective systems such as tropical cyclones is represented in CLaMS trajectory calculations driven by ERA-Interim (Li et al., 2017, 2020)."

CLaMS trajectory calculations using ECMWF's next-generation reanalysis ERA5 (Hersbach et al., 2020), demonstrate that diabatic trajectory calculations using ERA5 show much faster and stronger vertical transport than ERA-Interim primarily because of ERA5's higher spatial and temporal resolution, which likely resolves convective events more accurately (Li et al., 2020). Nonetheless, Li et al. (2020) demonstrate that the large scale convective uplift as represented in ERA-Interim does represent well the large scale uplift in convective systems.

Detailed comments:

l126: 'last accessed' info not needed in citation?

The last accessed info is now removed in the main text.

l164: 'essential' would be better than 'mandatory'. ('Mandatory' means 'required by some rule or regulation'.)

Good point, we changed "mandatory" to "essential".

l210-215: I found these sentences confusing. What is the distinction between 'pure CLaMS back trajectories', 'pure CLaMS trajectories' and 'back trajectories'? There seem to be two separate issues here – 'forward vs backward' and 'with CLaMS mixing vs without CLaMS mixing'.

We agree that this section was written a bit confusing and changed the text as follows:

“To support the interpretation of airborne measurements we use global three-dimensional simulations of the Chemical Lagrangian Model of the Stratosphere (CLaMS; McKenna, 2002a,b; Pommrich et al., 2014) as well as~~ pure~~ CLaMS back-trajectory calculations.~~ Pure~~ CLaMS back-trajectory calculations consider only the advective (reversible) transport, neglecting (irreversible) mixing processes entirely (e.g., Vogel et al., 2019; Hanumanthu et al., 2020).”

l221: ’lapsrate’ should be ’lapse rate’.

Thanks, it is corrected in the text now.

l239-240: This seems to repeat some information on back trajectories what has been given early (which potentially causes more confusion – ’is this intended to be subtly different to what has been said previously’).

No, it should not be different. We agree and removed in the revision in Section 2.3.2 the confusing statements. For details, we refer to the track change version of the manuscript.

l241: ’The spatial uncertainty of calculated back-trajectories increases with time because mixing processes occurring during transport are neglected’ – the uncertainty doesn’t just result from neglect mixing processes – the nature of chaotic advection is such that e.g. small errors in velocity fields convert into increasingly large errors in particle position. The idea that one could accurately calculate a trajectory for, e.g. 50 days, simply doesn’t make sense (whether or not one accounts for mixing). The key point for back-trajectory calculations on this sort of time scale is that ensembles of particles are used – so one is essentially calculation probabilities of location of origin rather than ’the’ location of origin’.

We agree and changed the respective text in Section 2.3.2 as follows:

“~~The spatial uncertainty of calculated back-trajectories increases with time because mixing processes occurring during transport are neglected. However, the back-trajectory analysis is used here in a statistical way (ensembles of about 100 to 200 trajectories) and not to consider single trajectories. In addition, t~~In general, trajectory calculations have limitations caused by trajectory dispersion increasing with the trajectory length, therefore ensembles of trajectories (of about 100 to 200 trajectories) are used here.”

l250: ’Thereby mainly air parcels of ... branch are from below the thermal TP’ – do you mean this – i.e. that most of the parcels from below the thermal tropopause are from the lower branch, or do you mean something slightly different, that most of the parcels from the lower branch are from below the thermal tropopause – in which case the ’mainly’ should before ’from below’.

Actually both versions are true. However, we wrote the sentence as intended thus no corrections are made here.

Figure 15: You use the term ’convective updraft’ in this Figure. There seems to be potentially an unfortunate confusion with the use of ’updrafts’ and ’downdrafts’ as description of rather small-scale features (perhaps 1km) of convective clouds. ’Convective transport’ might be a better term (and a better fit to the fact that, as noted above, your model calculations are incorporating some kind of global re-analysis scale representation of large-scale transport by convective systems.

Many thanks for this interesting remark! The labeling in Figure 15 is updated now as suggested.

In situ observations of CH_2Cl_2 and $CHCl_3$ show efficient transport pathways for very short-lived species into the lower stratosphere via the Asian and the North American summer monsoon~~s~~

Valentin Lauther[1], Bärbel Vogel[2], Johannes Wintel[1,a], Andrea Rau[1], Peter Hoor[3], Vera Bense[3],
Rolf Müller[2], and C. Michael Volk[1]

[1]Institute for Atmospheric and Environmental Research, University of Wuppertal, Wuppertal, Germany
[2]Forschungszentrum Jülich, Institute of Energy and Climate Research – Stratosphere (IEK-7), Jülich, Germany
[3]Institute for Atmospheric Physics, Johannes Gutenberg University, Mainz, Germany
[a]now at: Elementar GmbH, Langenselbold, Germany

Correspondence: Valentin Lauther (lauther@uni-wuppertal.de)

Abstract.

Efficient transport pathways for ozone depleting very short-lived substances (VSLS) from their source regions into the stratosphere are a matter of current scientific debate, however they have yet to be fully identified on an observational basis. Understanding the increasing impact of chlorine containing VSLS (Cl-VSLS) on stratospheric ozone depletion is important in order to validate and improve model simulations and future predictions. We report on~~ the first~~ a transport study using airborne in situ measurements of the Cl-VSLS dichloromethane (CH_2Cl_2) and trichloromethane (chloroform, $CHCl_3$) to derive a detailed description of~~ the~~ two~~ most efficient and fast~~ transport pathways from (sub-)tropical source regions into the extratropical lower stratosphere and upper troposphere (Ex-UTLS) in northern hemisphere (NH) late summer. The Cl-VSLS measurements were obtained in the ~~upper troposphere and lower stratosphere (~~UTLS~~)~~ above Western Europe and the mid latitude Atlantic Ocean in the frame of the WISE (Wave-driven ISentropic Exchange) aircraft campaign in autumn 2017 and are combined with the results from a three-dimensional simulation of a Lagrangian transport model as well as back-trajectory calculations. Compared to background measurements of similar age we find up to 150 % enhanced CH_2Cl_2 and up to 100 % enhanced $CHCl_3$ mixing ratios in the Ex-LS. We link the measurements of enhanced CH_2Cl_2 and $CHCl_3$ mixing ratios to emissions in the region of southern and eastern Asia. Transport from this area to the Ex-LS at potential temperatures in the range of 370 – 400 K takes about ~~5 – 10~~6 – 11 weeks via the Asian summer monsoon anticyclone (ASMA). Our measurements suggest anthropogenic sources to be the cause of these strongly elevated Cl-VSLS concentrations observed at the top of the lowermost stratosphere (LMS). A faster transport pathway into the Ex-LS is derived from particularly low CH_2Cl_2 and $CHCl_3$ mixing ratios in the UTLS. These low mixing ratios reflect weak emissions~~ sources~~ and a local seasonal minimum of both species in the boundary layer of Central America and the tropical Atlantic. We show that air masses uplifted by hurricanes, the North American monsoon, and general convection above Central America into the tropical tropopause layer to potential temperatures of about 360 – 370 K are transported isentropically within ~~1 – 5~~5 – 9 weeks from the boundary layer into the Ex-LS. This transport pathway linked to the North American monsoon mainly impacts the middle and lower part of the LMS with particularly low

CH_2Cl_2 and $CHCl_3$ mixing ratios. In a case study, we specifically analyze air samples directly linked to the uplift by the category 5 hurricane Maria that occurred during October 2017 above the Atlantic Ocean. ~~Regionally differing $CHCl_3$:CH_2Cl_2 emission ratios derived from our UTLS measurements suggest a clear similarity between $CHCl_3$ and CH_2Cl_2 when emitted by anthropogenic sources and differences between the two species mainly caused by additional, likely biogenic, $CHCl_3$ sources.~~ CH_2Cl_2 and $CHCl_3$ have similar atmospheric sinks and lifetimes but the fraction of biogenic emissions is clearly higher for $CHCl_3$ than for the mainly anthropogenically emitted CH_2Cl_2, consequently lower $CHCl_3$:CH_2Cl_2 ratios are expected in air parcels showing a higher impact of anthropogenic emissions. The observed $CHCl_3$:CH_2Cl_2 ratio suggests clearly stronger anthropogenic emissions in the region of southern and eastern Asia compared to those in the region of Central America and the tropical Atlantic. Overall, the transport of strongly enhanced CH_2Cl_2 and $CHCl_3$ mixing ratios from southern and eastern Asia via the ASMA is the main factor for increasing the chlorine loading from the analyzed VSLS in the Ex-LS during NH late summer. Thus, further increases in Asian CH_2Cl_2 and $CHCl_3$ emissions, as frequently reported in recent years, will further increase the impact of Cl-VSLS on stratospheric ozone depletion.

Copyright statement.

1 Introduction

Within the last two decades emissions of the chlorine containing very short-lived substances (Cl-VSLS) dichloromethane (CH_2Cl_2) and trichloromethane (chloroform, $CHCl_3$) increased significantly by about 8 %/year (Hossaini et al., 2015) and 3.5 %/year (Fang et al., 2018), respectively. With both Cl-VSLS not being regulated by the Montreal Protocol on Substances that Deplete the Ozone Layer and its amendments and adjustments their influence on stratospheric ozone depletion is currently an important topic of investigation. ~~Due~~Owing to the sparseness of Cl-VSLS measurements in the stratosphere (e.g., Schauffler et al., 1993, 2003; Laube et al., 2008; Park et al., 2010; Adcock et al., 2021) the impact of changes in Cl-VSLS surface emissions on their distribution in the stratosphere has yet to be fully characterized on an observational basis. Particularly important is the identification of rapid and efficient transport pathways for Cl-VSLS from their source regions into the stratosphere. ~~T~~In the present study~~ is the first to~~ we use airborne in situ measurements of CH_2Cl_2 and $CHCl_3$ in the extratropical upper troposphere and lower stratosphere (Ex-UTLS) to analyze the impact of different source regions onto the stratospheric chemical composition and to identify transport pathways of CH_2Cl_2 and $CHCl_3$ into the stratosphere.

CH_2Cl_2 is almost exclusively emitted by anthropogenic sources with only about 10 % of its emission being of natural origin (Engel et al., 2018). Thereby CH_2Cl_2 mixing ratios in the troposphere at northern hemisphere (NH) mid latitudes are by a factor of three larger than those in the southern hemisphere (Hossaini et al., 2017). Global CH_2Cl_2 emissions in 2017 are estimated to be about 1 (Tg Cl)/year ~~(Claxton et al., 2020) which is even higher than emissions of CFC-11 at its emission peak in 1986 with about 0.3 (Tg Cl)/year~~ (Daniel et al., 2007, however, CFC-11 is practically inert in the troposphere, which is not the case for CH_2Cl_2)~~. A~~ and almost 90 % of the global CH_2Cl_2 emission sources are located in Asia (Claxton et al., 2020). Other, more localized studies, estimate that about 10 % of global CH_2Cl_2 emissions originate in India (Say et al., 2019) and that 25 − 37 % (Feng et al., 2018) or even 45 % (Oram et al., 2017) of global CH_2Cl_2 emissions originate in China. Collected air samples from IAGOS-CARIBIC confirm particularly high emissions in the broad region of southern and eastern Asia (Leedham-Elvidge et al., 2015) as similarly shown for the north Indian subcontinent from air sampled during the StratoClim aircraft campaign in summer 2017 (Adcock et al., 2021). European and American CH_2Cl_2 sources in 2017 were estimated to contribute less than 10 % to the global CH_2Cl_2 emissions (Claxton et al., 2020).

Based on ~~AGAGE~~ ground-based measurements from the AGAGE network Engel et al. (2018) estimate the global $CHCl_3$ emissions in 2017 to be about 0.29 (Tg Cl)/year. Compared to CH_2Cl_2 the distribution of $CHCl_3$ emission sources is rather unclear. On global average Engel et al. (2018) estimate $CHCl_3$ emissions from anthropogenic sources to be equally high as from biogenic sources. However, emission estimates of anthropogenic $CHCl_3$ sources range between 60 % (Trudinger et al., 2004), 30 % (Worton et al., 2006), and 10 % (McCulloch, 2003) of the total emissions. While CH_2Cl_2 is believed to have no significant oceanic sources and is only temporarily taken up by the oceans to be re-released to the atmosphere later, a process that is not yet fully understood (Moore, 2004), $CHCl_3$ is estimated to have about 50 % of its biogenic emission sources located in offshore seawater (Laturnus et al., 2002; McCulloch, 2003). The increase in global $CHCl_3$ emissions during the last decade was traced back entirely to an increase in eastern Chinese $CHCl_3$ emissions of most likely anthropogenic origin (Fang et al., 2018). In addition, Chinese $CHCl_3$ emissions amount to almost 90 % of all East Asian $CHCl_3$ emissions (Fang et al., 2018). Nevertheless, on a global scale $CHCl_3$ has a significant fraction of biogenic emission sources in contrast to CH_2Cl_2 which is almost exclusively emitted by anthropogenic sources.

~~Anthropogenic emissions of CH_2Cl_2 and $CHCl_3$ partly arise from the non-chemical industry like pulp and paper manufacture and water treatment, as well as from the chemical and pharmaceutical industry (Aucott et al., 1999; McCulloch, 2003). Both CH_2Cl_2 and $CHCl_3$ are the main co-products needed for any manufacturing process of chloromethanes. CH_2Cl_2 is also strongly used in the production of the hydrofluorocarbon HFC-32 (Chipperfield et al., 2020). The fraction of produced CH_2Cl_2 and $CHCl_3$ used as feedstock to manufacture other halogens is not further released into the atmosphere. This fraction has been estimated for $CHCl_3$ to be over 95 % (McCulloch, 2003; Chipperfield et al., 2020) but only 15 % for CH_2Cl_2~~ (Chipperfield et al., 2020)~~. The remaining fraction not used as feedstock for the production of other halogens (about 5 % of $CHCl_3$; about 85 % of CH_2Cl_2) is emitted into the atmosphere in form of chemical solvent, paint stripper, and degreasing agent~~ (McCulloch and Midgley, 1996; Montzka et al., 2011)~~ as well as through foam blowing and agricultural fumigation (Oram et al., 2017).~~

~~While CH_2Cl_2 is believed to have no significant oceanic sources and is only temporarily taken up by the oceans to be re-released to the atmosphere later, a process that is not yet fully understood (Moore, 2004), $CHCl_3$ is estimated to have about 50 % of its biogenic emission sources located in offshore seawater (Laturnus et al., 2002; McCulloch, 2003). Biomass burning was reported to play a significant role in CH_2Cl_2 emissions (Rudolph et al., 1995) but more recent studies could not confirm that finding (Simmonds et al., 2006; Simpson et al., 2011; Leedham-Elvidge et al., 2015). In contrast, biomass burning was observed to be a small but significant $CHCl_3$ emission source~~ (Rudolph et al., 1995; Scheeren et al., 2002; Bourtsoukidis et al., 2017).

For CH_2Cl_2 Hossaini et al. (2019) suggest an average tropospheric lifetime of 168 days (about 6 months) and a stratospheric lifetime of $1-2$ years (outside the poles) was estimated by Hossaini et al. (2017). The main atmospheric sink of both CH_2Cl_2 and $CHCl_3$ is the reaction with hydroxyl radicals (OH) in the troposphere. Both species have similar reaction rates with OH implying similar photochemical lifetimes for both Cl-VSLS (Hsu and DeMore, 1994). Time series of background mixing ratios of both species are anticorrelated to the seasonal cycle of OH (Cox et al., 2003). In the NH seasonal anthropogenic use of products releasing $CHCl_3$ to the atmosphere (e.g., landfill and chlorination of water) have been observed to have a small local impact on the seasonality of $CHCl_3$ (Gentner et al., 2010). In addition, the global distribution of OH shows significant regional differences (Spivakovsky et al., 2000; Hanisco et al., 2001; Lelieveld et al., 2016). Therefore, also the photochemical lifetimes of CH_2Cl_2 and $CHCl_3$ are regionally different. ~~For CH_2Cl_2 Hossaini et al. (2019) suggest an average tropospheric lifetime of 168 days (about 6 months) and a stratospheric lifetime of $1-2$ years (outside the poles) was estimated by Hossaini et al. (2017). Both species have similar reaction rates with OH implying similar photochemical lifetimes for both Cl-VSLS (Hsu and DeMore, 1994).~~

In the tropical tropopause layer (TTL) the lifetime of both CH_2Cl_2 and $CHCl_3$ is estimated to be about $6-10$ months, being long enough for both Cl-VSLS to enter the stratosphere under normal dynamic conditions (Park et al., 2010). For the level of zero radiative heating Hossaini et al. (2015) simulated an increase in average CH_2Cl_2 mixing ratios of about 83 % between 2005 and 2013. Hossaini et al. (2019) estimate an increase of total stratospheric chlorine from Cl-VSLS from about 69 ppt in 2000 to about 111 ppt in 2017 of which $> 80\,\%$ enter the stratosphere as source gases and the rest as product gases of Cl-VSLS. Hossaini et al. (2019) further state that CH_2Cl_2 and $CHCl_3$ contribute with about 68 % and 19 % to this increase, respectively. However, due to high Asian emissions and an efficient transport into the stratosphere via the Asian summer monsoon (ASM), the estimation of stratospheric chlorine from Cl-VSLS could even be underestimated by $8-26\,\%$ (Adcock et al., 2021).

Between June and September the ASM is a wide spread convective system located above the Indian subcontinent, East and Southeast Asia (e.g., Yihui and Chan, 2005). The ASM provides fast vertical transport of surface air into the large scale anticyclone (ASMA) above, which spans from the upper troposphere at about 360 K potential temperature to the lower stratosphere at about 450 K potential temperature (e.g., Park et al., 2007, 2009; Bergman et al., 2013; Vogel et al., 2019). Within the ASMA air masses are somewhat confined and separated from the surrounding UTLS air by a strong gradient of potential vorticity (e.g., Ploeger et al., 2015). Several studies have shown that these air masses are transported further vertically into the tropical pipe or break out of the ASMA to enter the extratropical lowermost stratosphere (LMS) quasi-horizontally by Rossby wave breaking events (e.g., Popovic and Plumb, 2001; Garny and Randel, 2016; Vogel et al., 2014, 2016). Thus, the ASM has a strong impact on the chemical composition of the stratosphere in boreal summer (e.g., Randel et al., 2010; Randel and Jensen, 2013; Vogel et al., 2015; Santee et al., 2017).

~~The specific transport pathways of Cl-VSLS from their source regions into the stratosphere have not been identified on an observational basis.~~ The most efficient transport pathway for Cl-VSLS into the stratosphere is suggested to be via the ASMA. This is why Cl-VSLS emissions from the region of continental Asia are suggested to have the highest ozone depletion potential (ODP) compared to emissions from other source regions (Claxton et al., 2019). ~~Their regionally dependent ODP is estimated to be in the range of $0.0097-0.0208$ (CH_2Cl_2) and $0.0143-0.0264$ ($CHCl_3$)~~ (for comparison here the ODPs of some other chlorocarbons: CFC-11: 1; CCl_4: 0.87; HCFC-22: 0.034; CH_3Cl: 0.015; Carpenter et al., 2018; Claxton et al., 2019). Projecting different past CH_2Cl_2 emission rates Hossaini et al. (2017) predict a possibly significant delay of the recovery date of stratospheric ozone ranging from a few years up to no recovery at all compared to estimations including only long-lived chlorinated species. ~~They also found a doubling of southern hemispheric spring time ozone loss caused by CH_2Cl_2 between 2010 and 2016. Their study emphasizes the importance of studying Cl-VSLS on a regular observational basis.~~ However, the estimated impact of Cl-VSLS on stratospheric ozone trends is small compared to that of long-lived chlorinated species or even the impact of meteorology or the 11-year solar cycle (Chipperfield et al., 2018). Nevertheless, with the expected decrease of long-lived chlorinated trace gases during the next decades due to the Montreal Protocol and its amendments and adjustments the relative importance of Cl-VSLS on stratospheric ozone depletion will further increase.

Observational evidence for Cl-VSLS being transported into the stratosphere is extremely rare ~~and their main transport pathways into the stratosphere have not been described on an observational basis~~ (e.g., Schauffler et al., 1993; Woodbridge et al., 1995; Schauffler et al., 2003; Laube et al., 2008; Park et al., 2010; Adcock et al., 2021). Transport pathways into the stratosphere for VSLS have been derived from observations of bominated VSLS (Br-VSLS; e.g., Sturges et al., 2000; Ashfold et al., 2012; Wales et al., 2018; Filus et al., 2020; Keber et al., 2020; Rotermund et al., 2021) or modeled specifically for Br-VSLS (e.g., Levine et al., 2007; Aschmann et al., 2009; Ashfold et al., 2012; Liang et al., 2014) which have mainly natural emission sources (Engel et al., 2018). However, the only Br-VSLS with a photochemical lifetime comparable to those of CH_2Cl_2 and $CHCl_3$ is CH_2Br_2 (150 days; WMO, 2018) which is mostly emitted by the oceans and, consequently, is differently distributed in the troposphere than the mainly anthropogenically (land-based) emitted CH_2Cl_2 and most Cl-VSLS (e.g., Engel et al., 2018). Thus, transport studies of Br-VSLS focus on transport into the stratosphere from likely different source regions than those of Cl-VSLS and their results might not necessarily be directly applicable to the transport into the stratosphere of CH_2Cl_2 and $CHCl_3$. In addition, in order to specifically study transport into the stratosphere via the ASM it is beneficial to observe VSLS with their strongest sources being located in the core region of the ASM. This is the case for CH_2Cl_2 while most Asian Br-VSLS sources are located only in adjacent regions of the ASM.

In the present paper we use in situ measurements of CH_2Cl_2 and $CHCl_3$ to identify two efficient transport pathways ~~for Cl-VSLS~~ from the boundary layer into the extratropical lower stratosphere (Ex-LS). In addition we provide observational evidence for different impacts on the stratospheric chemical composition depending on the transport pathway the two Cl-VSLS take to enter the Ex-LS in NH late summer. A study by Rotermund et al. (2021) employed similar methods to identify source regions and the impact on the Ex-LS of Br-VSLS using measurements from the same aircraft campaign as the measurements used in the present paper and is compared to our results in Section 4.

2 Airborne observations and model simulations

2.1 The WISE campaign 2017

All measurements presented in this study were obtained in the frame of the WISE (Wave-driven Isentropic Exchange) campaign ~~(Riese et al., 2017, last accessed: 2021-01-14)~~(Riese et al., 2017) which took place in September and October 2017. A total of 15 scientific flights were carried out with the German HALO (High Altitude and LOng range) research aircraft mainly from Shannon (Ireland) and from Oberpfaffenhofen (Germany) probing a wide area above the Atlantic Ocean and Western Europe. Among other goals, the WISE campaign aimed at investigating transport and mixing processes in the extratropical tropopause layer and the Ex-LS, the impact of the Asian monsoon system on the chemical composition of the extratropical ~~lowermost stratosphere (~~LMS~~)~~, as well as the role of halogenated VSLS for ozone depletion and radiative forcing in the ~~upper troposphere/lower stratosphere (~~UTLS~~)~~ region. In this study we present UTLS measurements ~~up to~~between a potential temperature of 315 K and 404 K (i.e., 7.4 – 14.5 km altitude; 388 – 130 hPa pressure) of the last ten WISE flights, i.e., from 28 September to 21 October 2017 (Figure 1). Due to technical issues of the instrument, CH_2Cl_2 and $CHCl_3$ measurements below the given range and during earlier flights of the WISE campaign were not performed (cf. Section 2.2.1).

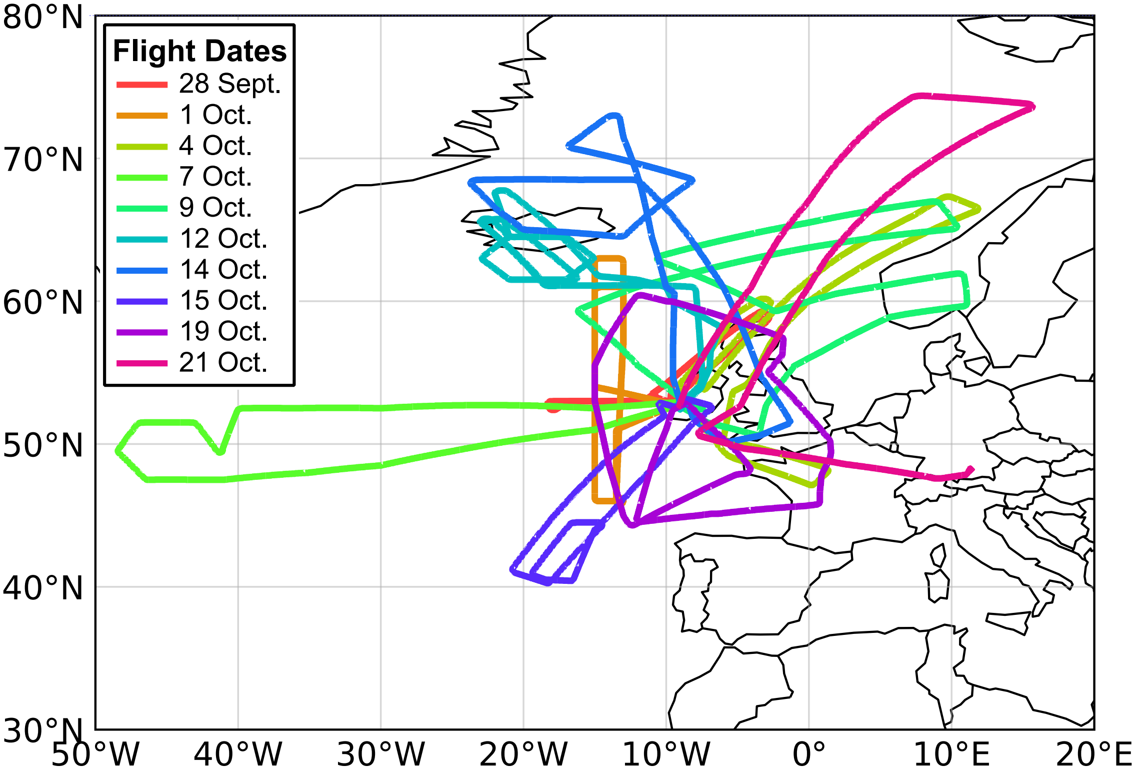

Figure 1. Map of ten flight tracks carried out with the German HALO (High Altitude and LOng range) research aircraft from and to Shannon (Ireland) with one flight from Shannon to Oberpfaffenhofen (Germany). The flights were conducted from 28 September to 21 October in 2017 in the frame of the WISE campaign (details see text).

2.2 In situ trace gas measurements

Our analysis is mainly based on airborne in situ observations of the trace gas instruments HAGAR-V (CH_2Cl_2 and $CHCl_3$) and UMAQS (N_2O) (as described below). The corresponding avionic data is provided by the Basic HALO Measurement and

Sensor System (BAHAMAS) (Krautstrunk and Giez, 2012; Giez et al., 2017). The different measurement frequencies of the instruments were matched to that of HAGAR-V's MS module of $1/180$ Hz. Exceptions are the flights on 28 September and 1 October where the MS measurement frequency is $1/240$ Hz. Each data point is the average of a time interval of 40 s, except for the flights on 28 September, 1 October, and 4 October where it is 60 s, corresponding to a spatial resolution at maximum cruising speed of 10 km and 15 km along the flight path, respectively. The used time and location of a data point is the respective center of the averaged time interval.

2.2.1 High Altitude Gas AnalyzeR - 5 channel version (HAGAR-V)

HAGAR-V is a novel airborne in situ instrument. It is a modernized and largely extended version of the airborne in situ instrument HAGAR (Werner et al., 2010) and is mounted in a HALO standard rack (R-G550SM). Similar to HAGAR, HAGAR-V comprises a two-channel gas chromatograph with electron capture detection (GC/ECD) as well as a non dispersive infrared absorption module for the detection of CO_2 (LI-COR 7000). In contrast to HAGAR, HAGAR-V additionally comprises a mass spectrometer (MS) coupled to two GC channels by a two-position valve which allows to switch between the two channels. This novel MS module can thus be used either for the detection of a wide range of atmospheric trace gases (different target species on each channel) or to double the measurement frequency (same target species on both channels). However, during WISE only one of the two GC/MS channels was used, measuring nine different species (CH_2Cl_2, $CHCl_3$, CH_3Cl, CFC-11, CFC-113, HFC-125, HFC-134a, iso-, and n-Pentane). In this study, the focus is on CH_2Cl_2 and $CHCl_3$ measurements by HAGAR-V's novel MS module, thus the instrumental description is confined only to the GC/MS part of the instrument. A more detailed description of HAGAR-V is given by Lauther (2020).

The general MS sampling process during WISE was as follows: Ambient air is drawn from outside the aircraft to the instrument and is further compressed to 3 bar (a) by two diaphragm pumps (KNF 813.5 and 814) connected in series. The sample passes through a preconcentration tube packed with about 70 mg Carboxen 572 (Supelco) at 20 °C to adsorb the target species. At a usual adsorption time of 40 s the preconcentrated sample volume is about 130 ml. Afterwards the sample is desorbed by flash heating the trap to about 270 °C and injected on to the separation columns by applying a helium carrier gas flow. The sampled species are separated within two 0.25 mm J&W Scientific Al_2O_3/Na_2SO_4 PLOT capillary columns of 4 m and 5 m length (pre- and main-column, respectively). Both columns are temperature controlled changing from initial 35 °C to final 160 °C in 20 s (pre-column) and 35 s (main-column), providing two sample refocusing steps in the process. The sample is detected by a quadrupole MS detector (5975C, Agilent Technologies) using electron ionization (EI) mode.

Fast GC/MS measurements are ~~mandatory~~essential when operating from aboard an aircraft. To achieve a sample frequency of $1/180$ Hz per MS channel particularly the heating and cooling rates of the preconcentration traps and the columns were optimized during the MS module development process. Both units are self built, keeping the design and the application as adaptable as possible.

The cooling of the preconcentration traps is realized by a Stirling cooler (Twinbird, SC-UD08) and each trap is heated by a self regulating Ni heating wire (which is also used as temperature sensor) convoluted around the trap tube. To our knowledge, HAGAR-V is the only state-of-the-art airborne GC/MS instrument using indirect trap heating and our thermodesorption design provides consistent heating and cooling rates of 80 °C s^{-1} and −25 °C s^{-1} (from 270 °C down to 20 °C) inside the trap tube. In addition, our thermodesorption concept avoids large variable currents at relatively low voltages (peak current < 7 A at 48 V for < 2 s, then < 2 A) and is thus well suited to be used aboard an aircraft with stringent constraints regarding electromagnetic compatibility.

The self built separation column ovens are conceptually comparable to the principles of regular modern Low Thermal Mass capillary column systems (e.g., Luong et al., 2006). In parallel to the column a heating wire and a temperature sensor wire are coiled to a torus of 7 cm in diameter acquiring fast and homogenous heat application to the column (up to 20 °C s^{-1}) and temperature read-out. Deactivated capillary columns emerge from the torus functioning as connecting lines and particle traps to enhance the measurement stability. The cooling of the columns is realized by fans providing a setback from final to initial temperatures within 60 s.

Following the compression by the inlet pumps, usually the air sample is dehydrated because water vapor can strongly affect the reproducibility of MS measurements. However, during WISE the dehydration system of HAGAR-V was malfunctioning. ~~could not be used. Consequently,~~ For the last 10 WISE flights that system was bypassed and the MS module measured only at low ambient water vapor levels (mainly at H_2O < 100 ppm; median: 5.6 ppm), i.e., in the UTLS region~~. With this solution the MS module measured~~ thus yielding measurements during about 90% of a typical~~ WISE~~ flight's duration (i.e., about 7.6 h per flight). MS measurements of WISE flights before 28 September could not be used for analysis due to the malfunctioning sample dehydration unit.

HAGAR-V uses two different working standards for in-flight calibration to enhance the accuracy in case of non-linear system responses. Both working standards consist of compressed clean ambient air; one of them is additionally diluted with about 25 % synthetic air. The main bottles of the working standards were calibrated by the University of Frankfurt against a calibration gas that was calibrated in second generation against an AGAGE standard on the SIO-14 (CH_2Cl_2) and SIO-98 ($CHCl_3$) scale. Every second or third flight the in-flight calibration gas bottles were refilled from the main bottles after a calibration between main and flight bottles. Considering possible differences between main and flight bottles, uncertainties of the mixing ratios within the main bottles, as well as potential influence from HAGAR-V's inlet pump system, the MS relative accuracy was estimated to be 2.0 % and 4.4 % for CH_2Cl_2 and $CHCl_3$, respectively.

Measurement precisions were optimized during data processing, using a strongly adapted version of the IGOR Pro analysis package called NOAHChrom, originally developed by NOAA, USA. Exponentially modified Gaussian (EMG) functions were fitted to the MS signal peaks within individual time windows. Thereby peak tailing could be accurately treated and neighboring peaks were included in the background fit. In addition, the MS data were corrected for small system contamination and an occasional systematic measurement bias of one calibration gas. The measurement precision was derived for each flight from the standard deviation of one of the two in-flight calibration gases relative to its mixing ratio. The median precisions during WISE were 1.7 % (1 ppt) and 2.7 % (0.4 ppt) for CH_2Cl_2 and $CHCl_3$, respectively.

2.2.2 University of Mainz Airborne Quantum cascade Laser Spectrometer (UMAQS)

UMAQS simultaneously measures CO and N_2O from aboard HALO. The instrument uses the principle of direct absorption spectroscopy of a continuous-wave quantum cascade laser operating at a sweep rate of 2 kHz (Müller et al., 2015). In this study we use UMAQS' measurements of N_2O with a total drift-corrected uncertainty of 0.18 ppb (Kunkel et al., 2019). Note, for this study the N_2O measurements are averaged over $40-60$ s to fit the integration times of HAGAR-V's MS module, thereby smoothing out instrumental noise which most likely further improves the N_2O precision. The instrument is calibrated regularly in-flight using a secondary standard which is calibrated against a NOAA standard before and after the campaign. The accuracy of the used N_2O mixing ratios is 0.39 ppb.

2.3 CLaMS simulations

To support the interpretation of airborne measurements we use global three-dimensional simulations of the Chemical Lagrangian Model of the Stratosphere (CLaMS; McKenna, 2002a,b; Pommrich et al., 2014) as well as~~ pure~~ CLaMS back-trajectory calculations.~~ Pure~~ CLaMS back-trajectory calculations consider only the advective (reversible) transport, neglecting (irreversible) mixing processes entirely (e.g., Vogel et al., 2019; Hanumanthu et al., 2020). However, in this study back-trajectories are useful to trace back the detailed transport pathway and transport time of an air parcel in the UTLS to possible source regions in the boundary layer and therefore provide added value compared to three-dimensional CLaMS simulations including irreversible mixing. Both three-dimensional CLaMS simulations and back-trajectory calculations are driven by ECMWF ERA-Interim reanalysis data with a horizontal resolution of $1^\circ \times 1^\circ$ (Dee et al., 2011).~~ The irreversible part of transport was set to discrete mixing steps every 24 h in the three-dimensional CLaMS simulation~~

In CLaMS, the diabatic approach was applied using the diabatic heating rate as the vertical velocity with contributions from radiative heating including the effects of clouds, latent heat release, mixing, and diffusion (for details, see Ploeger et al., 2010). CLaMS employs a hybrid vertical coordinate (ζ) which, in this study, transforms from a strictly isentropic coordinate (Θ) to a pressure-based orography-following coordinate system (σ coordinates) below a threshold of approximately 300 hPa(Pommrich et al., 2014). In both three-dimensional simulations as well as in trajectory calculations, the upward transport in CLaMS is driven by ERA-Interim reanalysis data in which changes are implemented to improve deep and mid-level convection compared to previous reanalysis data (Dee et al., 2011). However small-scale rapid uplift in convective cores is not included, therefore small-scale convection is most likely underestimated in CLaMS simulations driven by ERA-Interim. Nevertheless, upward transport in larger convective systems such as tropical cyclones is represented in CLaMS trajectory calculations driven by ERA-Interim (Li et al., 2017, 2020). More detailed information about CLaMS is given by Pommrich et al. (2014) and references therein. Equivalent latitudes and the location of the thermal tropopause (lapse rate, according to WMO) along the flight path was calculated from ERA-Interim reanalysis data.

2.3.1 Artificial tracers of air mass origin

In this study CLaMS simulations of artificial tracers of air mass origin (also referred to as surface origin tracers, Ω_i; Vogel et al., 2015, 2016, 2019) are used to identify the location of the origin of air masses whose impact can be seen in the concentration data gathered during WISE. The surface origin tracers are released within 24 defined regions in the boundary layer ($\zeta = 120\,\mathrm{K} \sim 2-3\,\mathrm{km}$ above ground, including orography) as shown in Figure 2, top panel. The different surface origin tracers are continuously released (every $24\,\mathrm{h}$) at the model boundary and are subsequently transported (advected and mixed) to the free atmosphere during the course of the simulation. Here, the irreversible part of transport was set to discrete mixing steps every $24\,\mathrm{h}$. The simulation was initialized with the meteorological data from 1 May, 2017, implying that all air parcels residing in the free troposphere and the stratosphere at this date are not marked with the surface origin tracers. As a consequence, the fraction of all surface origin tracers ($\Omega = \sum_{i=1}^{n=24} \Omega_i$) of an air parcel can be $< 100\,\%$ during the course of the simulation because also air masses older than 1 May 2017 can contribute to the composition of an air parcel. In this study we examine short-lived species measured in October 2017 with the focus on relatively fast transport, therefore a simulation period of approximately $5-6$ months is chosen here. The used model simulation is spatially constrained from the surface to $\Theta = 900\,\mathrm{K}$ (about $37\,\mathrm{km}$ altitude) with a horizontal resolution of $100\,\mathrm{km}$ and a maximum vertical resolution of about $400\,\mathrm{m}$ (at the tropopause).

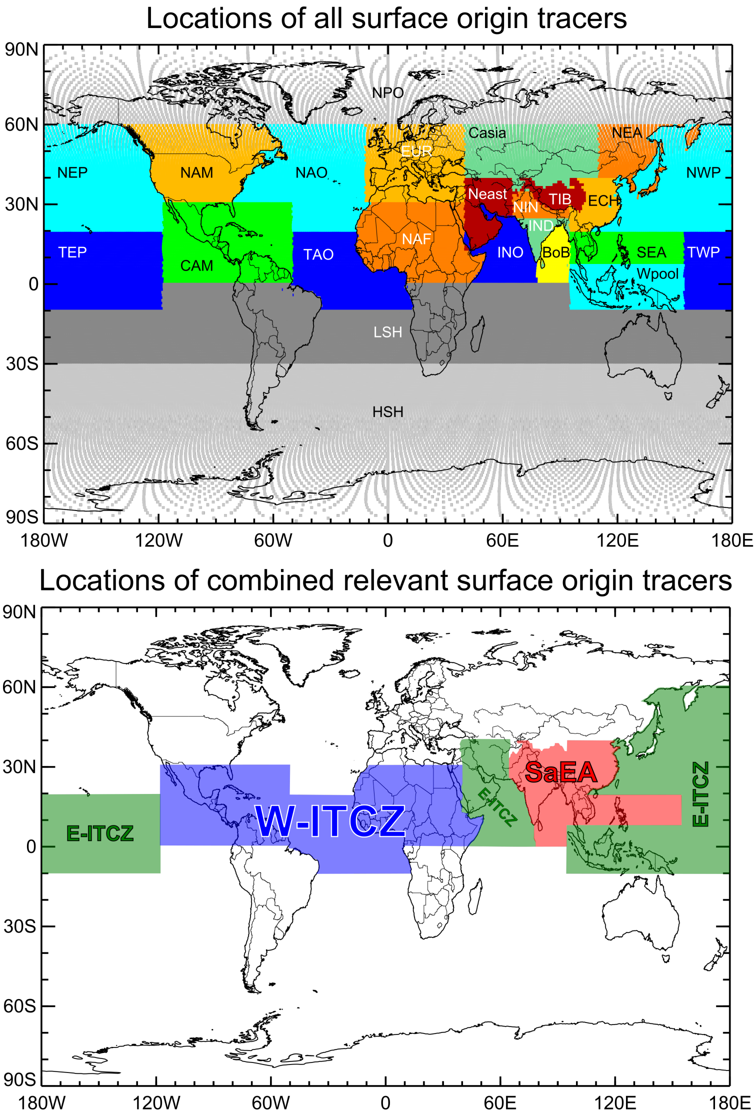

BoB	Bay of Bengal
CAM	Central America
Casia	Central Asia
ECH	Eastern China
EUR	Europe
HSH	High Southern Hemisphere
IND	Indian Subcontinent
INO	Indian Ocean
LSH	Lower Southern Hemisphere
NAF	Northern Africa
NAM	Northern America
NAO	Northern Atlantic Ocean
NEA	Northern Eastern Asia
Neast	Near East
NEP	Northern Eastern Pacific
NIN	Northern India / Pakistan / Himalayan foothills
NPO	North Polar Region
NWP	Northern Western Pacific
SEA	Southeast Asia
TAO	Tropical Atlantic Ocean
TEP	Tropical Eastern Pacific
TIB	Tibetan Plateau
TWP	Tropical Western Pacific
Wpool	Warm Pool
SaEA	BoB + ECH + IND + NIN + SEA + TIB
W-ITCZ	CAM + NAF + TAO
E-ITCZ	INO + Neast + NWP + TEP + TWP + Wpool

Figure 2. World map depicting the boundaries of CLaMS's 24 surface origin tracers (top) and three surface origin tracers combining several tracers from regions of significant (> 90 %) impact on the WISE measurements (bottom). The tracer names corresponding to their abbreviations are listed next to the maps. Also included in the list are the tracers of combined regions (cf. Section 3.1.2).

2.3.2 Back-trajectory calculations

In order to investigate the transport pathways corresponding to the WISE measurements analyzed here, the trajectory module of CLaMS was used to calculate back-trajectories. ~~Other than in the three-dimensional CLaMS simulation, trajectories are calculated using only the advective part of transport without mixing. The advantage is that a single pathway for each air parcel can be calculated and analyzed with the additional information of its transport time.~~ The back-trajectories are initialized at the time and location of the center of the respective MS sample integration time window and end at the first contact with the model boundary layer (below $2-3$ km above surface). In general, the maximum length of a trajectory is confined to 120 days, however most of the trajectories reach the model boundary layer much earlier.

~~The spatial uncertainty of calculated back-trajectories increases with time because mixing processes occurring during transport are neglected. However, the back-trajectory analysis is used here in a statistical way (ensembles of about 100 to 200 trajectories) and not to consider single trajectories. In addition, t~~In general, trajectory calculations have limitations caused by trajectory dispersion increasing with the trajectory length, therefore ensembles of trajectories (of about 100 to 200 trajectories) are used here. The maximum trajectory length of 120 days was chosen to match a large part of the time frame of the three-dimensional CLaMS simulation but the average length of the used back-trajectories is 50 days. We will show (in sections 3.1.2 and 3.1.3) that the results of the three-dimensional CLaMS simulation in which mixing of air parcels is included agrees very well with the results of the back-trajectory analysis.

3 Results

3.1 CH_2Cl_2-N_2O ~~correlation~~relationship during WISE

The analysis presented in this paper is mainly based on the CH_2Cl_2-N_2O ~~correlation~~relationship observed during WISE (Figure 3). With a photochemical lifetime of 123 years (Ko et al., 2013) N_2O is well mixed in the troposphere and has a much longer lifetime than CH_2Cl_2 which exhibits strongly varying mixing ratios throughout the boundary layer (e.g., Simmonds et al., 2006). As expected, the ~~correlation~~CH_2Cl_2-N_2O relationship is relatively compact for data points with low N_2O mixing ratios (i.e., $N_2O < 325$ ppb, relatively old, mixed and processed air). Towards younger air masses ($N_2O > 325$ ppb) there is a distinct split of the ~~correlation~~compact relationship into two branches. In the stratosphere, the upper branch of the CH_2Cl_2-N_2O ~~correlation~~relationship shows up to 150 % enhanced CH_2Cl_2 mixing ratios compared to data of the lower branch at the same N_2O mixing ratios. For $N_2O > 328.5$ ppb, data points with low CH_2Cl_2 mixing ratios even ~~anticorrelate~~decrease with increasing N_2O (Figure 3, inlay). In general, the majority of measurements was obtained in the stratosphere above the thermal tropopause (TP) with an increasing number of observations below the thermal TP for increasing N_2O mixing ratios. Thereby mainly air parcels of the lower branch of the CH_2Cl_2-N_2O ~~correlation~~relationship ~~branch~~ are from below the thermal TP.

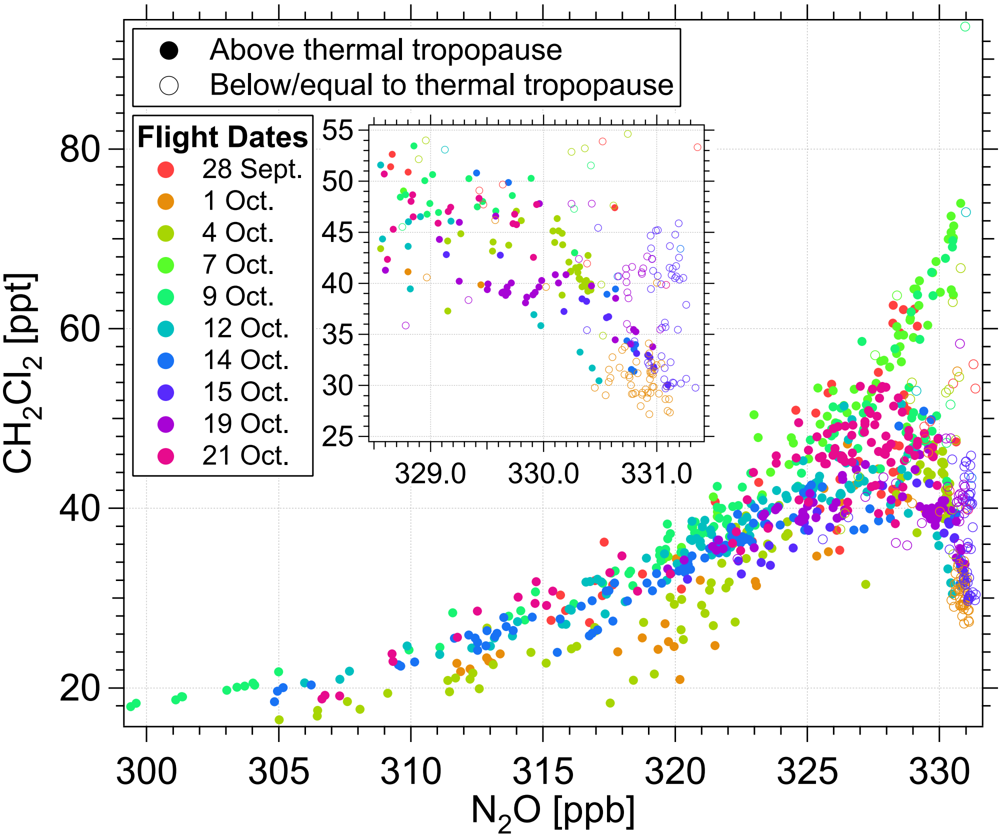

Figure 3. CH_2Cl_2-N_2O ~~correlation~~relationship color coded by flight date. The embedded figure shows a detailed magnification of ~~the anticorrelation~~decreasing CH_2Cl_2 mixing ratios with increasing N_2O within the lower branch of the CH_2Cl_2-N_2O relationship. Air parcels below the thermal tropopause are marked as open circles, air parcels above by closed circles.

The most frequent convection to potential temperatures on the order of 360 K is expected to originate in the tropics. Therefore, tropical monthly averaged ground-based ~~CH_2Cl_2~~ measurements of CH_2Cl_2 from the AGAGE network at Ragged Point, Barbados (Figure 4; Prinn et al., 2018) were analyzed. These AGAGE observations suggest an explanation for the lower branch of the CH_2Cl_2-N_2O ~~anticorrelation~~relationship observed during WISE. The mainly OH induced CH_2Cl_2 seasonality results in minimum tropical CH_2Cl_2 surface mixing ratios in September 2017. This September minimum is comparable to WISE data of low CH_2Cl_2 mixing ratios in the UTLS region in October (Figure 4, at $N_2O \approx 330.9$ ppb) assuming a transport time from Earth's surface to the UTLS region of a few weeks. The observed decrease of low CH_2Cl_2 mixing ratios for increasing N_2O mixing ratios (from older to younger air) agrees well with the decreasing tropical monthly averaged CH_2Cl_2 mixing ratios from about July to September 2017, as observed by AGAGE. Extratropical NH ground-based ~~AGAGE~~ observations from the AGAGE network yield significantly higher CH_2Cl_2 mixing ratios than those in the tropics. It is thus very likely that the lower branch of the CH_2Cl_2-N_2O ~~correlation~~relationship is caused by the tropical Atlantic CH_2Cl_2 surface seasonality. However, the low CH_2Cl_2 mixing ratios observed during WISE could also be impacted by air uplifted from regions less influenced by

CH_2Cl_2 sources than the observations from the AGAGE network at Barbados. Ground-based observations of CH_2Cl_2 surface mixing ratios from the AGAGE and the NOAA network show strong regional differences particularly in the NH tropics. However, it is unclear if these differences are caused by calibration biases or are of a natural origin (Engel et al., 2018).

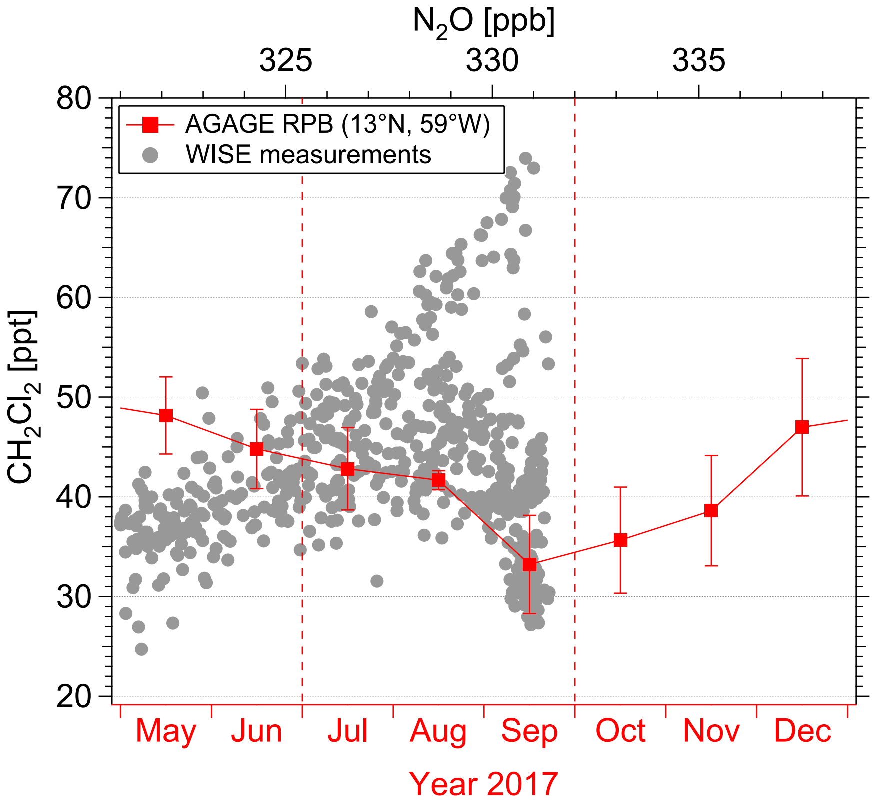

Figure 4. Monthly averaged ground-based ~~CH_2Cl_2~~ measurements of CH_2Cl_2 from the AGAGE network at Ragged Point, Barbados (13° N Prinn et al., 2018) overlayed by a detailed plot of the CH_2Cl_2-N_2O ~~correlation~~relationship observed during WISE. The AGAGE CH_2Cl_2 time series (shown in red) shows CH_2Cl_2's seasonality and is overlayed by the ~~correlation~~CH_2Cl_2-N_2O relationship such that the CH_2Cl_2 minimum at $N_2O \geq 325$ ppb measured during WISE in October 2017 matches the surface CH_2Cl_2 minimum at Barbados in September 2017. Further, the axis of the time series is adjusted so that 1 month corresponds to a change of ≈ 2 ppb N_2O, which is the typical N_2O change per month of age in the UTLS (Andrews et al., 2001). The gradient of the CH_2Cl_2-N_2O ~~correlation~~relationship's lower branch (low CH_2Cl_2 mixing ratios between dashed red lines) qualitatively fits the temporal variation of the ground-based CH_2Cl_2 measurements. The graph illustrates the congruence of ground-based tropical ~~AGAGE~~ measurements of CH_2Cl_2 ~~measurements~~ from the AGAGE network and airborne extratropical ~~WISE~~ measurements of CH_2Cl_2 ~~measurements~~ from the WISE campaign when assuming that the variation of stratospheric CH_2Cl_2 with age (here expressed in terms of N_2O mixing ratio) arises from the temporal variation of CH_2Cl_2 at the ground ("tape recorder effect"). Although this simplified view ignores the impact of mixing processes and chemical reduction of CH_2Cl_2 it qualitatively explains the lower branch of the ~~correlation curve~~CH_2Cl_2-N_2O relationship for air parcels younger than a few months.

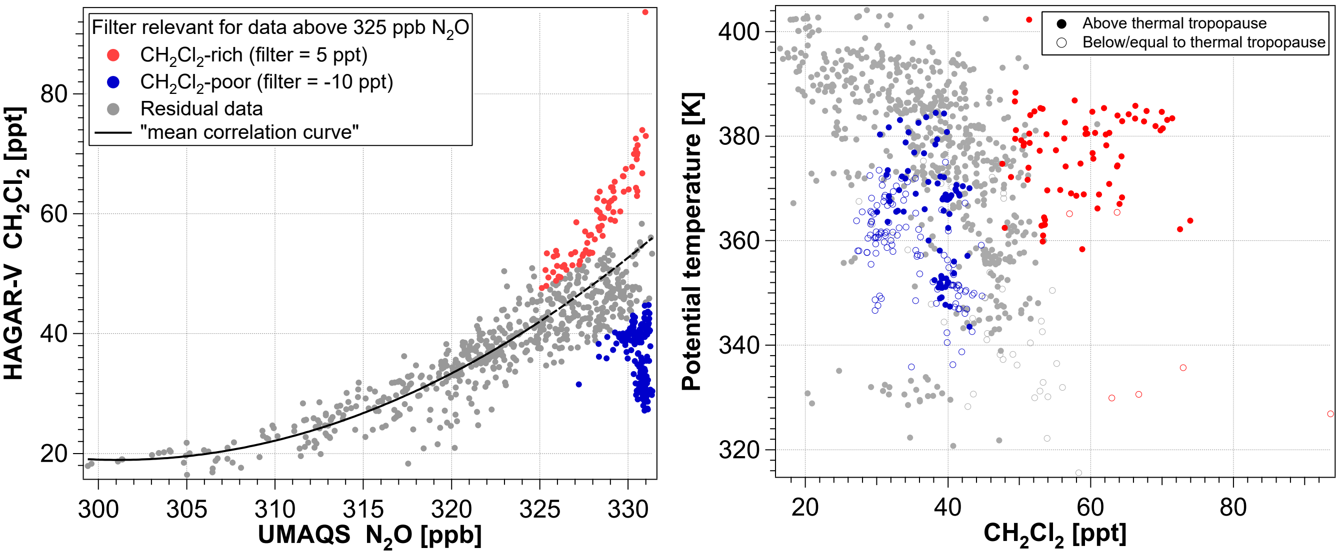

Figure 5. Left panel: CH_2Cl_2-N_2O ~~correlation~~relationship color coded with the used definition of the data filter. Red data points are considered measurements of CH_2Cl_2-rich air, consisting of measurements more than 5 ppt higher than the "mean correlation curve" and $N_2O \geq 325$ ppb. Blue data points are considered measurements of CH_2Cl_2-poor air, consisting of measurements more than 10 ppt lower than the "mean correlation curve" and $N_2O \geq 325$ ppb. The "mean correlation curve" is derived from a quadratic fit to the ~~correlation~~CH_2Cl_2-N_2O relationship for $N_2O < 325$ ppb extrapolated to higher mixing ratios relevant for the data filter (dashed line). Right panel: Scatter plot of CH_2Cl_2 as a function of the potential temperature and color coded to highlight CH_2Cl_2-rich (red) and CH_2Cl_2-poor (blue) air. On average the CH_2Cl_2-rich air is found at higher potential temperatures than the CH_2Cl_2-poor air.

3.1.1 ~~Correlation~~Data filter

In order to separately analyze the CH_2Cl_2-N_2O ~~correlation~~relationship's distinct features, the measurements are filtered relative to a "mean correlation curve". The "mean correlation curve" is derived from a quadratic fit applied to the CH_2Cl_2-N_2O ~~correlation~~relationship for $N_2O < 325$ ppb, i.e., where ~~there is no visible split of the correlation~~ the relationship clearly correlates (Figure 5, left). In order to identify chemically contrasting air masses of potentially different origin, we focus on the most extreme differences in the chemical composition: Measurements more than 5 ppt higher than the "mean correlation curve" are considered CH_2Cl_2-rich air; measurements more than 10 ppt lower than the "mean correlation curve" are considered CH_2Cl_2-poor air. In addition, only measurements with $N_2O > 325$ ppb (corresponding to $\Theta < 390$ K) are considered. The choice of these filter conditions allows the CH_2Cl_2-rich and -poor air masses to be clearly discriminated. It will further be shown below that this filter definition yields a good correspondence with the impact of different air mass origins on the CH_2Cl_2-N_2O ~~correlation~~relationship.

The thus defined measurements of CH_2Cl_2-rich air contain on ~~average 66~~median 64 % higher mixing ratios than those of CH_2Cl_2-poor air (~~(59 ± 8)~~59 ppt vs ~~(36 ± 5)~~36 ppt, respectively). In addition, the median potential temperature of mea-

Table 1. Median fractions of different surface origin tracers from CLaMS in measurements of CH_2Cl_2-rich and CH_2Cl_2-poor air parcels, and the respective ratios of the median fractions. The last row shows the median fraction of Ω. Ω is the sum of all (non-normalized) surface origin tracers of the respective air parcels ($\Omega = \sum_{i=1}^{n=24} \Omega_i$; cf. Section 2.3.1) which is the fraction of an air parcel actually considered in the tracer analysis of CH_2Cl_2-rich and -poor air. The fraction $(100 - \Omega)$ % is the part of an air parcel that has already been in the free atmosphere on 1 May, 2017. The geographical location of each surface origin tracer is given in Figure 2.

Surface origin tracer		CH_2Cl_2-rich [%]	CH_2Cl_2-poor [%]	rich/poor	poor/rich
W-ITCZ	CAM	7.3	24.9	0.29	3.40
	TAO	2.3	6.9	0.34	2.98
	NAF	3.8	6.9	0.54	1.90
	LSH	1.9	2.3	0.83	1.20
E-ITCZ	TEP	9.8	10.7	0.92	1.09
	Neast	4.3	4.1	1.04	0.96
	Wpool	7.7	5.7	1.35	0.74
	NWP	5.0	3.4	1.49	0.67
	TWP	6.7	4.5	1.49	0.67
	INO	6.7	4.1	1.64	0.61
SaEA	SEA	10.8	5.8	1.87	0.54
	NIN	4.9	2.6	1.90	0.53
	BoB	7.1	3.7	1.92	0.52
	ECH	6.0	3.1	1.94	0.52
	IND	5.2	2.6	1.97	0.51
	TIB	6.5	3.3	2.00	0.50
	Ω	63.2	81.4	0.78	1.29

surements of CH_2Cl_2-rich air is 16.2 K higher than that of CH_2Cl_2-poor air (377.8 K vs 361.6 K, respectively). 93 % of CH_2Cl_2-rich air was observed in the Ex-LS which is the case only for 40 % of CH_2Cl_2-poor air. However, only slightly smaller differences between the two types of air masses are visible in observations above the thermal TP (58 ppt vs 39 ppt and 378.7 K vs 368.3 K, respectively). These findings not only indicate tropospheric intrusions of air from two different source regions into the stratosphere, the different levels of potential temperature also suggest two different transport mechanisms. One is transporting CH_2Cl_2-rich air mainly to the top of the LMS ($\Theta \approx 380$ K) and the other is transporting CH_2Cl_2-poor air mainly to the middle and lower part of the LMS ($\Theta \approx 3$~~5~~$60 - 370$ K; Figure 5, right).

3.1.2 Impact of different air mass origin on the extratropical UTLS

In order to investigate the impact of different air mass origin on the WISE trace gas measurements, tracers of air mass origin simulated with CLaMS are analyzed. To focus on fast transport into the LMS in the range of approximately 6 months reflecting the mean tropospheric lifetime of CH_2Cl_2 and $CHCl_3$ (see Section 1), only the fraction of air parcels released from the boundary layer since 1 May is considered. Therefore, in every air parcel each surface origin tracer fraction (Ω_i) is normalized to the sum of all fractions of surface origin tracers ($\Omega = \sum_{i=1}^{n=24} \Omega_i \leq 100\,\%$) in the air parcel, thus neglecting the fraction of air that was in the free atmosphere at the initialization date of the CLaMS simulation at 1 May, 2017 (i.e., air older than 6 months). The start time of our simulations on 1 May, 2017, is further chosen to be before the onset of the Asian summer monsoon (pre-monsoon) in order to include all transport processes into the LS impacted by the Asian monsoon circulation. In the following, all analyzed surface origin tracers are normalized as described above, if not stated otherwise.

Further, to work out differences of air mass origin between CH_2Cl_2-rich and -poor air, ~~for each surface origin tracer the median fraction~~ the median fraction of a surface origin tracer in CH_2Cl_2-rich air parcels is compared to that in CH_2Cl_2-poor air parcels. To combine regions of air mass origin with a particularly high relative impact on either CH_2Cl_2-rich or -poor air, the ratio of these median surface origin tracer fractions in CH_2Cl_2-rich and -poor air is analyzed. Surface origin tracers with particularly high relative median fractions in either CH_2Cl_2-rich or -poor air are combined following these two criteria:

(1) considered are only surface origin tracers with median fractions $\geq 1\,\%$ in CH_2Cl_2-rich or -poor air parcels, and

(2) the ~~median~~ ratio of a median surface origin tracer fraction (CH_2Cl_2-rich/CH_2Cl_2-poor air respectively CH_2Cl_2-poor/CH_2Cl_2-rich air) must be > 1.8.

With this definition, regions of air mass origin – as defined for the model simulation – of significantly enhanced influence on measurements of CH_2Cl_2-rich (-poor) air relative to CH_2Cl_2-poor (-rich) air are combined. Table 1 lists the median fractions in CH_2Cl_2-rich and -poor air of each surface origin tracer fulfilling criterion (1).

The surface origin tracers also fulfilling criterion (2) for CH_2Cl_2-rich air are all located in the region of southern and eastern Asia (SaEA) including India, China, and Southeast Asia (cf. Figure 2). The source region of this SaEA tracer is mostly land-based and located in the core region of the Asian summer monsoon (ASM) from where the highest CH_2Cl_2 emissions globally are expected (Claxton et al., 2020). The median fraction of the SaEA surface origin tracer in CH_2Cl_2-rich air is about twice that in CH_2Cl_2-poor air ($41.5\,\%$ vs $20.7\,\%$, respectively).

The surface origin tracers fulfilling criterion (1) and (2) for CH_2Cl_2-poor air are all located in the tropics along the mostly western part of the Intertropical Convergence Zone (ITCZ) from 120° W to about 45° E (W-ITCZ; cf. Figure 2, bottom). The source region of this W-ITCZ tracer includes a large maritime region and is not known for significant CH_2Cl_2 emissions. The median fraction of the W-ITCZ surface origin tracer in CH_2Cl_2-poor air is about three times higher than in CH_2Cl_2-rich air ($40.6\,\%$ vs $13.5\,\%$, respectively) with a particularly high contribution from the region of Central America (CAM).

The surface origin tracers fulfilling criterion (1) but not (2) are all geographically connected. To focus on NH regions of air mass origin and because its fraction in both CH_2Cl_2-rich and -poor air is very low ($< 2.5\,\%$), the surface origin tracer for the lower southern hemisphere (LSH, Figure 2, top) will not be considered in the following analysis. Without LSH, the third major region of air mass origin significantly influencing the WISE measurements by relatively fast transport mainly includes an extended region of the summertime ITCZ mostly in the eastern hemisphere and the Pacific Ocean (E-ITCZ), excluding the regions of W-ITCZ and SaEA. The region of this E-ITCZ tracer combines a vast maritime region and areas adjacent to the core region of the ASM. The fractions of the E-ITCZ surface origin tracer in CH_2Cl_2-rich and -poor air parcels do not strongly favor either over the other.

With mainly fractions above 40 % the SaEA tracer dominates the CH_2Cl_2-N_2O ~~correlation~~relationship both below 325 ppb N_2O and the upper branch above 325 ppb N_2O including CH_2Cl_2-rich air (Figure 6, bottom left). Towards CH_2Cl_2-poor air, the SaEA tracer gradually decreases while the W-ITCZ tracer increases up to fractions above 50 % (Figure 6, bottom right). In fact, both surface origin tracers, SaEA and W-ITCZ, show significant correlations with all WISE CH_2Cl_2 measurements at $N_2O > 325$ ppb. Thereby the Spearman's correlation coefficients $R_{\mathrm{SaEA}} = 0.7$ and $R_{\mathrm{W\text{-}ITCZ}} = -0.72$ indicate a significant monotone but not necessarily linear positive and negative correlation, respectively, with fractions of the SaEA tracer ranging from 8.5 % to 48 % and those of the W-ITCZ tracer ranging from 9.3 % to 70.8 %.

On the one hand, of all measured air masses entering the LS in the course of NH summer a large fraction originated in southern and eastern Asia. In addition, these air masses are preferably composed of CH_2Cl_2-rich air and thus strongly contribute to steepening the slope of the CH_2Cl_2-N_2O ~~correlation slope~~relationship (upper branch). On the other hand, young air from the region of the central and western part of the ITZC strongly influences the UTLS with CH_2Cl_2-poor air (lower branch). Further, measurements in between CH_2Cl_2-rich and -poor air in the CH_2Cl_2-N_2O ~~correlation~~relationship contain moderate fractions (in the range of $20 - 40$ %) from both regions of air mass origin.

It has to be noted that the ground-based measurements of CH_2Cl_2 from the AGAGE network (Section 3.1) were obtained in the CAM surface origin tracer region, which is included in the W-ITCZ tracer. The extraordinarily high impact of the CAM tracer (24.9 %) on the measurements of CH_2Cl_2-poor air strongly supports the comparison made in Section 3.1 and underlines our conclusion of CH_2Cl_2's tropical Atlantic surface seasonality being reflected in the measurements within the UTLS region.

The influence of the E-ITCZ surface origin tracer on the CH_2Cl_2-N_2O ~~correlation~~relationship is about equal in all air parcels with fractions of around 40 % (Figure 6, top right). This region of air mass origin is thus generally important for the composition of young air masses in the LMS without a specifically strong influence on either CH_2Cl_2-rich or -poor air.

3.1.3 Results of back-trajectory calculations

The back-trajectories calculated for CH_2Cl_2-rich and -poor air are analyzed in two steps. First, the location of maximum rate of change in potential temperature (diabatic ascent rate) along each back-trajectory is derived and the transport time from the measurement to this location is calculated. Second, the back-trajectories are considered up to the point where they reach the model boundary layer. General transport pathways are derived for measurements of CH_2Cl_2-rich and -poor air. Within the maximum of 120 days the model boundary layer is reached by 59 out of 80 back-trajectories of CH_2Cl_2-rich air (74 %) and 170 out of 189 back-trajectories of CH_2Cl_2-poor air (90 %), and only these back-trajectories are analyzed in the following. The median time for an air parcel at the boundary layer to reach the location of measurement is 48 days; CH_2Cl_2-poor air in general shows shorter transport times (43 days) than CH_2Cl_2-rich air (64 days). The locations of trajectory end points at the model boundary layer color coded with transport time are given in the appendix (Figure B1).

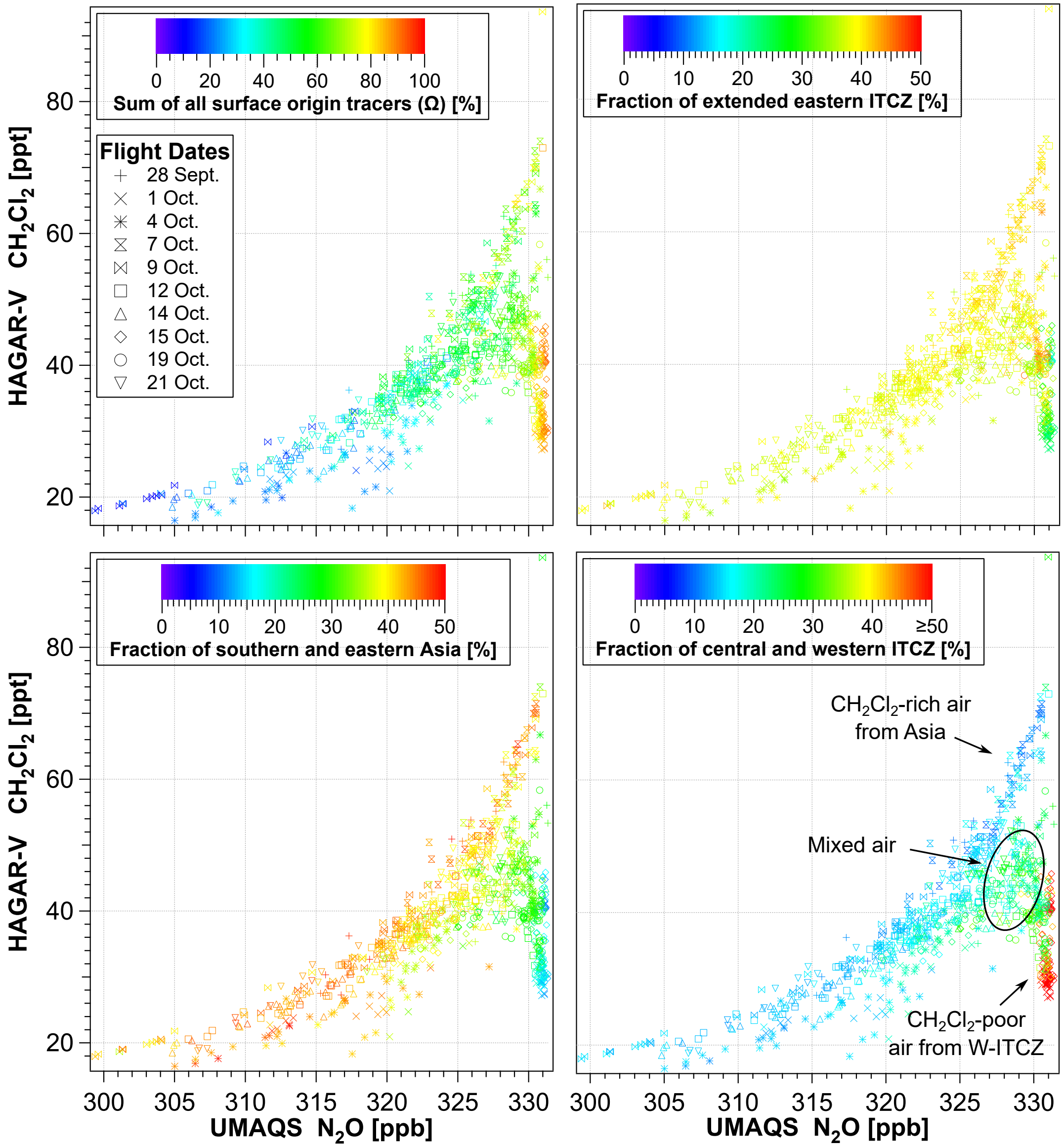

Figure 6. CH_2Cl_2-N_2O ~~correlation~~relationship color coded with the sum of all (non-normalized) surface origin tracers (Ω, top left), the SaEA (bottom left), the W-ITCZ (bottom right) and the E-ITCZ (top right) surface origin tracer. The SaEA, W-ITCZ, and E-ITCZ surface origin tracers are each normalized to the sum of all surface origin tracers (i.e., of each air parcel only the fraction of the sum of all surface origin tracers is considered), thereby neglecting the fraction of older air that has been above the model boundary layer on the simulation's initialization date (1 May, 2017; cf. Section 2.3.1). The CH_2Cl_2-N_2O ~~correlation~~relationship color coded with the absolute fraction of SaEA and W-ITCZ is shown in Figure A1 in Appendix A.

Locations of maximum diabatic ascent rate and transport times

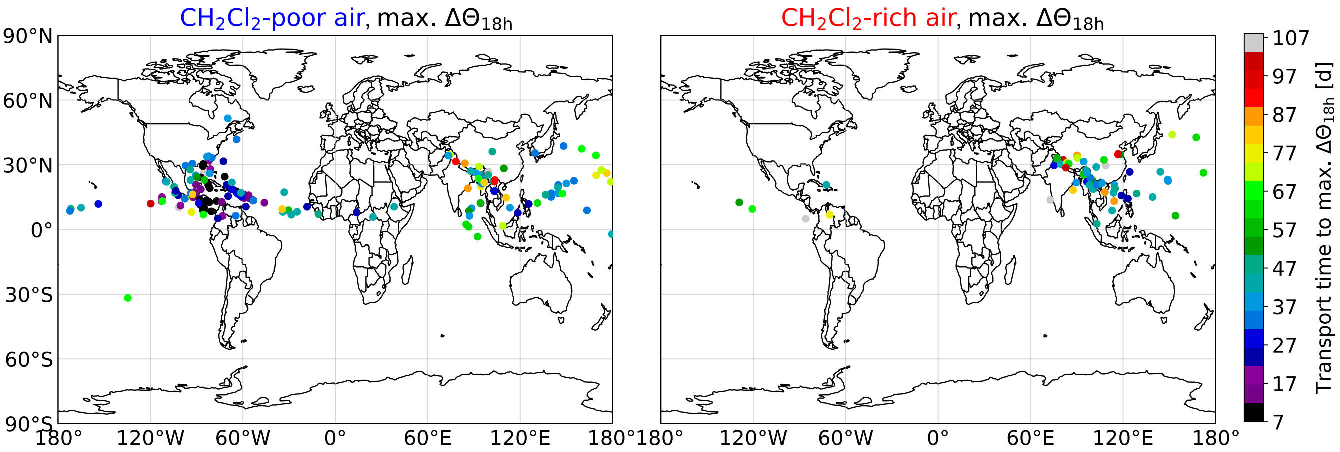

Figure 7. Location of maximum change in potential temperature over a time interval of 18 h (max. $\Delta\Theta_{18\mathrm{h}}$) along back-trajectories, color coded with the transport time from the location of measurement to the location of max. $\Delta\Theta_{18\mathrm{h}}$. Left panel: CH_2Cl_2-poor air; right panel: CH_2Cl_2-rich air. Shown are the locations of max. $\Delta\Theta_{18\mathrm{h}}$ for CH_2Cl_2-rich and -poor air from all WISE flights between 28 September and 21 October.

The location of maximum change in potential temperature over a time interval of 18 h (max. $\Delta\Theta_{18\mathrm{h}}$) along each trajectory is used to identify the locations of strong uplift along the trajectories of sampled CH_2Cl_2-rich and -poor air. This uplift occurs in the troposphere. Details about the calculation and use of max. $\Delta\Theta_{18\mathrm{h}}$ are given by Hanumanthu et al. (2020).

Almost all trajectories of CH_2Cl_2-rich air show their max. $\Delta\Theta_{18\mathrm{h}}$ above the region of southern and eastern Asia, in particular above the region of the Tibetan Plateau, northern India, China, and Southeast Asia (Figure 7, right). This uplift mostly occurred about $5-10$ weeks prior to the measurement (cf. Table 2), i.e., in July and August, the peak season of the ASM. This strongly suggests that the measurements of CH_2Cl_2-rich air were almost exclusively uplifted within the ASM. There is a clear overlap between the Asian region of concentrated locations of max. $\Delta\Theta_{18\mathrm{h}}$ and the region of the SaEA surface origin tracer with the highest relative contribution to air parcels of CH_2Cl_2-rich air (cf. Section 3.1.2) suggesting a consistency between trajectory calculations and the three-dimensional CLaMS simulation.

Table 2. Median transport times derived from back-trajectories calculated for air parcels of CH_2Cl_2-poor air uplifted above Central America (location of max. $\Delta\Theta_{18h}$ within $0° - 35°$ N and $50° - 120°$ W) labeled as NAM and for air parcels of CH_2Cl_2-rich air uplifted above southern and eastern Asia (location of max. $\Delta\Theta_{18h}$ within $0° - 40°$ N and $60° - 160°$ E) labeled as ASM. The median transport times are calculated from the model boundary layer and from the location of max. $\Delta\Theta_{18h}$ each to the location of measurement in the UTLS, only for samples above the thermal TP (LS), and only for samples below or equal to the thermal TP (UT). The medians are given within the range of the 25. and the 75. percentile. N is the number of trajectories used to calculate the respective median. Note that the number of CH_2Cl_2-rich air samples observed in the UT and uplifted above southern and eastern Asia is too small to provide reliable transport times.

	NAM		ASM	
	Transp. time [d]	N	Transp. time [d]	N
BL to meas. (UTLS)	25 +23/-10	92	61 +17/-18	51
max. $\Delta\Theta_{18h}$ to meas. (UTLS)	20 +15/-8		48 +20/-9	
BL to meas. (UT)	20 +14/-6	69		4
max. $\Delta\Theta_{18h}$ to meas. (UT)	13 +12/-2			
BL to meas. (LS)	47 +17/-16	23	64 +15/-21	47
max. $\Delta\Theta_{18h}$ to meas. (LS)	38 +5/-8		48 +20/-9	

Of all trajectories related to CH_2Cl_2-poor air more than ~~6~~50 % exhibit the location of max. $\Delta\Theta_{18h}$ above the region of Central America with the rest being located above southern and eastern Asia and along the ITZC (Figure 7, left). The transport times to the UTLS since the ascent above Central America mainly range between ~~1~~2 – 5 weeks~~ and are much shorter than for those air parcels lifted up above Asia~~ (cf. Table 2). The main uplift of CH_2Cl_2-poor air above Central America thus falls in the time period of late August and throughout the entire September. ~~T~~With transport times from the BL being only about one week longer (Table 2), this result supports the comparison of CH_2Cl_2-poor air with the seasonal minimum CH_2Cl_2 mixing ratios observed by AGAGE at Barbados (cf. Figure 4). During the time period of late August and September the region around Central America is influenced by several convective systems: (1) the North American monsoon, (2) the ITCZ, and (3) tropical cyclones, i.e., hurricanes. It is very likely that all of these convective systems contributed to the fast uplift of CH_2Cl_2-poor air. The convection systems of the North American monsoon and the ITCZ share many characteristics and overlap geographically which makes it difficult to distinguish between the two systems (e.g., Siu and Bowman, 2019). The uplift of air parcels by hurricanes can be distinguished and localized more clearly which is analyzed below. The back-trajectory analysis suggests that the most important region for vertical transport of CH_2Cl_2-poor air is above Central America, which was also identified as the most significant region of air mass origin of CH_2Cl_2-poor air in the three-dimensional CLaMS simulation (cf. Section 3.1.2).

Analysis of transport pathways

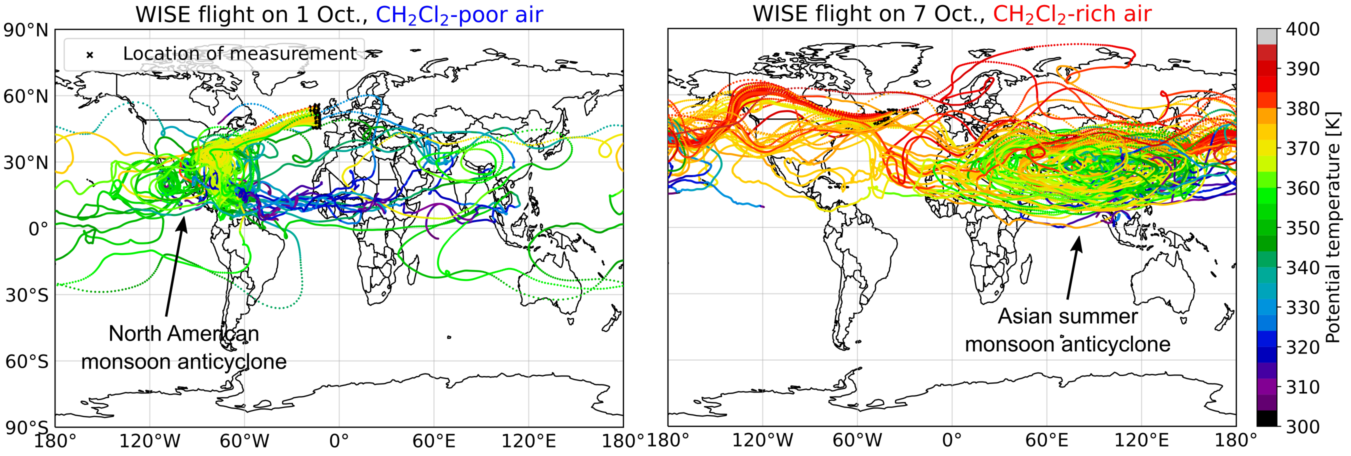

Figure 8. Back-trajectories from the location of measurement to the model boundary layer for CH_2Cl_2-poor air sampled on 1 October (left panel) and for CH_2Cl_2-rich air sampled on 7 October (right panel) color coded with the potential temperature of the trajectory. The trajectories of CH_2Cl_2-poor air show an uplift above Central America to about 365 K, an isentropic northward drag towards an anticyclonic system above North America, an eastward breakout, and a direct and isentropic pathway into the extratropics above the Atlantic Ocean. The trajectories of CH_2Cl_2-rich air show an uplift above southern and eastern Asia up to about 360 K with further upward transport by the ASMA to about 385 K and a breakout eastward following the subtropical jet stream until they quasi-isentropically enter the extratropics above the eastern Pacific or western Atlantic Ocean.

The back-trajectories from the location of measurement to the model boundary layer are analyzed to identify the main transport pathways of CH_2Cl_2-rich and -poor air into the ~~stratosphere~~UTLS. As representative examples, Figure 8 shows the trajectories of the WISE flights on 1 October (left) and 7 October (right) for CH_2Cl_2-poor and -rich air, respectively.

Almost all trajectories of CH_2Cl_2-rich air show the following general pathway: The air parcels are convectively lifted up above southern and eastern Asia to $\Theta \approx 360$ K. Further ascent of the air parcels occurs in a clockwise upward spiraling motion (Vogel et al., 2019), following the dynamics of the Asian summer monsoon anticyclone (ASMA) mainly to potential temperatures in the range of $370 - 400$ K. Preferably within this potential temperature range, the air parcels break out of the ASMA eastwards (e.g., Honomichl and Pan, 2020), following the subtropical jet stream at about 40° N until, eventually, they quasi-isentropically enter the extratropics above the eastern Pacific or western Atlantic Ocean (e.g., Vogel et al., 2014, 2016). All trajectories suggest that the air parcels arrived from the west to the location of measurement and most trajectories suggest a slight diabatic descent of up to -10 K in the extratropics a few days before the measurement. The transport time from the boundary layer to the location of measurement in the Ex-LS via this pathway ranges between $6 - 11$ weeks (cf. Table 2).

The majority (>~~6~~50 %) of trajectories of CH_2Cl_2-poor air show a strong uplift above the region of Central America up to potential temperatures mainly in the range of $360 - 370$ K. After convection, the trajectories experience a northward drag towards an anticyclonic structure located above North America, and most of these trajectories further directly enter the extratropics above the Atlantic Ocean or the North American east coast leading to short transport times to the location of measurement.

Of all CH_2Cl_2-poor air parcels transported via this pathway only 25 % (N = 23) were observed in the LS with transport times from the BL to the location of measurement in the LS ranging between 5 and 9 weeks (Table 2).

Some trajectories lifted up above the region of Central America eventually follow the subtropical jet stream eastwards around the globe before entering the extratropics. This significantly increases the transport time of an air parcel by about 3 weeks and has the potential to cause it to descend by up to about -10 K as indicated by the back-trajectory calculations. ~~However, this concerns a minority of air parcels and has only a minor effect on the median transport time of all observed air parcels lifted up above the region of Central America (max. $\Delta\Theta_{18h}$ between 0° – 30° N and 50° – 120° W) which is still 44 days shorter than that of the observed air parcels lifted up above southern and eastern Asia (max. $\Delta\Theta_{18h}$ between 0° – 40° N and 60° – 160° E; 24 vs 68 days, respectively).~~ However, the median transport time from the BL to the location of measurement in the Ex-LS of CH_2Cl_2-poor air parcels by convection above Central America (max. $\Delta\Theta_{18h}$ between 0° – 35° N and 50° – 120° W) is still 17 days shorter than for CH_2Cl_2-rich air parcels lifted up above southern and eastern Asia (max. $\Delta\Theta_{18h}$ between 0° – 40° N and 60° – 160° E; 47 vs 64 days, respectively; Table 2) and their median potential temperature differs by 10.7 K (369.7 K vs 380.4 K, respectively). Below~~, in Section 4,~~ the transport pathway from Central America to the Ex-LS is discussed in more detail.

The analysis of the entire set of back-trajectories shows that for the majority of measurements there are two distinct transport pathways into the Ex-UTLS. CH_2Cl_2-rich air is transported by the ASMA into the Ex-LS and CH_2Cl_2-poor air mainly by convection above Central America, which includes the North American monsoon, the ITCZ and hurricanes into the Ex-UTLS. In general, air parcels are lifted up to similar potential temperature levels by the convection of the ASM in Asia and the convection above Central America. The key difference yielding the observed higher potential temperatures of CH_2Cl_2-rich air from Asia compared to those of CH_2Cl_2-poor air from Central America is the additional uplift by the ASMA following the convection within the ASM (e.g., Müller et al., 2016; Brunamonti et al., 2018; Vogel et al., 2019; von Hobe et al., 2021). The slow upward spiraling dynamics within the ASMA also contributes to the longer transport time from the boundary layer to the location of the measurement of CH_2Cl_2-rich air compared to that of CH_2Cl_2-poor air. Another aspect adding to the different transport times is the longer transport pathway from Asia because simulations indicated air masses ~~were always observed to reach~~ reached the location of measurement always from the west. Nevertheless, air parcels observed in the Ex-LS are impacted more strongly by air masses transported via the ASMA than via the NAMA (cf. figures 6 and 14).

Case study: convective uplift by hurricane Maria

In order to investigate the role of tropical cyclones for the transport of Cl-VSLS into the extratropical UTLS region, the locations of max. $\Delta\Theta_{18h}$ were compared with the tracks of several tropical cyclones. Significant matches with the category 5 hurricane Maria (Pasch et al., 2019) were found for back-trajectories of measurements of four WISE flights (on 1, 14, 15, and 19 October). A total of 27 trajectory locations of max. $\Delta\Theta_{18h}$ agreed within a time window of 0.2 days and a 1° radius with the center of hurricane Maria at some point along its track (Figure 9). The 1° radius of tolerance was chosen because it corresponds to the spatial resolution of the ERA-Interim reanalysis data used for the trajectory calculation, as well as (roughly) to the hurricane's radius from its core. This analysis directly links 27 WISE measurements (five were observed above the thermal TP) to the convection of hurricane Maria with transport times since convection ranging between one week and one month.

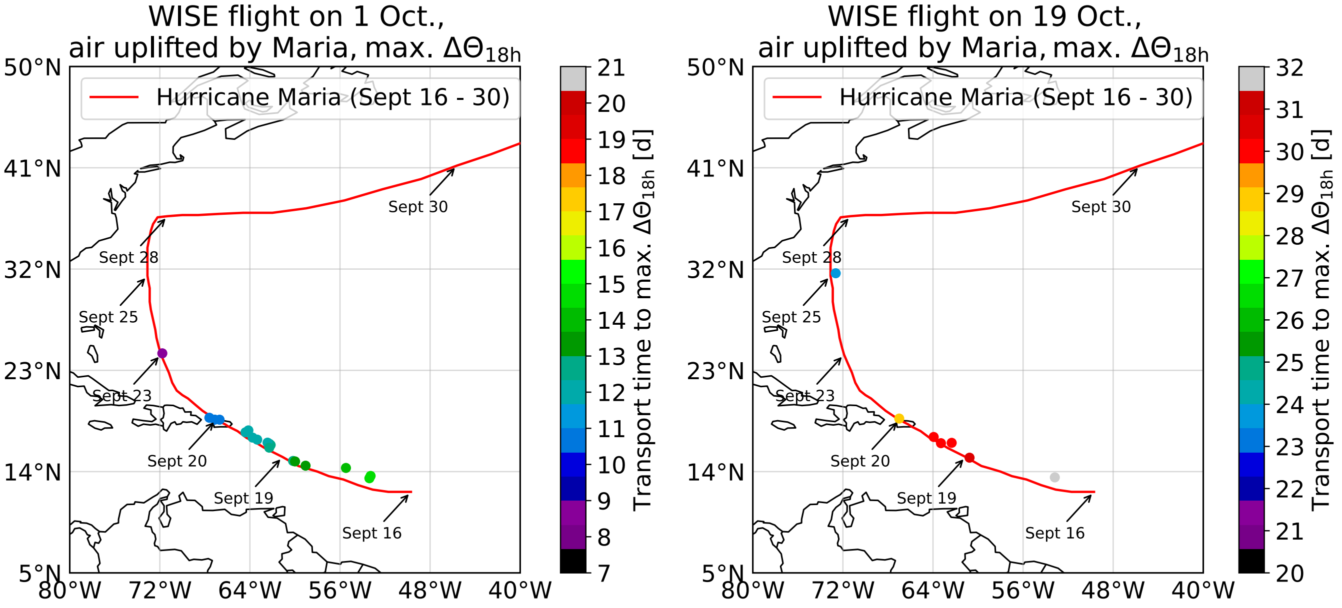

Figure 9. Trajectory locations of max. $\Delta\Theta_{18\mathrm{h}}$ color coded with the transport time from the location of measurement to the position of max. $\Delta\Theta_{18\mathrm{h}}$ along the trajectory. The red line indicates the storm track of the center of hurricane Maria (Pasch et al., 2019) with arrows marking the location at which the hurricane resided at the indicated date. Left panel: Flight on 1 Ocober; right panel: Flight on 19 October.

Interestingly, CH_2Cl_2 mixing ratios of measurements linked to hurricane Maria positively correlate with transport time since maximum convection ($R_{\mathrm{Pearson}} = 0.85$; Figure 10, top right. Note, these CH_2Cl_2 mixing ratios also correlate with transport time since the model BL but with a lower $R_{\mathrm{Pearson}} = 0.64$ and transport times between 9 and 48 days. However, here we focus on the transport since convection by hurricane Maria to derive impacts on the air parcels induced by processes in the UTLS region). Those air samples related to short transport times contain the lowest CH_2Cl_2 mixing ratios at $N_2O > 325$ ppb measured during WISE (Figure 10, top left). According to the back-trajectories, most of the air parcels lifted up by hurricane Maria left the model boundary layer above the tropical Atlantic in September where CH_2Cl_2 sources are small (Figure 10, bottom). In addition, in that region the seasonal minimum of CH_2Cl_2 mixing ratios is in September (cf. Section 3.1). This implies that when air masses lifted up by hurricane Maria mix, they can only increase their CH_2Cl_2 mixing ratio, i.e., mixing with air of higher CH_2Cl_2 mixing ratio. Air parcels related to longer transport times did not take a direct path to the extratropics after being lifted up by hurricane Maria and rather followed the subtropical jet stream eastwards around the globe, thereby enhancing the chances of mixing with air of higher CH_2Cl_2 mixing ratios.

In general, despite being a significant source of convection, hurricane Maria did not contribute to the transport of enhanced CH_2Cl_2 mixing ratios into the stratosphere and rather led to the transport of CH_2Cl_2-poor air, a consequence of

CH_2Cl_2's tropical Atlantic boundary layer seasonality. This result is consistent with the lack of strong CH_2Cl_2 sources in the oceanic region of convection. Nevertheless, our analysis shows that large hurricanes can provide a fast transport into the extratropical UTLS. ~~Below in Section 4 it is discussed how tropospheric air masses observed on 1 October are mixed into the LS a few days after the observation. For instance, this is of particular importance for brominated short-lived substances (e.g., CH_2Br_2 and $CHBr_3$) that have a high ODP and some of their largest emission sources located in tropical oceans (e.g., Hepach et al., 2015; Rotermund et al., 2021).~~

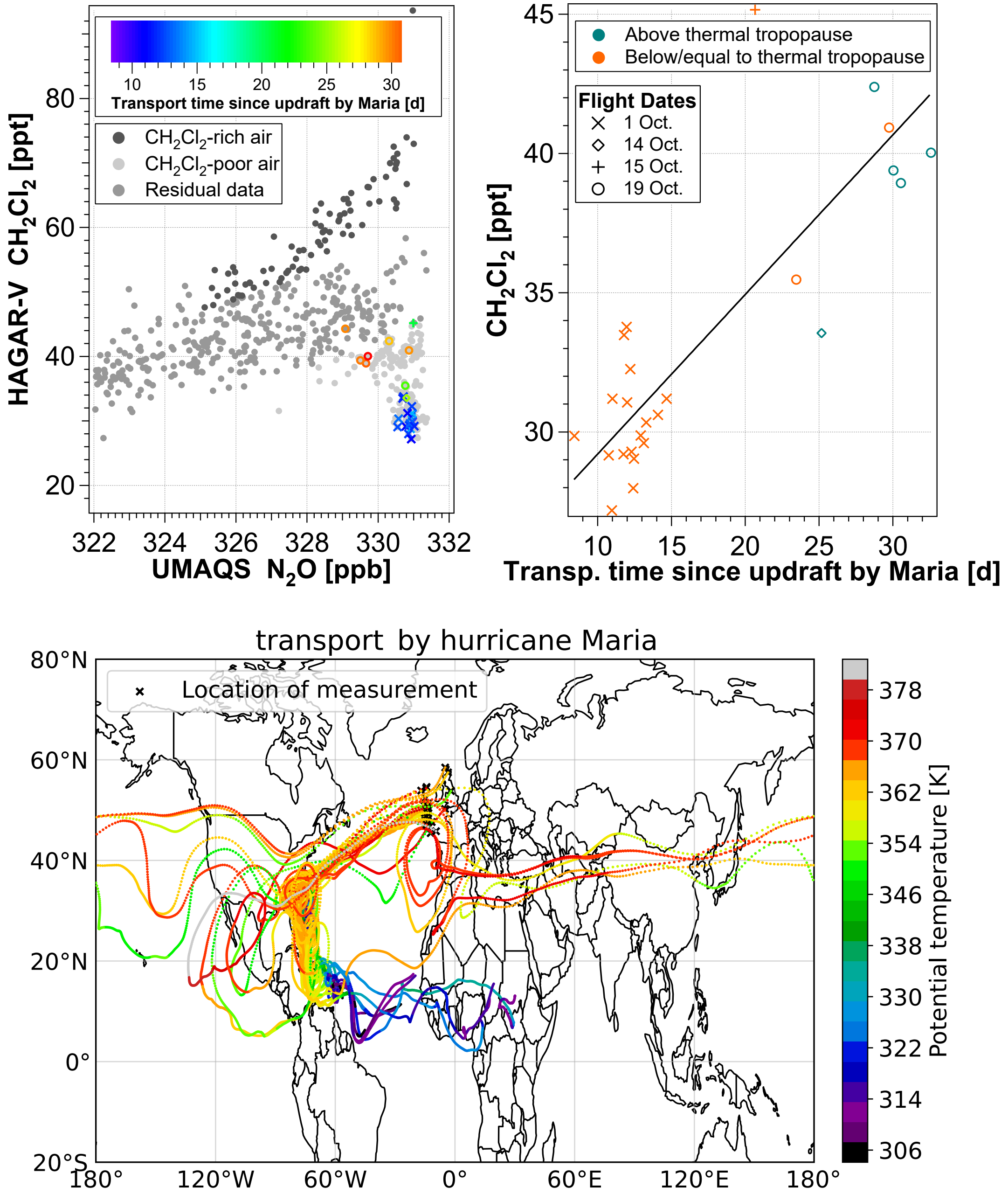

Figure 10. Upper left panel: Detailed graph of the CH_2Cl_2-N_2O ~~correlation~~relationship color coded with the transport time since uplift by hurricane Maria. The CH_2Cl_2-N_2O ~~correlation~~relationship in the background is plotted in different shades of gray indicating the measurements of CH_2Cl_2-rich air (dark gray) and CH_2Cl_2-poor air (light gray). Upper right panel: Correlation of CH_2Cl_2 and the transport time since uplift by hurricane Maria, color coded according to the air parcels' location above (blue-green) or below/equal to the thermal tropopause (orange). Lower panel: back-trajectories from the location of measurement to the model boundary layer of air parcels lifted up by hurricane Maria, color coded with the potential temperature of the air parcels at the respective trajectory location.

Particularly during the WISE flight on 1 October when we sampled the largest number of air parcels uplifted by hurricane Maria the measurements were highly impacted by air originating in the region of Central America (cf. Figure ~~14~~6). With a median transport time from the BL of 18 days these measurements agree well with the fast transport pathway into the stratosphere described by Wang et al. (2021). However, despite the fact that we observed most of these air masses at latitudes around 50° N and potential temperatures in the range of $350-370$ K, the majority of measurements were below the thermal TP. Figure 11 shows the meteorological situation of this particular WISE flight on 1 October based on ERA-Interim reanalysis data (Dee et al., 2011). Obviously, the air masses breaking out of the anticyclone above the North American east coast (cf. Figure 8, left) turned into a streamer carrying a local high TP to higher latitudes. A few days after our observation, this streamer became unstable and mixed into the LS. This implies that tropical air lifted up by hurricanes and other convective systems in the region of Central America can enter the Ex-LS quasi-isentropically during NH autumn even if the convection in the tropics has not transported the air above the TP. ~~This transport pathway, described by Wang et al. (2021) as the fastest and most efficient transport of tropical tropospheric air into the North American LMS region, has been corroborated for the first time on the basis of in situ Cl-VSLS observations by the present study.~~ We have thereby shown that tropical surface mixing ratios of VSLS from the region of Central America and the Atlantic Ocean can be efficiently transported into the Ex-LS during the late North American monsoon season. For instance, this is of particular importance for brominated short-lived substances (e.g., CH_2Br_2 and $CHBr_3$) that have a high ODP and some of their largest emission sources located in tropical oceans (e.g., Hepach et al., 2015; Rotermund et al., 2021). However, it has to be noted that only 25 % of air parcels transported by this pathway were observed in the Ex-LS and stratospheric air masses showed relatively low fractions of air originating in the region of central and western ITCZ compared to those originating in southern and eastern Asia (cf. Figure 14). Transport and mixing processes in the TP region below the aircraft during the flight on 1 October are analyzed by Schäfler et al. (2021).

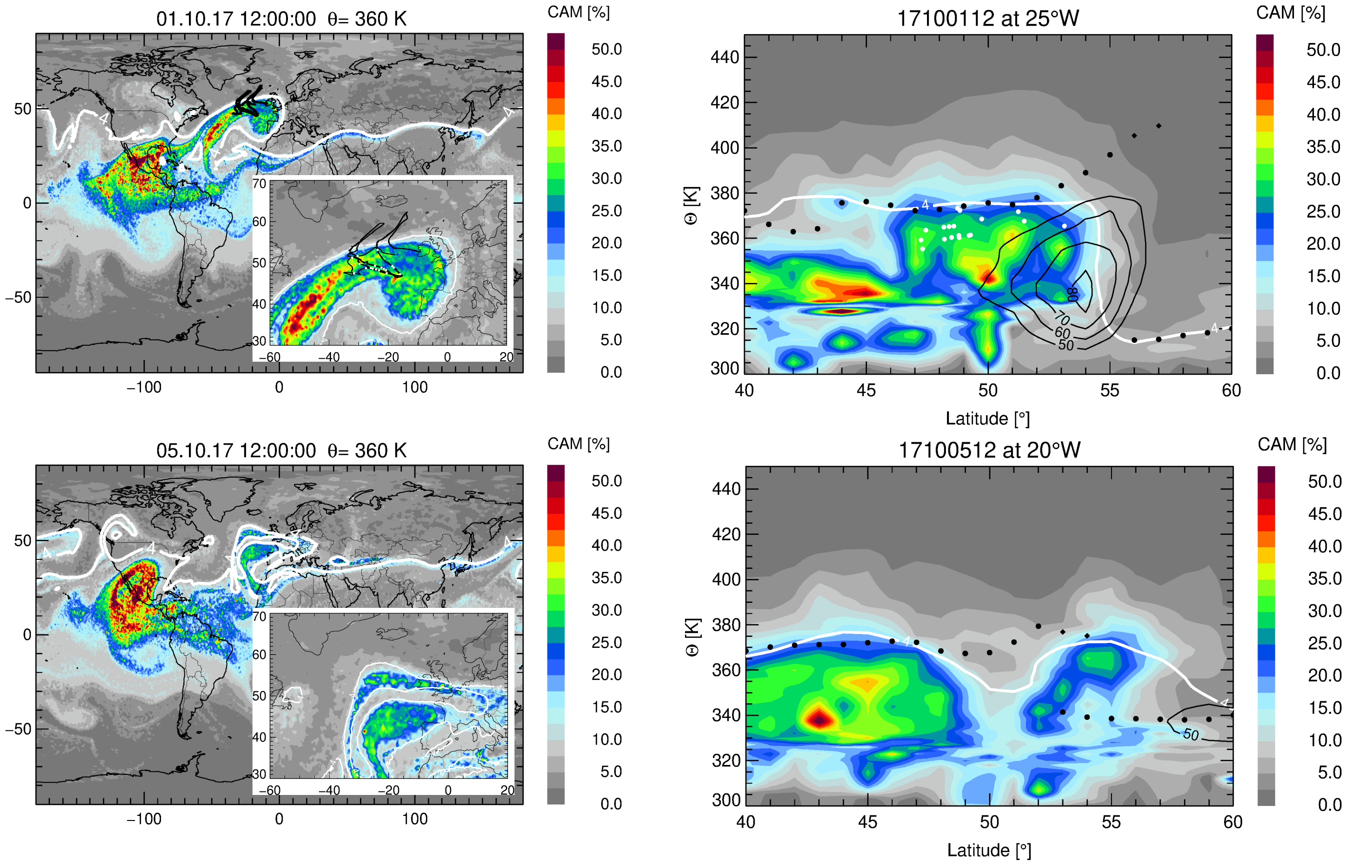

Figure 11. Meteorological situation at noon time for the WISE flight on 1 October (top) and four days later (bottom) using ERA-Interim reanalysis data. The colors indicate the absolute surface origin tracer fraction of the region of Central America (CAM) at 360 K of potential temperature (left panels) and as a vertical cross section at 20° W (top, right) and 25° W (bottom, left). The flight track (transferred to noontime) is shown as a black line on the isentropic view (top, left); on the vertical cross sections the black lines indicate zonal wind speed. White dots mark the measurement location of air lifted up by hurricane Maria. Note that these measurement locations, as well as the shown flight path, are not necessarily located exactly at 360 K (top, left) or at 25° W (top, right). Black dots indicate the location of the first thermal tropopause (TP), black diamonds indicate the second thermal TP; the white line shows the 4 PVU surface. The plots show the probing of a high TP streamer of air originating in Central America at midlatitudes on 1 October. Four days later, the streamer became unstable and a large volume mixed into the LS above the thermal TP. This figure illustrates the intrusion of tropical air into the LS: Air within the streamer has been lifted up by a hurricane into the TTL and was further transported to higher latitudes by an upper level anticyclone above North America (cf. Figure 8, left) to be finally mixed into the LS by Rossby wave breaking.

3.2 Comparison of CH_2Cl_2 and $CHCl_3$

In this section the results of the CH_2Cl_2 analysis are used to investigate $CHCl_3$ data measured during WISE. Figure 12 (left) shows the $CHCl_3$-N_2O ~~correlation~~relationship color coded to highlight air parcels of CH_2Cl_2-rich (red) and -poor (blue) air (cf. Section 3.1.1). In general, the $CHCl_3$-N_2O ~~correlation~~relationship reveals similar but less clearly pronounced structures as observed for the CH_2Cl_2-N_2O ~~correlation~~relationship. The $CHCl_3$-N_2O ~~correlation~~relationship similarly is less compact for higher N_2O mixing ratios. However, a distinct split of the ~~correlation~~compact relationship, as observed for CH_2Cl_2, is not clearly visible, but a broad scatter on the $CHCl_3$ axis with mixing ratios in the stratosphere being enhanced by up to 100 % compared to the lowest measurements at similar N_2O values. Measurements of CH_2Cl_2-rich air also show clearly enhanced $CHCl_3$ mixing ratios and measurements of CH_2Cl_2-poor air also contain the lowest $CHCl_3$ mixing ratios at given N_2O values. Nevertheless, there are a few significant differences which will be analyzed in the following.

The seasonal cycle of $CHCl_3$ is less pronounced but in phase with that of CH_2Cl_2 (cf. Figure C1 in Appendix C). Based on a comparison with ground-based ~~AGAGE~~ observations from the AGAGE network, $CHCl_3$ data for measurements of CH_2Cl_2-poor air between N_2O values of 229.5 ppb and 331 ppb reflect $CHCl_3$'s tropical surface seasonality as it similarly was observed for CH_2Cl_2.

In our data, high CH_2Cl_2 concentrations coincide with high $CHCl_3$ concentrations in many, but not in all cases. There are examples of high $CHCl_3$ concentrations where CH_2Cl_2 concentrations are relatively low. This suggests that air from regions with relatively stronger $CHCl_3$ than CH_2Cl_2 sources was measured. However, air masses of CH_2Cl_2-rich air clearly stand out by their elevated $CHCl_3$ mixing ratios in the region of $\Theta \approx 380$ K (Figure 12, center). Based on the results of Section 3.1.3, we therefore suggest that the ASMA is the dominant factor also for the transport of enhanced $CHCl_3$ mixing ratios to the Ex-LS at $\Theta \approx 380$ K.

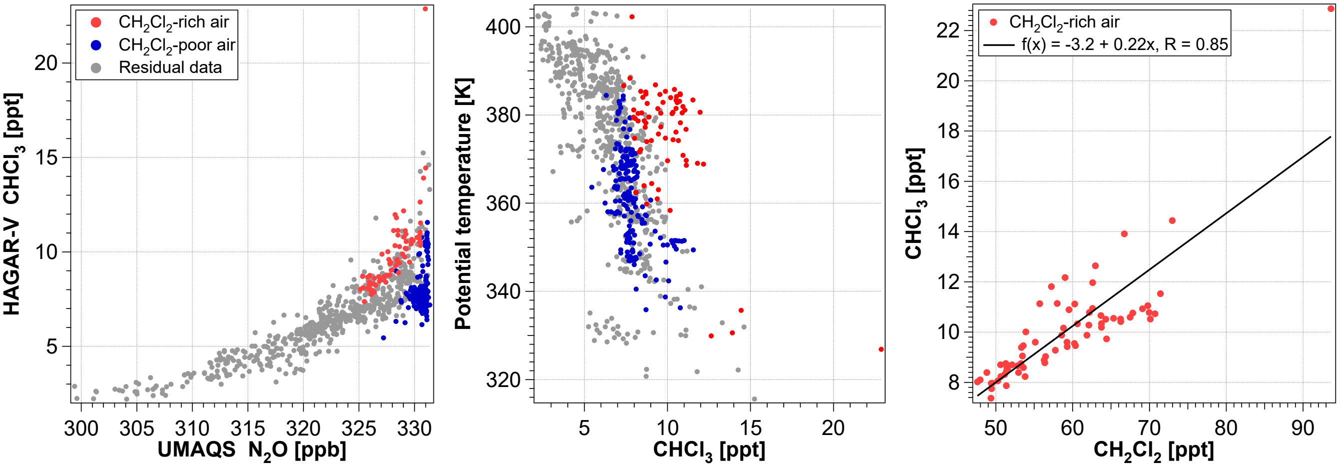

Figure 12. $CHCl_3$-N_2O ~~correlation~~relationship (left) and $CHCl_3$ as a function of potential temperature (center) color coded to highlight measurements of CH_2Cl_2-rich and -poor air; $CHCl_3$-CH_2Cl_2 ~~correlation~~relationship of measurements of only CH_2Cl_2-rich air (right).

Due to their similar photochemical lifetime CH_2Cl_2 and $CHCl_3$ are expected to linearly correlate in the stratosphere; however varying correlation slopes can arise due to different emission ratios in the source regions defining the respective composition of the air parcel. The measurements of CH_2Cl_2-rich air show a significant positive linear correlation with $CHCl_3$ (Figure 12, right) suggesting sources or source regions with similar emission ratios of these species. Due to the strong evidence for CH_2Cl_2-rich air being significantly affected by anthropogenic sources, the significant positive correlation with $CHCl_3$ suggests that this also holds for $CHCl_3$. The highest anthropogenic emissions of $CHCl_3$ are expected to originate from China (Fang et al., 2018), which is within the region of sources particularly impacting the air masses of CH_2Cl_2-rich air analyzed here (Section 3.1.2). This suggests a significant anthropogenic impact that clearly enhances $CHCl_3$ concentrations in the upper LMS.

At a closer look, the $CHCl_3$-CH_2Cl_2 ~~correlation~~relationship in Figure 12 (right) reveals two correlation lines with different slopes. The nature of the different slopes can be better understood when looking at the $CHCl_3$-CH_2Cl_2 ~~correlation~~relationship of all WISE measurements color coded with CLaMS's surface origin tracers (Figure 13; left and center). The $CHCl_3$-CH_2Cl_2 ~~correlation~~relationship fans out towards higher mixing ratios giving the impression of several correlation lines with different slopes. The data points forming the steepest correlation slope show the highest W-ITCZ tracer fractions and the lowest SaEA tracer fractions while for the data points forming the lowest correlation slope the opposite is the case. The $CHCl_3$-CH_2Cl_2 correlation slope thus flattens with increasing entry of air masses originating from southern and eastern Asia.~~T~~ Knowing that both species have similar sinks and photochemical lifetimes but $CHCl_3$ has a larger fraction of emissions from biogenic sources than CH_2Cl_2, this suggests larger $CHCl_3$:CH_2Cl_2 emission ratios in the region of the central and western ITCZ region (with presumably mostly biogenic sources) than in southern and eastern Asia (where anthropogenic sources likely dominate).

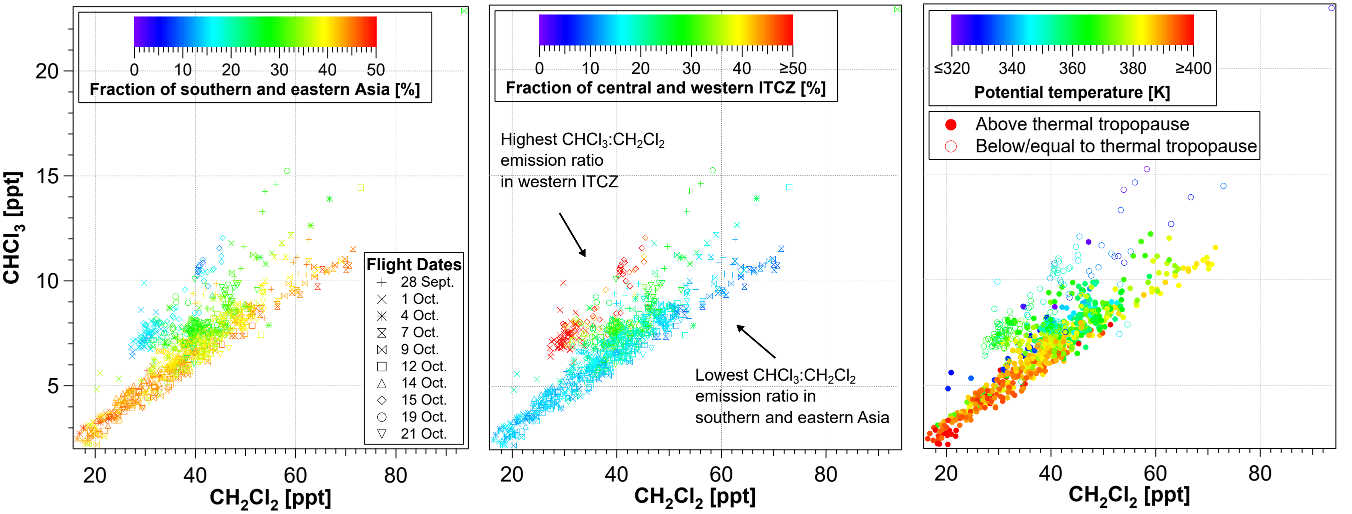

Figure 13. $CHCl_3$-CH_2Cl_2 ~~correlation~~relationship color coded with the SaEA (left) and the W-ITCZ (center) surface origin tracer, and the potential temperature (right). The ~~correlation~~relationship exhibits different correlation slopes clearly depending on the origin of air. A large impact of sources from southern and eastern Asia coincides with a low correlation slope dominating the larger part of the ~~correlation~~relationship. A large impact of sources from the central and western part of the ITCZ coincides with the steepest correlation slope implying a relatively larger $CHCl_3$:CH_2Cl_2 emission ratio in this region compared to the emission ratio in southern and eastern Asia. The highest $CHCl_3$ mixing ratios and the majority of measurements with the steepest correlation slope were observed in the tropopause region and the upper troposphere.

Compared to the lowest correlation line, the wider range of surface origin tracer fractions apparent in the correlation lines with steeper slopes might be due to the different strengths of seasonality of CH_2Cl_2 and $CHCl_3$ possibly affecting the linear relationship between $CHCl_3$ and CH_2Cl_2. In addition, the highest mixing ratios pertain to the steeper correlation lines. However, all of those were observed at low potential temperature levels and below the thermal TP (Figure 13, right) where mixing ratios can easily exceed those in the stratosphere above. The evolution of tropospheric air masses at potential temperatures above 350 K as shown in the steeper correlation line ~~is~~was discussed ~~further below~~above in Section ~~4~~3.1.3. In summary the analysis suggests clear similarities between CH_2Cl_2 and $CHCl_3$ when emitted by anthropogenic sources and differences between the two species mainly due to additional (presumably biogenic) $CHCl_3$ sources.

4 Discussion

Figure 14 shows measured and simulated WISE tracers as a function of equivalent latitude and potential temperature. It illustrates the air masses of enhanced CH_2Cl_2 and $CHCl_3$ that were transported from southern and eastern Asian sources by the ASMA to potential temperatures of around 380 K and to the Ex-LS. At slightly lower potential temperatures and equivalent latitudes we observed particularly low CH_2Cl_2 mixing ratios and partly low $CHCl_3$ mixing ratios. The corresponding air masses were sampled at potential temperatures mainly above 360 K but mostly below the thermal tropopause and were uplifted from Central American as well as tropical Atlantic and Northern African source regions via convection by hurricanes, by the ITCZ and the North American monsoon and transported further towards the location of measurement at higher latitudes; therefore these air masses are characterized by low values of equivalent latitude.

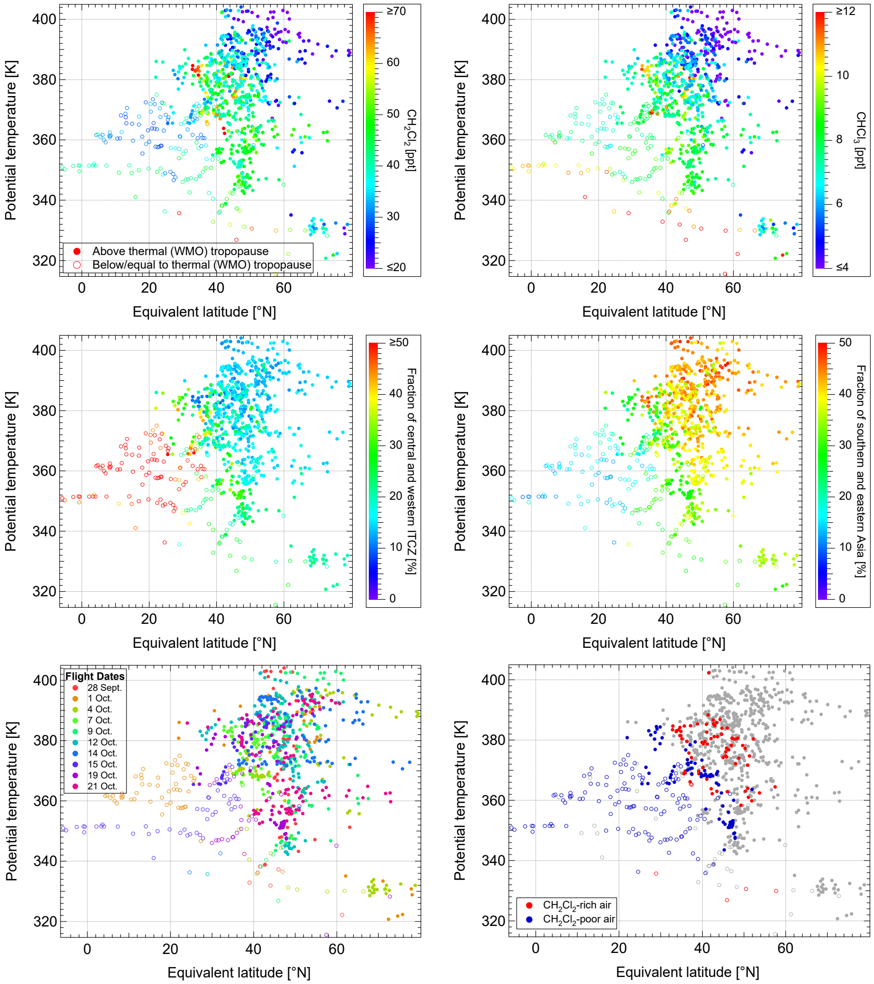

Figure 14. Measured (top) and simulated (middle) tracers of the WISE flights (bottom, left) from 28 September to 21 October, 2017, as a function of equivalent latitude and potential temperature. Note that equivalent latitudes $\leq 0°$ N are likely calculated artifacts due to a negative bias induced by convection (Pan et al., 2012). The open symbols indicate a measurement location below or equal to the thermal tropopause (TP) and the location of full symbol data points is above the thermal TP. The coloration of the panel at bottom right correspond to the lower branch (blue) and to the upper branch (red) of the CH_2Cl_2-N_2O ~~correlation~~relationship (referred to as CH_2Cl_2-poor and -rich air, respectively; cf. Section 3.1.1). CH_2Cl_2-poor air measured at potential temperatures generally up to 375 K mostly originated from the Central American as well as tropical Atlantic and Northern African boundary layer (central and western ITCZ) and has mostly not (yet) entered the lower stratosphere at the time of measurement. CH_2Cl_2-rich air is strongly influenced by air masses from southern and eastern Asia and was measured almost exclusively in the extratropical lower stratosphere. Note that the fraction of surface origin tracers given in the graphs is not an absolute fraction of the whole air parcels but of the air masses younger than 6 months within the air parcels (cf. Section 3.1.2). The two different transport pathways from the boundary layer into the extratropical UTLS region are described in the text.

The presented distribution of air masses from different source regions in the NH UTLS is in good agreement with a similar study by Rotermund et al. (2021) also based on WISE measurements, but using bromine observations. However, the lower stratospheric region of high bromine concentrations from Asian source regions described by Rotermund et al. (2021) is at lower potential temperatures and higher equivalent latitudes than the CH_2Cl_2-rich air described in the present paper. This could be due to relatively stronger (mostly biogenic) bromine emission sources in the adjacent region of the ASM compared to the mostly anthropogenic CH_2Cl_2 emission sources mainly located in the core region of the ASM. In addition, in the present paper the first five research flights in September are not analyzed in contrast to the study by Rotermund et al. (2021). Nevertheless, compared to the very short-lived bromine species analyzed by Rotermund et al. (2021), the combination of a longer lifetime, highly significant Asian emission sources~~, and a strong seasonal cycle~~ and very low mixing ratios in other regions of strong convection clearly benefits the use of CH_2Cl_2 observations to derive details about the different transport mechanisms and pathways from the source region into the NH summertime UTLS. In addition, using the $CHCl_3$:CH_2Cl_2 ratio to support the analysis of air mass origin is a unique and helpful tool in the analysis of transport pathways.

Further, elevated quantities of peroxyacetyl nitrate (PAN) were measured in the NH LMS during the WISE flight on 13 September 2017 by the GLORIA instrument with main sources in South Asia and Southeast Asia uplifted by the ASMA (Wetzel et al., 2021). Moreover, the transport pathway into the LS via the ASMA derived from ~~back-trajectories of air originating~~CLaMS simulations identifying the air mass origin in southern and eastern Asia was also observed for other measurements taken in the NH UTLS over Europe and the Atlantic Ocean during the HALO TACTS campaign in August and September 2012 (Vogel et al., 2014, 2016; Müller et al., 2016; Rolf et al., 2018). In the present study, we have~~ for the first time~~ directly related this transport pathway to in situ Cl-VSLS measurements in the LS and observed that air masses strongly enhanced in CH_2Cl_2 and $CHCl_3$ are rather rapidly transported to the top of the NH LMS at about 380 K by this pathway. This finding supports the modeled results of Claxton et al. (2019) who show that Cl-VSLS sources located in tropical Asia have a higher potential for stratospheric ozone depletion than those from any other source region. In addition, $CHCl_3$ has significant biogenic sources (Engel et al., 2018). Our study suggests that not only the enhanced CH_2Cl_2 mixing ratios but also the enhanced $CHCl_3$ mixing ratios observed at about 380 K are significantly impacted by anthropogenic sources which are expected to be strongest in the region of southern and eastern Asia (Claxton et al., 2020) and eastern China (Fang et al., 2018), respectively.

There are several studies analyzing the transport of air into the stratosphere by convection above Central and North America and its further distribution by the North American monsoon anticyclone (NAMA) (e.g., Gettelman et al., 2004; Ray, 2004; Pittman et al., 2007; Weinstock et al., 2007; Herman et al., 2017; Wang et al., 2021; Clapp et al., 2021). Studies based on observational data mostly focus on the equatorward transport of air out of the NAMA (e.g., Gettelman et al., 2004; Ray, 2004; Pittman et al., 2007; Weinstock et al., 2007). Mainly model based simulations (e.g., Li, 2005; Ploeger et al., 2013; Nützel et al., 2019) and a study based on satellite observations (Clapp et al., 2021) have addressed north- and northeastward outflow of the NAMA. Here, we have described a transport pathway from the marine boundary layer in Central America and the tropical Atlantic into the NH midlatitude UTLS based on in situ Cl-VSLS observations.~~ To our knowledge in situ Cl-VSLS measurements have never been used before to study transport from the tropics south of the NAMA to the midlatitude UTLS.~~

The horizontal advection northwards following the convection in the tropics might be related to the NAMA as described in a recent model study by Wang et al. (2021). Further, Clapp et al. (2021) observed the main outflow (68 %) of the NAMA to be in north-eastward direction between 35° N and 60° N in July and August. In good agreement with both studies, the trajectories of WISE measurements uplifted above Central America show a northward drag towards a location of circular movement resembling the NAMA with a north-eastward escape from the circulation (cf. Figure 8, left).

Many studies have addressed the topic of tropospheric intrusions into the stratosphere above Central and North America by analyzing direct injections via overshooting convection (e.g., Smith et al., 2017; Anderson et al., 2017; Herman et al., 2017; Cooney et al., 2018; Clapp et al., 2019, 2021). The results of Wang et al. (2021) suggest that for air uplifted in the region of Central America (15° N to 20° N) overshooting convection is not the main transport pathway into the stratosphere during NH summer. Above this region of Central America the TP usually is at potential temperatures on the order of 380 K and most convection in this region does not uplift air higher than that. Drawn towards the NAMA, the uplifted air gets further transported horizontally to higher latitudes (Wang et al., 2021) where the TP is $1-2$ km higher than usual due to the NAMA (Schoeberl et al., 2020). Further horizontal transport northeastward out of the anticyclone, as shown in our study, eventually causes the tropical air masses (being on high potential temperatures) to isentropically enter the LS.

Our results further show a regional dependency of the slope of the NH UTLS $CHCl_3$-CH_2Cl_2 ~~correlation~~relationship. Observations by Say et al. (2019) in the Indian boundary layer suggest a similarly flat $CHCl_3$-CH_2Cl_2 correlation slope as observed during WISE for air masses strongly impacted by Asian sources. However, measurements from the AGAGE ~~measurements~~ network (Prinn et al., 2018) ~~from~~ at Barbados in 2017 show seasonally varying $CHCl_3$-CH_2Cl_2 correlation slopes not necessarily matching the steep slope observed for air masses strongly impacted by Central American source regions during WISE. The here presented regional dependency of the $CHCl_3$-CH_2Cl_2 correlation slope could thus be a seasonal phenomenon depending on transport efficiency and locally varying emissions. Obviously, more in situ observations of CH_2Cl_2 and $CHCl_3$ in the UTLS (particularly in different seasons) and ground-based (particularly in Asia) are needed to better understand the correlation behavior of CH_2Cl_2 and $CHCl_3$ in the UTLS.

5 Conclusions

We have presented ~~the first~~ a study on transport of Cl-VSLS into the Ex-UTLS based on tracer-tracer ~~correlation~~relationships using in situ Cl-VSLS observations. A schematic of the transport pathways we deduced in this study is shown in Figure 15. Our measurements in the LS above the midlatitude Atlantic Ocean in autumn 2017 revealed up to 150 % enhanced CH_2Cl_2 and up to 100 % enhanced $CHCl_3$ mixing ratios compared to measurements with similar N_2O mixing ratios, i.e., similarly processed air. In the stratosphere, the samples of CH_2Cl_2-rich air also contained most of the observed $CHCl_3$-rich air and the highest mixing ratios of both species detected in the stratosphere at $\Theta \approx 380$ K. In contrast to $CHCl_3$, CH_2Cl_2 is almost exclusively of anthropogenic origin (Engel et al., 2018) and a good correlation of CH_2Cl_2-rich air with $CHCl_3$-rich air suggests anthropogenic sources also impacting the enhanced $CHCl_3$ mixing ratios observed in the region at about 380 K potential temperature. Using a global three-dimensional Lagrangian model simulation we have shown a particularly strong influence of southern and eastern Asian sources in these air masses of enhanced CH_2Cl_2 and $CHCl_3$ mixing ratios.

Back-trajectory calculations agree well with the global three-dimensional model simulation and reveal a distinct transport pathway via the Asian summer monsoon for the air masses of enhanced CH_2Cl_2 and $CHCl_3$ mixing ratios. This pathway implies convection over southern and eastern Asia to about 360 K potential temperature ~~$4-10$ weeks prior to the measurement (i.e.,~~ in July and August~~)~~ and a slow circular upwelling to $370-400$ K in the ASMA. The observed air masses broke out of the anticyclone eastward following the subtropical jet stream before entering the extratropics above the eastern Pacific or western Atlantic Ocean (horizontal red arrow in Figure 15). Air parcels following this pathway were observed in the Ex-LS $6-11$ weeks after they left the BL. This transport pathway was also observed during the HALO TACTS campaign in 2012 (Vogel et al., 2014, 2016; Müller et al., 2016; Rolf et al., 2018).

Our results provide observational evidence to support the findings of model studies (e.g., Hossaini et al., 2015, 2019; Claxton et al., 2019) which connect the recent increase in Asian CH_2Cl_2 and $CHCl_3$ emissions (e.g., Leedham-Elvidge et al., 2015; Oram et al., 2017; Feng et al., 2018; Fang et al., 2018; Adcock et al., 2021) with an increase in the contribution to stratospheric chlorine levels by the two species. Particularly the region at about 380 K potential temperature is dominated by young air masses from southern and eastern Asia thereby strongly increasing the chlorine loading from VSLS in this layer in NH late summer. Our results emphasize that further increases in Asian $CHCl_3$ emissions will inevitably lead to similarly clear signatures of enhanced $CHCl_3$ mixing ratios in the Ex-LS as we already observe for CH_2Cl_2.

Another ~~faster~~ pathway from the (sub-)tropical boundary layer into the NH Ex-UTLS ~~with transport times of $1-5$ weeks~~ was derived from particularly low CH_2Cl_2 mixing ratios observed in the UTLS region. The CH_2Cl_2-poor air mainly originated from Central America as well as from the the tropical Atlantic Ocean and Northern Africa (central and western ITCZ) and was uplifted above Central America during the course of September. Ground-based ~~AGAGE~~ measurements from the AGAGE network (Prinn et al., 2018) within that region show minimum background mixing ratios of both CH_2Cl_2 and $CHCl_3$ in September. This seasonal minimum is clearly reflected in our UTLS measurements and allows these air masses to be distinguished from the strongly enhanced mixing ratios transported via the ASMA.

The transport pathway derived from CH_2Cl_2-poor air follows a general pattern: Air masses are convectively uplifted into the TTL above Central America to about $360-370$ K potential temperature (vertical blue arrow in Figure 15). The ~~convection~~vertical transport is induced by the general ~~updraft~~convection in the ITCZ region, by the North American monsoon, and by hurricanes. We could directly link measurements of CH_2Cl_2-poor air to the uplift by the category 5 hurricane Maria (Pasch et al., 2019). After the convection, the air masses were horizontally transported to higher latitudes and drawn towards an anticyclonic structure above North America. Resolved by back-trajectories, the anticyclone above North America was much smaller than the ASMA and was located mostly at 35° N and 80° W above Florida, likely being a remnant of the NAMA which usually declines in late September (e.g., Vera et al., 2006). Other than observed for the ASMA, the circulating air parcels above North America did not significantly increase their potential temperature. Further, the air masses broke out of the anticyclone northeastward forming a streamer which carried a local high TP into higher latitudes. Eventually, these air masses mixed into the LS by Rossby wave breaking and influenced the chemical composition of the NH Ex-LS $10-20$ K below the air masses dominated by transport via the ASMA. However, only 25 % of air parcels transported via this pathway were observed above the thermal TP with transport times from the BL to the location of measurement ranging from 5 to 9 weeks.

Our study shows that air masses lifted by convection in the tropical region of Central America do not need to directly cross the TP or to slowly enter the tropical pipe to be transported into the stratosphere. In the TTL, fast horizontal transport northward on high potential temperature levels provides an efficient and fast pathway for air lifted up in the tropics above Central America to quasi-isentropically enter the Ex-LS during NH late summer. Air transported along this pathway was observed to be mostly CH_2Cl_2-poor and $CHCl_3$-poor air. However, transport along this pathway may cause other ozone depleting short-lived substances with stronger sources in the region of the central and western ITCZ (such as tropical maritime and coastal sources, e.g., CH_2Br_2 and $CHBr_3$, Hepach et al., 2015) to be significantly enhanced in the middle and lower part of the LMS (e.g., Rotermund et al., 2021).

Particularly the use of in situ CH_2Cl_2 measurements as a very short-lived tracer has clearly revealed the differences between the two main transport pathways into the NH Ex-LS described in this study. In addition, we have deduced a higher $CHCl_3$:CH_2Cl_2 emission ratio in the central and western ITCZ region compared to southern and eastern Asia. The difference might be due to additional biogenic $CHCl_3$ sources in the ocean-rich central and western ITCZ region, while the emissions in southern and eastern Asia are most likely dominated by anthropogenic continental sources. However, more UTLS observations of CH_2Cl_2 and $CHCl_3$ in different seasons as well as more ground-based long-term observations of the two species in Asia are needed to complete the understanding of the seasonal and inter-annual variability of the transport pathways identified in our study. Figure 15 shows a schematic drawing of the two reported ~~main~~ transport pathways into the NH Ex-LS in late summer. The scheme summarizes the main findings of this paper.

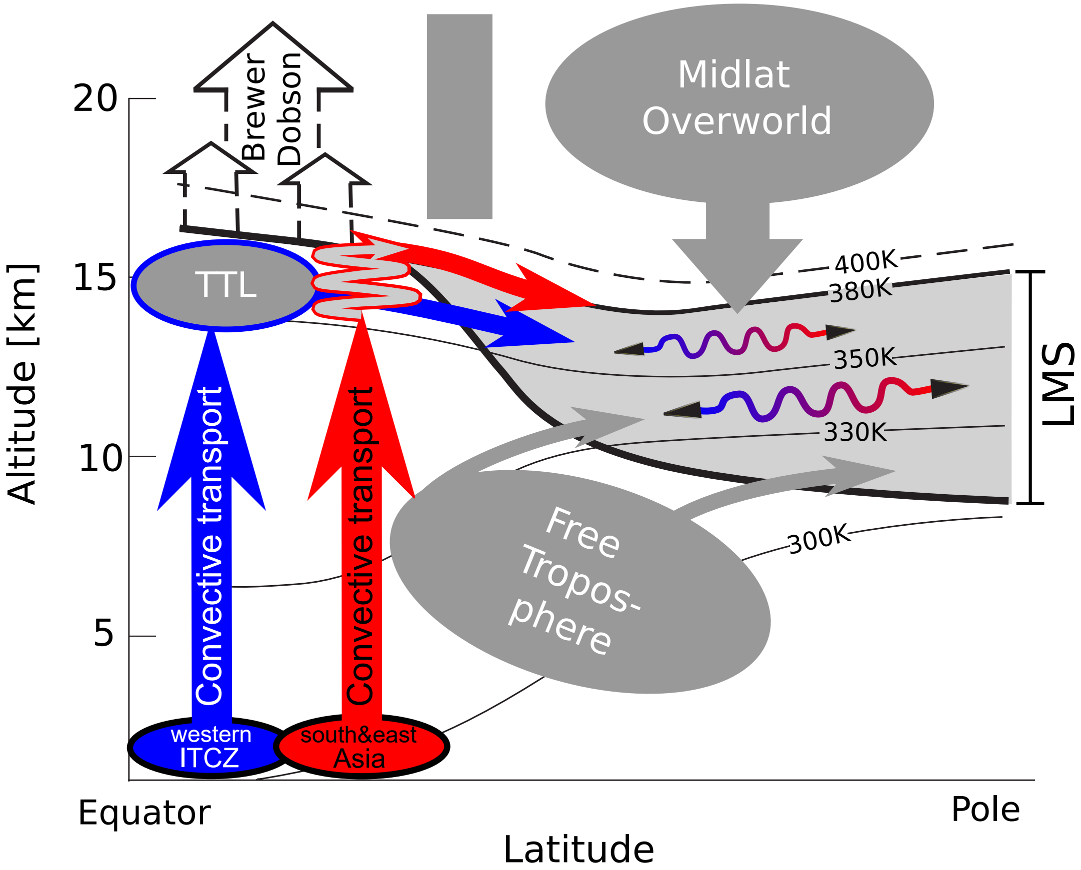

Figure 15. Schematic meridional view of the two major transport pathways for CH_2Cl_2-rich and $CHCl_3$-rich air (red) and CH_2Cl_2-poor and mainly $CHCl_3$-poor air (blue) from the source region into the NH LMS. The pathway from source regions located mostly in the western part of the ITCZ starts with convection into the tropical tropopause layer (TTL) above Central America by general updraft in the ITCZ, by the North American monsoon, and by hurricanes as shown for hurricane Maria in Section 3.1.3. Quasi-isentropic transport to the north and northeast eventually transports the air into the LMS at $\Theta \approx 360\,K$. Air masses from southern and eastern Asia are uplifted by the Asian summer monsoon (ASM) to $\Theta \approx 360\,K$ with subsequent slow upwelling within the monsoon anticyclone to $\Theta \approx 380\,K$. These air masses break out of the anticyclone to follow the subtropical jet stream eastwards before isentropically entering the Ex-LS above the eastern Pacific or western Atlantic Ocean.

Data availability. The following measured and simulated WISE data used in this paper is available at the HALO data depository (https://halo-db.pa.op.dlr.de/mission/96): HAGAR-V CH_2Cl_2 and $CHCl_3$ (Dataset #5917–#5926); UMAQS N_2O (Dataset #5979–#5988); BAHAMAS aircraft data (Dataset #5618–#5627); CLaMS equivalent latitude and tropopause (Dataset #5455–#5464). Signing a data protocol is mandatory to access the data from the HALO data depository. The CLaMS surface origin tracers and the back-trajectory calculations are available upon request (b.vogel@fz-juelich.de).

Appendix A: Absolute fractions of surface origin tracers

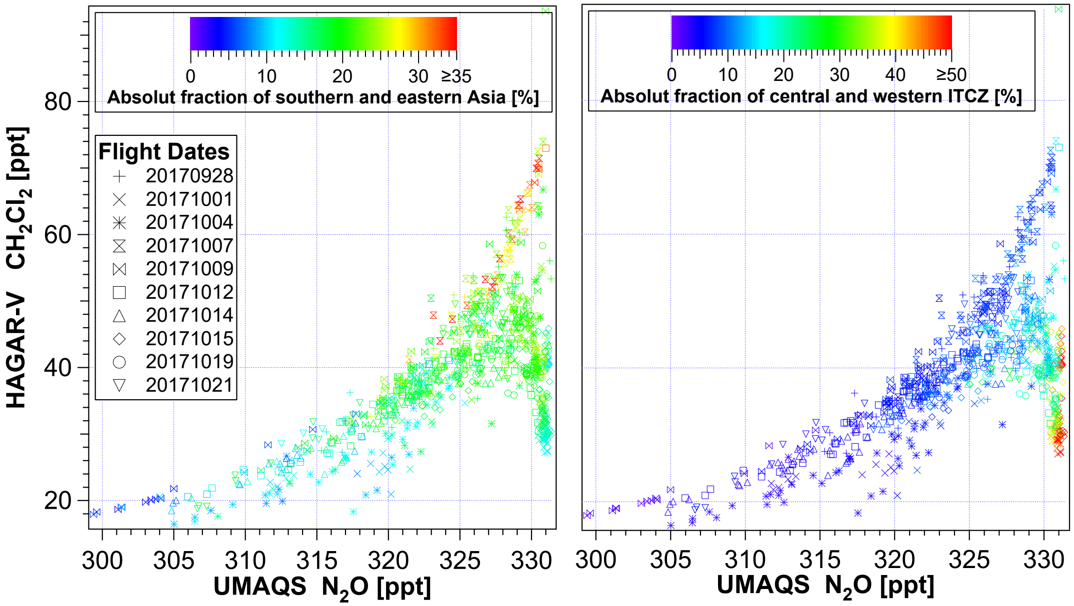

Figure A1. CH_2Cl_2-N_2O ~~correlation~~relationship color coded with different surface origin tracers. The shown tracer fractions are relative to the other surface origin tracers including the fraction of air that has already been above the model boundary layer at the initialization of the model simulation on 1 May, 2017.

Appendix B: Back-trajectory locations at boundary layer

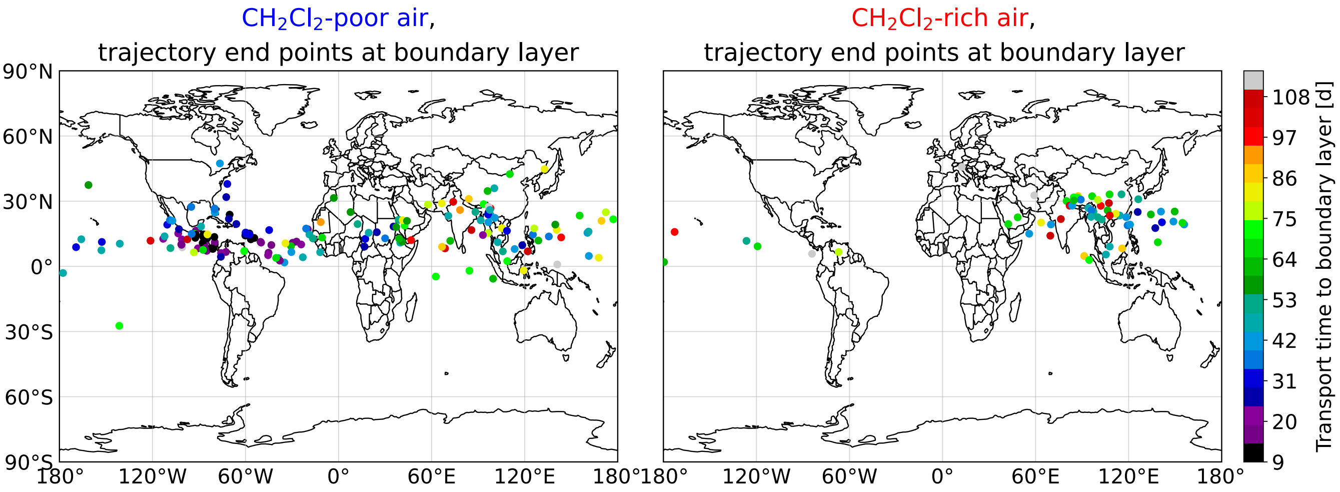

Figure B1. Location of back-trajectory end points at the model boundary layer, color coded with the transport time from the location of measurement to the location at the boundary layer. Shown are the locations at the boundary layer for CH_2Cl_2-poor (left panel) and -rich air (right panel) from all WISE flights between 28 September and 21 October.

Appendix C: CHCl$_3$-N$_2$O ~~correlation~~relationship vs ~~AGAGE~~ measurements from the AGAGE network

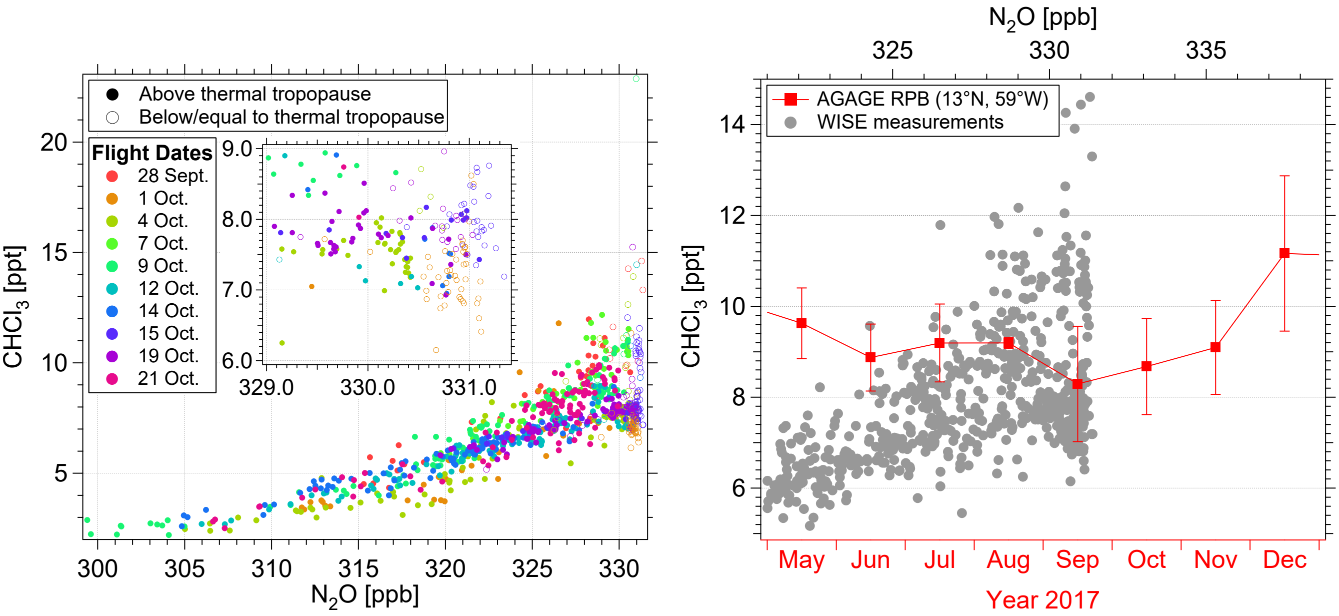

Figure C1. CHCl$_3$-N$_2$O ~~correlation~~relationship color coded by flight date (left) and monthly averaged ground-based ~~CHCl$_3$~~ measurements of CHCl$_3$ from the AGAGE network at Ragged Point, Barbados (right; Prinn et al., 2018) overlayed by a detailed plot of the CHCl$_3$-N$_2$O ~~correlation~~relationship. The right plot showing the ~~AGAGE~~ CHCl$_3$ time series of the AGAGE network is similar to Figure 4 where a detailed description is given.

Author contributions. VL, JW, AR, and CMV carried out the measurements with the HAGAR-V instrument; PH and VB provided the UMAQS N_2O data; the CLaMS simulations and the back-trajectory calculations were performed by BV. VL processed the HAGAR-V data and analyzed the measurements and simulations; CMV helped with interpreting the results. The results of the study were discussed by all the co-authors, with particular contributions by BV, RM and CMV. The paper was written by VL, with supporting comments from BV, RM, CMV, JW, and PH.

Competing interests. RM is an editor of ACP; otherwise the authors declare that they have no conflict of interest.

Disclaimer.

Acknowledgements. The authors would like to thank Simon O'Doherty and Dickon Young for the use of the AGAGE network ground-based CH_2Cl_2 and $CHCl_3$ measurements at Ragged Point obtained from http://www.agage.mit.edu/ (last access: 23 June 2021). Operation of the AGAGE laboratory at Ragged Point is supported by the National Aeronautics and Space Administration (NASA, grant NNX16AC98G to MIT) and the National Oceanic and Atmospheric Administration (NOAA, contract 1305M319CNRMJ0028 to the University of Bristol). We acknowledge the use of ERA-Interim reanalysis data obtained from the European Centre for Medium-Range Weather Forecasts (ECMWF). We also acknowledge the use of CLaMS calculations regarding the location of the tropopause and the equivalent latitude provided by Jens-Uwe Grooß (Forschungszentrum Jülich). We gratefully like to acknowledge Tanja Schuck (University of Frankfurt) for the calibration of the HAGAR-V laboratory standards. We warmly thank the whole WISE community, in particular the scientific coordinators of the campaign, the pilots, the management and ground support team of the Deutsches Zentrum für Luft- und Raumfahrt Flugexperimente (DLR-FX), and the flight planning team for making this campaign a success. We gratefully acknowledge the extended HAGAR-V team supporting the measurements of the WISE mission particularly Emil Gerhardt (software and field support), Peter Knieling (electronics), and Axel Frohschauer (mechanics). We acknowledge the use of water vapor data from the FISH instrument provided by Christian Rolf and Nicole Spelten (both Forschungszentrum Jülich) as well as the use of avionic data provided by the BAHAMAS team (Mess- und Sensortechnik, DLR-FX). We also want to thank Andreas Petzold (Forschungszentrum Jülich) for helpful remarks on the $CHCl_3$-CH_2Cl_2 ~~correlation~~relationship. We gratefully acknowledge the computing time for the CLaMS simulations granted on the supercomputer JURECA at Jülich Supercomputing Centre (JSC) under the VSR project ID JICG11. Our activities were mainly funded by the German Science Foundation (Deutsche Forschungsgemeinschaft, DFG) Priority Program SPP 1294: VO1530/5-1 (HAGAR-V), VO1276/5-1 (CLaMS), HO4225/7-1 and HO4225/8-1 (UMAQS). VL was partly funded by a HITEC (Helmholtz Interdisciplinary Doctoral Training in Energy and Climate Research) fellowship by the Forschungszentrum Jülich. We acknowledge support from the Open Access Publication Fund of the University of Wuppertal.

References

Adcock, K. E., Fraser, P. J., Hall, B. D., Langenfelds, R. L., Lee, G., Montzka, S. A., Oram, D. E., Röckmann, T., Stroh, F., Sturges, W. T., Vogel, B., and Laube, J. C.: Aircraft-Based Observations of Ozone-Depleting Substances in the Upper Troposphere and Lower Stratosphere in and Above the Asian Summer Monsoon, Journal of Geophysical Research: Atmospheres, 126, https://doi.org/10.1029/2020jd033137, 2021.

Anderson, J. G., Weisenstein, D. K., Bowman, K. P., Homeyer, C. R., Smith, J. B., Wilmouth, D. M., Sayres, D. S., Klobas, J. E., Leroy, S. S., Dykema, J. A., and Wofsy, S. C.: Stratospheric ozone over the United States in summer linked to observations of convection and temperature via chlorine and bromine catalysis, Proceedings of the National Academy of Sciences, 114, E4905–E4913, https://doi.org/10.1073/pnas.1619318114, 2017.

Andrews, A. E., Boering, K. A., Daube, B. C., Wofsy, S. C., Loewenstein, M., Jost, H., Podolske, J. R., Webster, C. R., Herman, R. L., Scott, D. C., Flesch, G. J., Moyer, E. J., Elkins, J. W., Dutton, G. S., Hurst, D. F., Moore, F. L., Ray, E. A., Romashkin, P. A., and Strahan, S. E.: Mean ages of stratospheric air derived from in situ observations of CO2, CH4, and N2O, Journal of Geophysical Research: Atmospheres, 106, 32 295–32 314, https://doi.org/10.1029/2001jd000465, 2001.

Aschmann, J., Sinnhuber, B.-M., Atlas, E. L., and Schauffler, S. M.: Modeling the transport of very short-lived substances into the tropical upper troposphere and lower stratosphere, 9, 9237–9247, https://doi.org/10.5194/acp-9-9237-2009, 2009.

Ashfold, M. J., Harris, N. R. P., Atlas, E. L., Manning, A. J., and Pyle, J. A.: Transport of short-lived species into the Tropical Tropopause Layer, Atmospheric Chemistry and Physics, 12, 6309–6322, https://doi.org/10.5194/acp-12-6309-2012, 2012.

Aucott, M. L., McCulloch, A., Graedel, T. E., Kleiman, G., Midgley, P., and Li, Y.-F.: Anthropogenic emissions of trichloromethane (chloroform, $CHCl_3$) and chlorodifluoromethane (HCFC-22): Reactive Chlorine Emissions Inventory, Journal of Geophysical Research: Atmospheres, 104, 8405–8415, https://doi.org/10.1029/1999jd900053, 1999.

Bergman, J. W., Fierli, F., Jensen, E. J., Honomichl, S., and Pan, L. L.: Boundary layer sources for the Asian anticyclone: Regional contributions to a vertical conduit, Journal of Geophysical Research: Atmospheres, 118, 2560–2575, https://doi.org/10.1002/jgrd.50142, 2013.

Bourtsoukidis, E., Helleis, F., Tomsche, L., Fischer, H., Hofmann, R., Lelieveld, J., and Williams, J.: An aircraft gas chromatograph–mass spectrometer System for Organic Fast Identification Analysis (SOFIA): design, performance and a case study of Asian monsoon pollution outflow, Atmospheric Measurement Techniques, 10, 5089–5105, https://doi.org/10.5194/amt-10-5089-2017, 2017.

Brunamonti, S., Jorge, T., Oelsner, P., Hanumanthu, S., Singh, B. B., Kumar, K. R., Sonbawne, S., Meier, S., Singh, D., Wienhold, F. G., Luo, B. P., Boettcher, M., Poltera, Y., Jauhiainen, H., Kayastha, R., Karmacharya, J., Dirksen, R., Naja, M., Rex, M., Fadnavis, S., and Peter, T.: Balloon-borne measurements of temperature, water vapor, ozone and aerosol backscatter on the southern slopes of the Himalayas during StratoClim 2016–2017, Atmospheric Chemistry and Physics, 18, 15 937–15 957, https://doi.org/10.5194/acp-18-15937-2018, 2018.

Carpenter, L. J., Daniel, J. S., (Lead Authors), Fleming, E. L., Hanaoka, T., Hu, J., Ravishankara, A. R., Ross, M. N., Tilmes, S., Wallington, T. J., and Wuebbles, D. J.: Scenarios and information for policymakers, Chapter 6 in *Scientific Assessment of Ozone Depletion: 2018*, pp. 1–69, Global Ozone Research and Monitoring Project – Report No. 58, WMO, 2018.

Chipperfield, M. P., Dhomse, S., Hossaini, R., Feng, W., Santee, M. L., Weber, M., Burrows, J. P., Wild, J. D., Loyola, D., and Coldewey-Egbers, M.: On the Cause of Recent Variations in Lower Stratospheric Ozone, Geophysical Research Letters, 45, 5718–5726, https://doi.org/10.1029/2018gl078071, 2018.

Chipperfield, M. P., Hossaini, R., Montzka, S. A., Reimann, S., Sherry, D., and Tegtmeier, S.: Renewed and emerging concerns over the production and emission of ozone-depleting substances, Nature Reviews Earth & Environment, 1, 251–263, https://doi.org/10.1038/s43017-020-0048-8, 2020.

Clapp, C. E., Smith, J. B., Bedka, K. M., and Anderson, J. G.: Identifying Source Regions and the Distribution of Cross-Tropopause Convective Outflow Over North America During the Warm Season, Journal of Geophysical Research: Atmospheres, 124, 13 750–13 762, https://doi.org/10.1029/2019jd031382, 2019.

Clapp, C. E., Smith, J. B., Bedka, K. M., and Anderson, J. G.: Identifying Outflow Regions of North American Monsoon Anticyclone-Mediated Meridional Transport of Convectively Influenced Air Masses in the Lower Stratosphere, Journal of Geophysical Research: Atmospheres, 126, https://doi.org/10.1029/2021jd034644, 2021.

Claxton, T., Hossaini, R., Wild, O., Chipperfield, M. P., and Wilson, C.: On the Regional and Seasonal Ozone Depletion Potential of Chlorinated Very Short-Lived Substances, Geophysical Research Letters, 46, 5489–5498, https://doi.org/10.1029/2018gl081455, 2019.

Claxton, T., Hossaini, R., Wilson, C., Montzka, S. A., Chipperfield, M. P., Wild, O., Bednarz, E. M., Carpenter, L. J., Andrews, S. J., Hackenberg, S. C., Mühle, J., Oram, D., Park, S., Park, M.-K., Atlas, E., Navarro, M., Schauffler, S., Sherry, D., Vollmer, M., Schuck, T., Engel, A., Krummel, P. B., Maione, M., Arduini, J., Saito, T., Yokouchi, Y., O'Doherty, S., Young, D., and Lunder, C.: A Synthesis Inversion to Constrain Global Emissions of Two Very Short Lived Chlorocarbons: Dichloromethane, and Perchloroethylene, Journal of Geophysical Research: Atmospheres, 125, https://doi.org/10.1029/2019jd031818, 2020.

Cooney, J. W., Bowman, K. P., Homeyer, C. R., and Fenske, T. M.: Ten Year Analysis of Tropopause-Overshooting Convection Using GridRad Data, Journal of Geophysical Research: Atmospheres, 123, 329–343, https://doi.org/10.1002/2017jd027718, 2018.

Cox, M. L., Sturrock, G. A., Fraser, P. J., Siems, S. T., Krummel, P. B., and O'Doherty, S.: Regional Sources of Methyl Chloride, Chloroform and Dichloromethane Identified from AGAGE Observations at Cape Grim, Tasmania, 1998–2000, Journal of Atmospheric Chemistry, 45, 79–99, https://doi.org/10.1023/a:1024022320985, 2003.

Daniel, J. S., Velders, G. J. M., Solomon, S., McFarland, M., and Montzka, S. A.: Present and future sources and emissions of halocarbons: Toward new constraints, Journal of Geophysical Research, 112, https://doi.org/10.1029/2006jd007275, 2007.

Dee, D. P., Uppala, S. M., Simmons, A. J., Berrisford, P., Poli, P., Kobayashi, S., Andrae, U., Balmaseda, M. A., Balsamo, G., Bauer, P., Bechtold, P., Beljaars, A. C. M., van de Berg, L., Bidlot, J., Bormann, N., Delsol, C., Dragani, R., Fuentes, M., Geer, A. J., Haimberger, L., Healy, S. B., Hersbach, H., Hólm, E. V., Isaksen, L., Kållberg, P., Köhler, M., Matricardi, M., McNally, A. P., Monge-Sanz, B. M., Morcrette, J.-J., Park, B.-K., Peubey, C., de Rosnay, P., Tavolato, C., Thépaut, J.-N., and Vitart, F.: The ERA-Interim reanalysis: configuration and performance of the data assimilation system, Quarterly Journal of the Royal Meteorological Society, 137, 553–597, https://doi.org/10.1002/qj.828, 2011.

Engel, A., Rigby, M., (Lead Authors), Burkholder, J. B., Fernandez, R. P., Froidevaux, L., Hall, B. D., Hossaini, R., Saito, T., Vollmer, M. K., and Yao, B.: Update on ozone-depleting substances (ODSs) and other gases of interest to the Montreal protocol, Chapter 1 in *Scientific Assessment of Ozone Depletion: 2018*, pp. 1–87, Global Ozone Research and Monitoring Project – Report No. 58, WMO, 2018.

Fang, X., Park, S., Saito, T., Tunnicliffe, R., Ganesan, A. L., Rigby, M., Li, S., Yokouchi, Y., Fraser, P. J., Harth, C. M., Krummel, P. B., Mühle, J., O'Doherty, S., Salameh, P. K., Simmonds, P. G., Weiss, R. F., Young, D., Lunt, M. F., Manning, A. J., Gressent, A., and Prinn, R. G.: Rapid increase in ozone-depleting chloroform emissions from China, Nature Geoscience, 12, 89–93, https://doi.org/10.1038/s41561-018-0278-2, 2018.

Feng, Y., Bie, P., Wang, Z., Wang, L., and Zhang, J.: Bottom-up anthropogenic dichloromethane emission estimates from China for the period 2005 - 2016 and predictions of future emissions, Atmospheric Environment, 186, 241–247, https://doi.org/10.1016/j.atmosenv.2018.05.039, 2018.

Filus, M. T., Atlas, E. L., Navarro, M. A., Meneguz, E., Thomson, D., Ashfold, M. J., Carpenter, L. J., Andrews, S. J., and Harris, N. R. P.: Transport of short-lived halocarbons to the stratosphere over the Pacific Ocean, Atmospheric Chemistry and Physics, 20, 1163–1181, https://doi.org/10.5194/acp-20-1163-2020, 2020.

Garny, H. and Randel, W. J.: Transport pathways from the Asian monsoon anticyclone to the stratosphere, Atmospheric Chemistry and Physics, 16, 2703–2718, https://doi.org/10.5194/acp-16-2703-2016, 2016.

Gentner, D. R., Miller, A. M., and Goldstein, A. H.: Seasonal Variability in Anthropogenic Halocarbon Emissions, Environmental Science & Technology, 44, 5377–5382, https://doi.org/10.1021/es1005362, 2010.

Gettelman, A., Kinnison, D. E., Dunkerton, T. J., and Brasseur, G. P.: Impact of monsoon circulations on the upper troposphere and lower stratosphere, Journal of Geophysical Research: Atmospheres, 109, n/a–n/a, https://doi.org/10.1029/2004jd004878, 2004.

Giez, A., Mallaun, C., Zöger, M., Dörnbrack, A., and Schumann, U.: Static Pressure from Aircraft Trailing-Cone Measurements and Numerical Weather-Prediction Analysis, Journal of Aircraft, 54, 1728–1737, https://doi.org/10.2514/1.c034084, 2017.

Hanisco, T. F., Lanzendorf, E. J., Wennberg, P. O., Perkins, K. K., Stimpfle, R. M., Voss, P. B., Anderson, J. G., Cohen, R. C., Fahey, D. W., Gao, R. S., Hintsa, E. J., Salawitch, R. J., Margitan, J. J., McElroy, C. T., and Midwinter, C.: Sources, Sinks, and the Distribution of OH in the Lower Stratosphere, The Journal of Physical Chemistry A, 105, 1543–1553, https://doi.org/10.1021/jp002334g, 2001.

Hanumanthu, S., Vogel, B., Müller, R., Brunamonti, S., Fadnavis, S., Li, D., Ölsner, P., Naja, M., Singh, B. B., Kumar, K. R., Sonbawne, S., Jauhiainen, H., Vömel, H., Luo, B., Jorge, T., Wienhold, F. G., Dirkson, R., and Peter, T.: Strong variability of the Asian Tropopause Aerosol Layer (ATAL) in August 2016 at the Himalayan foothills, Atmospheric Chemistry and Physics, https://doi.org/10.5194/acp-2020-552, 2020.

Hepach, H., Quack, B., Raimund, S., Fischer, T., Atlas, E. L., and Bracher, A.: Halocarbon emissions and sources in the equatorial Atlantic Cold Tongue, Biogeosciences, 12, 6369–6387, https://doi.org/10.5194/bg-12-6369-2015, 2015.

Herman, R. L., Ray, E. A., Rosenlof, K. H., Bedka, K. M., Schwartz, M. J., Read, W. G., Troy, R. F., Chin, K., Christensen, L. E., Fu, D., Stachnik, R. A., Bui, T. P., and Dean-Day, J. M.: Enhanced stratospheric water vapor over the summertime continental United States and the role of overshooting convection, Atmospheric Chemistry and Physics, 17, 6113–6124, https://doi.org/10.5194/acp-17-6113-2017, 2017.

Hersbach, H., Bell, B., Berrisford, P., Hirahara, S., Horányi, A., Muñoz-Sabater, J., Nicolas, J., Peubey, C., Radu, R., Schepers, D., Simmons, A., Soci, C., Abdalla, S., Abellan, X., Balsamo, G., Bechtold, P., Biavati, G., Bidlot, J., Bonavita, M., Chiara, G., Dahlgren, P., Dee, D., Diamantakis, M., Dragani, R., Flemming, J., Forbes, R., Fuentes, M., Geer, A., Haimberger, L., Healy, S., Hogan, R. J., Hólm, E., Janisková, M., Keeley, S., Laloyaux, P., Lopez, P., Lupu, C., Radnoti, G., Rosnay, P., Rozum, I., Vamborg, F., Villaume, S., and Thépaut, J.-N.: The ERA5 global reanalysis, Quarterly Journal of the Royal Meteorological Society, https://doi.org/10.1002/qj.3803, 2020.

Honomichl, S. B. and Pan, L. L.: Transport From the Asian Summer Monsoon Anticyclone Over the Western Pacific, Journal of Geophysical Research: Atmospheres, 125, https://doi.org/10.1029/2019jd032094, 2020.

Hossaini, R., Chipperfield, M. P., Saiz-Lopez, A., Harrison, J. J., von Glasow, R., Sommariva, R., Atlas, E., Navarro, M., Montzka, S. A., Feng, W., Dhomse, S., Harth, C., Mühle, J., Lunder, C., O'Doherty, S., Young, D., Reimann, S., Vollmer, M. K., Krummel, P. B., and Bernath, P. F.: Growth in stratospheric chlorine from short-lived chemicals not controlled by the Montreal Protocol, Geophysical Research Letters, 42, 4573–4580, https://doi.org/10.1002/2015gl063783, 2015.

Hossaini, R., Chipperfield, M. P., Montzka, S. A., Leeson, A. A., Dhomse, S. S., and Pyle, J. A.: The increasing threat to stratospheric ozone from dichloromethane, Nature Communications, 8, 15 962, https://doi.org/10.1038/ncomms15962, 2017.

Hossaini, R., Atlas, E., Dhomse, S. S., Chipperfield, M. P., Bernath, P. F., Fernando, A. M., Mühle, J., Leeson, A. A., Montzka, S. A., Feng, W., Harrison, J. J., Krummel, P., Vollmer, M. K., Reimann, S., O'Doherty, S., Young, D., Maione, M., Arduini, J., and Lunder, C. R.: Recent Trends in Stratospheric Chlorine From Very Short-Lived Substances, Journal of Geophysical Research: Atmospheres, 124, 2318–2335, https://doi.org/10.1029/2018jd029400, 2019.

Hsu, K.-J. and DeMore, W. B.: Rate constants for the reactions of OH with CH_3Cl, CH_2Cl_2, $CHCl_3$, and CH_3Br, Geophysical Research Letters, 21, 805–808, https://doi.org/10.1029/94gl00601, 1994.

Keber, T., Bönisch, H., Hartick, C., Hauck, M., Lefrancois, F., Obersteiner, F., Ringsdorf, A., Schohl, N., Schuck, T., Hossaini, R., Graf, P., Jöckel, P., and Engel, A.: Bromine from short-lived source gases in the extratropical northern hemispheric upper troposphere and lower stratosphere (UTLS), Atmospheric Chemistry and Physics, 20, 4105–4132, https://doi.org/10.5194/acp-20-4105-2020, 2020.

Ko, M. K. W., Newman, P. A., Reimann, S., and Strahan, S. E.: SPARC Report on Lifetimes of Stratospheric Ozone-Depleting Substances, Their Replacements, and Related Species, Tech. rep., http://www.sparc-climate.org/publications/sparc-reports/, 2013.

Krautstrunk, M. and Giez, A.: The Transition From FALCON to HALO Era Airborne Atmospheric Research, in: Atmospheric Physics, pp. 609–624, Springer Berlin Heidelberg, https://doi.org/10.1007/978-3-642-30183-4_37, 2012.

Kunkel, D., Hoor, P., Kaluza, T., Ungermann, J., Kluschat, B., Giez, A., Lachnitt, H.-C., Kaufmann, M., and Riese, M.: Evidence of small-scale quasi-isentropic mixing in ridges of extratropical baroclinic waves, Atmospheric Chemistry and Physics, 19, 12 607–12 630, https://doi.org/10.5194/acp-19-12607-2019, 2019.

Laturnus, F., Haselmann, K. F., Borch, T., and Grøn, C.: Terrestrial natural sources of trichloromethane (chloroform, $CHCl_3$) – An overview, Biogeochemistry, 60, 121–139, https://doi.org/10.1023/a:1019887505651, 2002.

Laube, J. C., Engel, A., Bönisch, H., Möbius, T., Worton, D. R., Sturges, W. T., Grunow, K., and Schmidt, U.: Contribution of very short-lived organic substances to stratospheric chlorine and bromine in the tropics – a case study, Atmospheric Chemistry and Physics, 8, 7325–7334, https://doi.org/10.5194/acp-8-7325-2008, 2008.

Lauther, V.: Airborne in situ measurements of short-lived chlorocarbons and investigation of their pathways from northern hemispheric source regions into the lowermost stratosphere, Ph.D. thesis, Bergische Universität Wuppertal, https://doi.org/10.25926/KQVQ-HB36, 2020.

Leedham-Elvidge, E. C., Oram, D. E., Laube, J. C., Baker, A. K., Montzka, S. A., Humphrey, S., O'Sullivan, D. A., and Brenninkmeijer, C. A. M.: Increasing concentrations of CH_2Cl_2 inferred from CARIBIC air samples collected 1998–2012, Atmospheric Chemistry and Physics, 15, 1939–1958, https://doi.org/10.5194/acp-15-1939-2015, 2015.

Lelieveld, J., Gromov, S., Pozzer, A., and Taraborrelli, D.: Global tropospheric hydroxyl distribution, budget and reactivity, Atmospheric Chemistry and Physics, 16, 12 477–12 493, https://doi.org/10.5194/acp-16-12477-2016, 2016.

Levine, J. G., Braesicke, P., Harris, N. R. P., Savage, N. H., and Pyle, J. A.: Pathways and timescales for troposphere-to-stratosphere transport via the tropical tropopause layer and their relevance for very short lived substances, Journal of Geophysical Research, 112, https://doi.org/10.1029/2005jd006940, 2007.

Li, D., Vogel, B., Bian, J., Müller, R., Pan, L. L., Günther, G., Bai, Z., Li, Q., Zhang, J., Fan, Q., and Vömel, H.: Impact of typhoons on the composition of the upper troposphere within the Asian summer monsoon anticyclone: the SWOP campaign in Lhasa 2013, Atmospheric Chemistry and Physics, 17, 4657–4672, https://doi.org/10.5194/acp-17-4657-2017, 2017.

Li, D., Vogel, B., Müller, R., Bian, J., Günther, G., Ploeger, F., Li, Q., Zhang, J., Bai, Z., Vömel, H., and Riese, M.: Dehydration and low ozone in the tropopause layer over the Asian monsoon caused by tropical cyclones: Lagrangian transport calculations using ERA-Interim and ERA5 reanalysis data, Atmospheric Chemistry and Physics, 20, 4133–4152, https://doi.org/10.5194/acp-20-4133-2020, 2020.

Li, Q.: North American pollution outflow and the trapping of convectively lifted pollution by upper-level anticyclone, Journal of Geophysical Research, 110, https://doi.org/10.1029/2004jd005039, 2005.

Liang, Q., Atlas, E., Blake, D., Dorf, M., Pfeilsticker, K., and Schauffler, S.: Convective transport of very short lived bromocarbons to the stratosphere, Atmospheric Chemistry and Physics, 14, 5781–5792, https://doi.org/10.5194/acp-14-5781-2014, 2014.

Luong, J., Gras, R., Mustacich, R., and Cortes, H.: Low Thermal Mass Gas Chromatography: Principles and Applications, Journal of chromatographic science, 44, 253–61, https://doi.org/10.1093/chromsci/44.5.253, 2006.

McCulloch, A.: Chloroform in the environment: occurrence, sources, sinks and effects, Chemosphere, 50, 1291–1308, https://doi.org/10.1016/s0045-6535(02)00697-5, 2003.

McCulloch, A. and Midgley, P. M.: The production and global distribution of emissions of trichloroethene, tetrachloroethene and dichloromethane over the period 1988–1992, Atmospheric Environment, 30, 601 – 608, https://doi.org/https://doi.org/10.1016/1352-2310(09)50032-5, http://www.sciencedirect.com/science/article/pii/1352231009500325, 1996.

McKenna, D. S.: A new Chemical Lagrangian Model of the Stratosphere (CLaMS) 1. Formulation of advection and mixing, Journal of Geophysical Research, 107, https://doi.org/10.1029/2000jd000114, 2002a.

McKenna, D. S.: A new Chemical Lagrangian Model of the Stratosphere (CLaMS) 2. Formulation of chemistry scheme and initialization, Journal of Geophysical Research, 107, https://doi.org/10.1029/2000jd000113, 2002b.

Müller, S., Hoor, P., Berkes, F., Bozem, H., Klingebiel, M., Reutter, P., Smit, H. G. J., Wendisch, M., Spichtinger, P., and Borrmann, S.: In situ detection of stratosphere-troposphere exchange of cirrus particles in the midlatitudes, Geophysical Research Letters, 42, 949–955, https://doi.org/10.1002/2014gl062556, 2015.

Müller, S., Hoor, P., Bozem, H., Gute, E., Vogel, B., Zahn, A., Bönisch, H., Keber, T., Krämer, M., Rolf, C., Riese, M., Schlager, H., and Engel, A.: Impact of the Asian monsoon on the extratropical lower stratosphere: trace gas observations during TACTS over Europe 2012, Atmospheric Chemistry and Physics, 16, 10 573–10 589, https://doi.org/10.5194/acp-16-10573-2016, 2016.

Montzka, S. A., Krol, M., Dlugokencky, E., Hall, B., Jöckel, P., and Lelieveld, J.: Small Interannual Variability of Global Atmospheric Hydroxyl, Science, 331, 67–69, https://doi.org/10.1126/science.1197640, 2011.

Moore, R. M.: Dichloromethane in North Atlantic waters, Journal of Geophysical Research, 109, https://doi.org/10.1029/2004jc002397, 2004.

Nützel, M., Podglajen, A., Garny, H., and Ploeger, F.: Quantification of water vapour transport from the Asian monsoon to the stratosphere, Atmospheric Chemistry and Physics, 19, 8947–8966, https://doi.org/10.5194/acp-19-8947-2019, 2019.

Oram, D. E., Ashfold, M. J., Laube, J. C., Gooch, L. J., Humphrey, S., Sturges, W. T., Leedham-Elvidge, E., Forster, G. L., Harris, N. R. P., Mead, M. I., Samah, A. A., Phang, S. M., Ou-Yang, C.-F., Lin, N.-H., Wang, J.-L., Baker, A. K., Brenninkmeijer, C. A. M., and Sherry, D.: A growing threat to the ozone layer from short-lived anthropogenic chlorocarbons, Atmospheric Chemistry and Physics, 17, 11 929–11 941, https://doi.org/10.5194/acp-17-11929-2017, 2017.

Pan, L. L., Kunz, A., Homeyer, C. R., Munchak, L. A., Kinnison, D. E., and Tilmes, S.: Commentary on using equivalent latitude in the upper troposphere and lower stratosphere, Atmospheric Chemistry and Physics, 12, 9187–9199, https://doi.org/10.5194/acp-12-9187-2012, 2012.

Park, M., Randel, W. J., Gettelman, A., Massie, S. T., and Jiang, J. H.: Transport above the Asian summer monsoon anticyclone inferred from Aura Microwave Limb Sounder tracers, Journal of Geophysical Research, 112, https://doi.org/10.1029/2006jd008294, 2007.

Park, M., Randel, W. J., Emmons, L. K., and Livesey, N. J.: Transport pathways of carbon monoxide in the Asian summer monsoon diagnosed from Model of Ozone and Related Tracers (MOZART), Journal of Geophysical Research, 114, https://doi.org/10.1029/2008jd010621, 2009.

Park, S., Atlas, E. L., Jiménez, R., Daube, B. C., Gottlieb, E. W., Nan, J., Jones, D. B. A., Pfister, L., Conway, T. J., Bui, T. P., Gao, R.-S., and Wofsy, S. C.: Vertical transport rates and concentrations of OH and Cl radicals in the Tropical Tropopause Layer from observations of CO_2 and halocarbons: implications for distributions of long- and short-lived chemical species, Atmospheric Chemistry and Physics, 10, 6669–6684, https://doi.org/10.5194/acp-10-6669-2010, 2010.

Pasch, R. J., Penny, A. B., and Berg, R.: Tropical Cyclone Report: Hurricane Maria (AL152017), Tech. rep., 2019.

Pittman, J. V., Weinstock, E. M., Oglesby, R. J., Sayres, D. S., Smith, J. B., Anderson, J. G., Cooper, O. R., Wofsy, S. C., Xueref, I., Gerbig, C., Daube, B. C., Richard, E. C., Ridley, B. A., Weinheimer, A. J., Loewenstein, M., Jost, H.-J., Lopez, J. P., Mahoney, M. J., Thompson, T. L., Hargrove, W. W., and Hoffman, F. M.: Transport in the subtropical lowermost stratosphere during the Cirrus Regional Study of Tropical Anvils and Cirrus Layers-Florida Area Cirrus Experiment, Journal of Geophysical Research, 112, https://doi.org/10.1029/2006jd007851, 2007.

Ploeger, F., Konopka, P., Günther, G., Grooß, J.-U., and Müller, R.: Impact of the vertical velocity scheme on modeling transport in the tropical tropopause layer, Journal of Geophysical Research, 115, https://doi.org/10.1029/2009jd012023, 2010.

Ploeger, F., Günther, G., Konopka, P., Fueglistaler, S., Müller, R., Hoppe, C., Kunz, A., Spang, R., Grooß, J.-U., and Riese, M.: Horizontal water vapor transport in the lower stratosphere from subtropics to high latitudes during boreal summer, Journal of Geophysical Research: Atmospheres, 118, 8111–8127, https://doi.org/10.1002/jgrd.50636, 2013.

Ploeger, F., Gottschling, C., Griessbach, S., Grooß, J.-U., Guenther, G., Konopka, P., Müller, R., Riese, M., Stroh, F., Tao, M., Ungermann, J., Vogel, B., and von Hobe, M.: A potential vorticity-based determination of the transport barrier in the Asian summer monsoon anticyclone, Atmospheric Chemistry and Physics, 15, 13 145–13 159, https://doi.org/10.5194/acp-15-13145-2015, 2015.

Pommrich, R., Müller, R., Grooß, J.-U., Konopka, P., Ploeger, F., Vogel, B., Tao, M., Hoppe, C. M., Günther, G., Spelten, N., Hoffmann, L., Pumphrey, H.-C., Viciani, S., D'Amato, F., Volk, C. M., Hoor, P., Schlager, H., and Riese, M.: Tropical troposphere to stratosphere transport of carbon monoxide and long-lived trace species in the Chemical Lagrangian Model of the Stratosphere (CLaMS), Geoscientific Model Development, 7, 2895–2916, https://doi.org/10.5194/gmd-7-2895-2014, 2014.

Popovic, J. M. and Plumb, R. A.: Eddy Shedding from the Upper-Tropospheric Asian Monsoon Anticyclone, Journal of the Atmospheric Sciences, 58, 93–104, https://doi.org/10.1175/1520-0469(2001)058<0093:esftut>2.0.co;2, 2001.

Prinn, R. G., Weiss, R. F., Arduini, J., Arnold, T., DeWitt, H. L., Fraser, P. J., Ganesan, A. L., Gasore, J., Harth, C. M., Hermansen, O., Kim, J., Krummel, P. B., Li, S., Loh, Z. M., Lunder, C. R., Maione, M., Manning, A. J., Miller, B. R., Mitrevski, B., Mühle, J., O'Doherty, S., Park, S., Reimann, S., Rigby, M., Saito, T., Salameh, P. K., Schmidt, R., Simmonds, P. G., Steele, L. P., Vollmer, M. K., Wang, R. H., Yao, B., Yokouchi, Y., Young, D., and Zhou, L.: History of chemically and radiatively important atmospheric gases from the Advanced Global Atmospheric Gases Experiment (AGAGE), Earth System Science Data, 10, 985–1018, https://doi.org/10.5194/essd-10-985-2018, 2018.

Randel, W. J. and Jensen, E. J.: Physical processes in the tropical tropopause layer and their roles in a changing climate, Nature Geoscience, 6, 169–176, https://doi.org/10.1038/ngeo1733, 2013.

Randel, W. J., Park, M., Emmons, L., Kinnison, D., Bernath, P., Walker, K. A., Boone, C., and Pumphrey, H.: Asian Monsoon Transport of Pollution to the Stratosphere, Science, 328, 611–613, https://doi.org/10.1126/science.1182274, 2010.

Ray, E. A.: Evidence of the effect of summertime midlatitude convection on the subtropical lower stratosphere from CRYSTAL-FACE tracer measurements, Journal of Geophysical Research, 109, https://doi.org/10.1029/2004jd004655, 2004.

Riese, M., Kaufmann, M., Kunkel, D., and Hoor, P.: Wave-driven Isentropic Exchange (WISE), https://www.wise2017.de/, last accessed: 2022-01-10, 2017.

Rolf, C., Vogel, B., Hoor, P., Afchine, A., Günther, G., Krämer, M., Müller, R., Müller, S., Spelten, N., and Riese, M.: Water vapor increase in the lower stratosphere of the Northern Hemisphere due to the Asian monsoon anticyclone observed during the TACTS/ESMVal campaigns, Atmospheric Chemistry and Physics, 18, 2973–2983, https://doi.org/10.5194/acp-18-2973-2018, 2018.

Rotermund, M. K., Bense, V., Chipperfield, M. P., Engel, A., Grooß, J.-U., Hoor, P., Hüneke, T., Keber, T., Kluge, F., Schreiner, B., Schuck, T., Vogel, B., Zahn, A., and Pfeilsticker, K.: Organic and inorganic bromine measurements around the extratropical tropopause and lowermost stratosphere: insights into the transport pathways and total bromine, 21, 15 375–15 407, https://doi.org/10.5194/acp-21-15375-2021, 2021.

Rudolph, J., Khedim, A., Koppmann, R., and Bonsang, B.: Field study of the emissions of methyl chloride and other halocarbons from biomass burning in Western Africa, Journal of Atmospheric Chemistry, 22, 67–80, https://doi.org/10.1007/bf00708182, 1995.

Santee, M. L., Manney, G. L., Livesey, N. J., Schwartz, M. J., Neu, J. L., and Read, W. G.: A comprehensive overview of the climatological composition of the Asian summer monsoon anticyclone based on 10 years of Aura Microwave Limb Sounder measurements, Journal of Geophysical Research: Atmospheres, 122, 5491–5514, https://doi.org/10.1002/2016jd026408, 2017.

Say, D., Ganesan, A. L., Lunt, M. F., Rigby, M., O'Doherty, S., Harth, C., Manning, A. J., Krummel, P. B., and Bauguitte, S.: Emissions of halocarbons from India inferred through atmospheric measurements, Atmospheric Chemistry and Physics, 19, 9865–9885, https://doi.org/10.5194/acp-19-9865-2019, 2019.

Schauffler, S. M., Heidt, L. E., Pollock, W. H., Gilpin, T. M., Vedder, J. F., Solomon, S., Lueb, R. A., and Atlas, E. L.: Measurements of halogenated organic compounds near the tropical tropopause, Geophysical Research Letters, 20, 2567–2570, https://doi.org/10.1029/93gl02840, 1993.

Schauffler, S. M., Atlas, E. L., Donnelly, S. G., Andrews, A., Montzka, S. A., Elkins, J. W., Hurst, D. F., Romashkin, P. A., Dutton, G. S., and Stroud, V.: Chlorine budget and partitioning during the Stratospheric Aerosol and Gas Experiment (SAGE) III Ozone Loss and Validation Experiment (SOLVE), 108, https://doi.org/10.1029/2001jd002040, 2003.

Scheeren, H. A., Lelieveld, J., de Gouw, J. A., van der Veen, C., and Fischer, H.: Methyl chloride and other chlorocarbons in polluted air during INDOEX, Journal of Geophysical Research, 107, https://doi.org/10.1029/2001jd001121, 2002.

Schäfler, A., Fix, A., and Wirth, M.: Mixing at the extratropical tropopause as characterized by collocated airborne H_2O and O_3 lidar observations, Atmospheric Chemistry and Physics, 21, 5217–5234, https://doi.org/10.5194/acp-21-5217-2021, 2021.

Schoeberl, M. R., Pfister, L., Wang, T., Kummer, J., Dessler, A. E., and Yu, W.: Erythemal Radiation, Column Ozone, and the North American Monsoon, Journal of Geophysical Research: Atmospheres, 125, https://doi.org/10.1029/2019jd032283, 2020.

Simmonds, P. G., Manning, A. J., Cunnold, D. M., McCulloch, A., O'Doherty, S., Derwent, R. G., Krummel, P. B., Fraser, P. J., Dunse, B., Porter, L. W., Wang, R. H. J., Greally, B. R., Miller, B. R., Salameh, P., Weiss, R. F., and Prinn, R. G.: Global trends, seasonal cycles, and European emissions of dichloromethane, trichloroethene, and tetrachloroethene from the AGAGE observations at Mace Head, Ireland, and Cape Grim, Tasmania, Journal of Geophysical Research, 111, https://doi.org/10.1029/2006jd007082, 2006.

Simpson, I. J., Akagi, S. K., Barletta, B., Blake, N. J., Choi, Y., Diskin, G. S., Fried, A., Fuelberg, H. E., Meinardi, S., Rowland, F. S., Vay, S. A., Weinheimer, A. J., Wennberg, P. O., Wiebring, P., Wisthaler, A., Yang, M., Yokelson, R. J., and Blake, D. R.: Boreal forest fire emissions in fresh Canadian smoke plumes: C_1-C_{10} volatile organic compounds (VOCs), CO_2, CO, NO_2, NO, HCN and CH_3CN, Atmospheric Chemistry and Physics, 11, 6445–6463, https://doi.org/10.5194/acp-11-6445-2011, 2011.

Siu, L. W. and Bowman, K. P.: Forcing of the Upper-Tropospheric Monsoon Anticyclones, Journal of the Atmospheric Sciences, 76, 1937–1954, https://doi.org/10.1175/jas-d-18-0340.1, 2019.

Smith, J. B., Wilmouth, D. M., Bedka, K. M., Bowman, K. P., Homeyer, C. R., Dykema, J. A., Sargent, M. R., Clapp, C. E., Leroy, S. S., Sayres, D. S., Dean-Day, J. M., Bui, T. P., and Anderson, J. G.: A case study of convectively sourced water vapor observed in the overworld stratosphere over the United States, Journal of Geophysical Research: Atmospheres, 122, 9529–9554, https://doi.org/10.1002/2017jd026831, 2017.

Spivakovsky, C. M., Logan, J. A., Montzka, S. A., Balkanski, Y. J., Foreman-Fowler, M., Jones, D. B. A., Horowitz, L. W., Fusco, A. C., Brenninkmeijer, C. A. M., Prather, M. J., Wofsy, S. C., and McElroy, M. B.: Three-dimensional climatological distribution of tropospheric OH: Update and evaluation, Journal of Geophysical Research: Atmospheres, 105, 8931–8980, https://doi.org/10.1029/1999jd901006, 2000.

Sturges, W. T., Oram, D. E., Carpenter, L. J., Penkett, S. A., and Engel, A.: Bromoform as a source of stratospheric bromine, Geophysical Research Letters, 27, 2081–2084, https://doi.org/10.1029/2000gl011444, 2000.

Trudinger, C. M., Etheridge, D. M., Sturrock, G. A., Fraser, P. J., Krummel, P. B., and McCulloch, A.: Atmospheric histories of halocarbons from analysis of Antarctic firn air: Methyl bromide, methyl chloride, chloroform, and dichloromethane, Journal of Geophysical Research: Atmospheres, 109, https://doi.org/10.1029/2004jd004932, 2004.

Vera, C., Higgins, W., Amador, J., Ambrizzi, T., Garreaud, R., Gochis, D., Gutzler, D., Lettenmaier, D., Marengo, J., Mechoso, C. R., Nogues-Paegle, J., Dias, P. L. S., and Zhang, C.: Toward a Unified View of the American Monsoon Systems, Journal of Climate, 19, 4977–5000, https://doi.org/10.1175/jcli3896.1, 2006.

Vogel, B., Günther, G., Müller, R., Grooß, J.-U., Hoor, P., Krämer, M., Müller, S., Zahn, A., and Riese, M.: Fast transport from Southeast Asia boundary layer sources to northern Europe: rapid uplift in typhoons and eastward eddy shedding of the Asian monsoon anticyclone, Atmospheric Chemistry and Physics, 14, 12 745–12 762, https://doi.org/10.5194/acp-14-12745-2014, 2014.

Vogel, B., Günther, G., Müller, R., Grooß, J.-U., and Riese, M.: Impact of different Asian source regions on the composition of the Asian monsoon anticyclone and of the extratropical lowermost stratosphere, Atmospheric Chemistry and Physics, 15, 13 699–13 716, https://doi.org/10.5194/acp-15-13699-2015, 2015.

Vogel, B., Günther, G., Müller, R., Grooß, J.-U., Afchine, A., Bozem, H., Hoor, P., Krämer, M., Müller, S., Riese, M., Rolf, C., Spelten, N., Stiller, G. P., Ungermann, J., and Zahn, A.: Long-range transport pathways of tropospheric source gases originating in Asia into the northern lower stratosphere during the Asian monsoon season 2012, Atmospheric Chemistry and Physics, 16, 15 301–15 325, https://doi.org/10.5194/acp-16-15301-2016, 2016.

Vogel, B., Müller, R., Günther, G., Spang, R., Hanumanthu, S., Li, D., Riese, M., and Stiller, G. P.: Lagrangian simulations of the transport of young air masses to the top of the Asian monsoon anticyclone and into the tropical pipe, Atmospheric Chemistry and Physics, 19, 6007–6034, https://doi.org/10.5194/acp-19-6007-2019, 2019.

von Hobe, M., Ploeger, F., Konopka, P., Kloss, C., Ulanowski, A., Yushkov, V., Ravegnani, F., Volk, C. M., Pan, L. L., Honomichl, S. B., Tilmes, S., Kinnison, D. E., Garcia, R. R., and Wright, J. S.: Upward transport into and within the Asian monsoon anticyclone as inferred from StratoClim trace gas observations, Atmospheric Chemistry and Physics, 21, 1267–1285, https://doi.org/10.5194/acp-21-1267-2021, 2021.

Wales, P. A., Salawitch, R. J., Nicely, J. M., Anderson, D. C., Canty, T. P., Baidar, S., Dix, B., Koenig, T. K., Volkamer, R., Chen, D., Huey, L. G., Tanner, D. J., Cuevas, C. A., Fernandez, R. P., Kinnison, D. E., Lamarque, J.-F., Saiz-Lopez, A., Atlas, E. L., Hall, S. R., Navarro, M. A., Pan, L. L., Schauffler, S. M., Stell, M., Tilmes, S., Ullmann, K., Weinheimer, A. J., Akiyoshi, H., Chipperfield, M. P., Deushi, M., Dhomse, S. S., Feng, W., Graf, P., Hossaini, R., Jöckel, P., Mancini, E., Michou, M., Morgenstern, O., Oman, L. D., Pitari, G., Plummer, D. A., Revell, L. E., Rozanov, E., Saint-Martin, D., Schofield, R., Stenke, A., Stone, K. A., Visioni, D., Yamashita, Y., and Zeng, G.: Stratospheric Injection of Brominated Very Short-Lived Substances: Aircraft Observations in the Western Pacific and Representation in Global Models, Journal of Geophysical Research: Atmospheres, 123, 5690–5719, https://doi.org/10.1029/2017jd027978, 2018.

Wang, X., Randel, W., and Wu, Y.: Infrequent, Rapid Transport Pathways to the Summer North American Upper Troposphere and Lower Stratosphere, Geophysical Research Letters, 48, https://doi.org/10.1029/2020gl089763, 2021.

Weinstock, E. M., Pittman, J. V., Sayres, D. S., Smith, J. B., Anderson, J. G., Wofsy, S. C., Xueref, I., Gerbig, C., Daube, B. C., Pfister, L., Richard, E. C., Ridley, B. A., Weinheimer, A. J., Jost, H.-J., Lopez, J. P., Loewenstein, M., and Thompson, T. L.: Quantifying the impact of the North American monsoon and deep midlatitude convection on the subtropical lowermost stratosphere using in situ measurements, Journal of Geophysical Research, 112, https://doi.org/10.1029/2007jd008554, 2007.

Werner, A., Volk, C. M., Ivanova, E. V., Wetter, T., Schiller, C., Schlager, H., and Konopka, P.: Quantifying transport into the Arctic lowermost stratosphere, Atmospheric Chemistry and Physics, 10, 11 623–11 639, https://doi.org/10.5194/acp-10-11623-2010, http://www.atmos-chem-phys.net/10/11623/2010/, 2010.

Wetzel, G., Friedl-Vallon, F., Glatthor, N., Grooß, J.-U., Gulde, T., Höpfner, M., Johansson, S., Khosrawi, F., Kirner, O., Kleinert, A., Kretschmer, E., Maucher, G., Nordmeyer, H., Oelhaf, H., Orphal, J., Piesch, C., Sinnhuber, B.-M., Ungermann, J., and Vogel, B.: Pollution trace gases C_2H_6, C_2H_2, HCOOH, and PAN in the North Atlantic UTLS: observations and simulations, 21, 8213–8232, https://doi.org/10.5194/acp-21-8213-2021, 2021.

WMO: Scientific Assessment of Ozone Depletion: 2018, Global Ozone Research and Monitoring Project-Report No. 56, Tech. rep., Geneva, Switzerland, 2018.

Woodbridge, E. L., Elkins, J. W., Fahey, D. W., Heidt, L. E., Solomon, S., Baring, T. J., Gilpin, T. M., Pollock, W. H., Schauffler, S. M., Atlas, E. L., Loewenstein, M., Podolske, J. R., Webster, C. R., May, R. D., Gilligan, J. M., Montzka, S. A., Boering, K. A., and Salawitch, R. J.: Estimates of total organic and inorganic chlorine in the lower stratosphere from in situ and flask measurements during AASE II, Journal of Geophysical Research, 100, 3057, https://doi.org/10.1029/94jd02744, 1995.

Worton, D. R., Sturges, W. T., Schwander, J., Mulvaney, R., Barnola, J.-M., and Chappellaz, J.: 20th century trends and budget implications of chloroform and related tri-and dihalomethanes inferred from firn air, Atmospheric Chemistry and Physics, 6, 2847–2863, https://doi.org/10.5194/acp-6-2847-2006, 2006.

Yihui, D. and Chan, J. C. L.: The East Asian summer monsoon: an overview, Meteorology and Atmospheric Physics, 89, 117–142, https://doi.org/10.1007/s00703-005-0125-z, 2005.